USING A BIOSENSOR PLATFORM FOR THE DETECTION AND CHARACTERIZATION OF AUTOANTIBODIES IN MYASTHENIA GRAVIS PATIENTS

by

Zahra Pakzad

B.Sc., The University of British Columbia, 2011

A THESIS SUBMITTED IN PARTIAL FULFILLMENT OF

THE REQUIREMENTS FOR THE DEGREE OF

MASTER OF SCIENCE

in

THE FACULTY OF GRADUATE AND POSTDOCTORAL STUDIES

(Pathology and Laboratory Medicine)

THE UNIVERSITY OF BRITISH COLUMBIA

(Vancouver)

April 2014

© Zahra Pakzad, 2014

Abstract

Myasthenia gravis (MG) is an antibody-mediated autoimmune disease of the neuromuscular junction, characterized by skeletal muscle weakness and fatiguability. 85-90% of MG patients have antibodies targeting the nicotinic acetylcholine receptor (AChR), an ion channel on the postsynaptic muscle membrane involved in neuromuscular transmission. A smaller proportion of MG patients have autoantibodies targeting muscle specific tyrosine kinase (MuSK), involved in AChR clustering. AChR and MuSK antibodies are highly specific for MG and serve as excellent diagnostic biomarkers. However, there is still a need for biomarkers to help predict response to treatment and disease course. Reasonable targets are antibody titer, isotype and IgG subclass, and binding affinity as these parameters dictate autoantibody pathogenicity.

Our first objective was to develop and optimize a sensitive assay using a biosensor platform (Biacore™) for the measurement of these parameters in MG patients with MuSK antibodies. MuSK antigen was immobilized onto Biacore™ sensor chips and diluted sera injected over the surface to measure binding levels. Antibody isotype and subclass were determined with sequential injections of anti-human Ig antibodies, and dissociation rate, as a measure of binding affinity, was determined by fitting the dissociation phase to a 1:1 model. This assay is specific, sensitive, and reproducible, and can be performed more rapidly and using low volumes of serum. We demonstrated the use of this assay in providing a comprehensive long-term profiling of MuSK antibodies that has the potential to be useful in a clinical setting for monitoring treatment response.

Developing a biosensor assay for the measurement and characterization of AChR antibodies involves the more complex process of immobilizing AChR in its native membrane-bound

conformation. Our secondary objective was to determine a method for immobilizing AChR onto a sensor chip in its membrane-bound form. We demonstrate a method using immobilized cell membrane vesicles which, with further study, may be viable for this purpose.

Collectively, these studies demonstrate the usefulness of biosensor methods in measuring and characterizing autoantibodies over the course of a patient's disease. Measuring and characterizing antibodies for use as clinical biomarkers in MG to help with assessing disease progression and response to treatment merits further study.

Preface

This thesis has been prepared by me in its entirety and is submitted in partial fulfillment of the requirements for the degree of Master of Science in Pathology and Laboratory Medicine. None of the text is taken from previously published or collaborative articles, with the exception of a published study presented in section 1.4.2 of the introduction, which was performed and written by me along with coauthors Aziz, T and Oger, J, and published prior to the start of my MSc.

The projects presented in this thesis were designed by me in conjunction with my supervisor, Dr. Joel Oger. Biacore™ experiments presented in Chapter 2 were conducted by me, with design help from Dr. Ebrima Gibbs. I was responsible for data collection and analysis. I performed all experimental design, data collection, and analysis for the project in Chapter 3.

Measuring MuSK antibodies in serum at the Neuroimmunology Laboratory was approved by the University of British Columbia Research Ethics Board (H09-02984).

Table of Contents

List of Tables

List of Figures

List of Abbreviations

αBT	Alpha-bungarotoxin
Ab	Antibody
ACh	Acetylcholine
AChR	Acetylcholine receptor
AChR-MG	Myasthenia gravis with acetylcholine receptor antibodies
AIRE	Autoimmune regulator gene
BC	British Columbia
BSA	Bovine serum albumin
CD20	Cluster of differentiation 20
CI	Confidence interval
CMD	Carboxymethylated dextran
CPM	Counts per minute
CT	Computed tomography
CV	Coefficient of variation
DMEM	Dulbecco's modified eagle's medium
DNA	Deoxyribonucleic acid
DPM	Disintegrations per minute
EAMG	Experimental autoimmune myasthenia gravis
EDC	1-ethyl-3-(3-dimethylaminopropyl)-carbodiimide
ELISA	Enzyme-linked immunosorbent assay
EPP	Endplate potential
FACS	Fluorescence-activated cell sorting
FBS	Fetal bovine serum

FITC	Fluorescein isothiocyanate
HLA	Human leukocyte antigen
IFC	Integrated microfluidic cartridge
Ig	Immunoglobulin
IR	Incidence rate
IvIg	Intravenous immunoglobulin
k_a / k_{on}	Association rate
k_d / k_{off}	Dissociation rate
LFH	Lymphoid follicular hyperplasia
LRP4	Lipoprotein receptor-related protein-4
mAb	Monoclonal antibody
MAC	Membrane attack complex
MFI	Median fluorescence intensity
MG	Myasthenia gravis
MG-ADL	Myasthenia gravis activities of daily living
MG-QOL	Myasthenia gravis quality of life
MHC	Major histocompatibility complex
MIR	Main immunogenic region
MRI	Magnetic resonance imaging
MuSK	Muscle-specific tyrosine kinase
MuSK-MG	Myasthenia gravis with muscle-specific tyrosine kinase antibodies
NHPS	Normal healthy pooled serum
NHS	N-hydroxysucciminide
NMJ	Neuromuscular junction
pI	Isoelectric point

PLEX	Plasma exchange
PML	Progressive multifocal leukoencephalopathy
QMG	Quantitative myasthenia gravis
RIPA	Radioimmunoprecipitation assay
RNS	Repetitive nerve stimulation
RU	Response (or resonance) unit
SCID	Severe combined immunodeficiency
SD	Standard deviation
SEM	Standard error of the mean
SFEMG	Single-fiber electromyography
SNMG	Seronegative myasthenia gravis
SPR	Surface plasmon resonance
Treg	Regulatory T cell
VGCC	Voltage-gated calcium channel
VGSC	Voltage-gated sodium channel

Acknowledgements

This project and my personal growth as a student in science has been a journey which would not have been possible without the insights and assistance of many individuals, for which I am most grateful.

First, I would like to give my utmost thanks to my supervisor, Dr. Joel Oger, for taking me on as a student and for his support, guidance, and mentorship throughout the course of my degree. Throughout my graduate studies, he provided me with the opportunity and independence to grow through the many challenges of planning and carrying out my research project. I thank him for granting me exposure not only to the world of research, but also for imparting his vast knowledge on the clinical aspects of neuroimmunology and the field of neurology, I have learned so much through him.

I would also like to thank the members of my supervisory committee, Drs. Haydn Pritchard, Jacqueline Quandt, and John Schrader for their time, guidance, and constructive suggestions during my project. I also thank Dr. Haydn Pritchard, advisor for the UBC Pathology and Laboratory Medicine program, for checking in with me and helping to keep me on track.

This work would not have been possible without the support of my fellow lab colleagues. I thank Tariq Aziz for his guidance and training since when I first started work at the lab as an undergraduate student, for his continuous help and support, and for helping make the lab an enjoyable place to work. I also thank Dr. Ebrima Gibbs for training me on all aspects of the Biacore™ technology, for his help in designing experiments, and for always providing coherent and extensive answers to my many questions. Anna Fronda and Jenah Alibhai deserve thanks for their friendship and moral support, and for being a continuous source of fun and laughter both in

and out of the lab. To all of the past members of the Neuroimmunology Lab, it has been a great pleasure to work alongside all of you. I also thank everyone outside of our lab that has ever helped me throughout the course of my graduate studies.

Finally, I would like to thank my family for continued moral support, and my friends for contagious enthusiasm and comic relief. I would especially like to thank my parents for always encouraging me to pursue my dreams and for their unwavering support. They have helped me become the person I am today, and for that I am truly grateful.

To my parents

Chapter 1: Introduction

1.1 Myasthenia gravis the disease

Myasthenia gravis (MG) is a prototypical antibody-mediated autoimmune disorder of the neuromuscular junction (NMJ). The disease is characterized by fluctuating skeletal muscle weakness and fatiguability, resulting from a deficiency in signal transmission between motor neurons and skeletal muscle. Its pathogenesis involves circulating pathogenic autoantibodies directed against proteins of the post-synaptic muscle membrane, the primary target being the nicotinic acetylcholine receptor (AChR), and less frequently muscle-specific tyrosine kinase (MuSK). MG is a heterogeneous disease with variable clinical presentation, disease course, and response to treatment.

1.2 History

One of the first cases of MG was likely described by English physician Thomas Willis, who in 1672 reported a female patient with fatiguable weakness of bulbar and limb muscles[1]. Over 200 years later, Wilhelm Erb and Samual Goldflam described the clinical features of MG in a series of patients, emphasizing the fatiguable weakness, ocular and bulbar features, and fluctuating symptoms[1]. For some time the disease was known as "Erb-Goldflam syndrome", until Friedrich Jolly in 1895 coined the term "myasthenia gravis pseudoparalytica", combing the Greek terms for muscle and weakness (myasthenia) and the Latin term for severe (gravis)[2].

In 1934, Mary Walker realized that the symptoms of MG were similar to those of curare poisoning, which was treated with the cholinesterase inhibitor physostigmine. She demonstrated

that treatment with physostigmine quickly improved myasthenic symptoms[3], after which treatment with anticholinesterase drugs became a staple in the management of MG. In 1937 Blalock began reporting that removal of the thymus improved MG symptoms, establishing thymectomy as a treatment[1].

In 1959-1960, Simpson and Nastuck both independently proposed that MG has an autoimmune etiology, caused by an antibody specific for a NMJ protein[4, 5]. In 1973, Patrick and Lindstrom developed the first experimental autoimmune model of MG (EAMG) when they demonstrated that rabbits immunized with AChR purified from electric organs of electric eels developed MG-like symptoms[6].

1.3 Clinical features and subgroups

MG is characterized by fluctuating skeletal muscle weakness that is worsened by activity and improves with rest. The weakness fluctuates from day to day or even from hour to hour[7]. MG is a very heterogeneous disease ("snowflake disease") and can be classified into several clinical subtypes based on muscle groups affected (ocular, bulbar, and generalized MG), age at onset (early-onset and late-onset MG), autoantibody profile (AChR-MG and MuSK-MG), and presence or absence of thymic pathology.

The particular muscle groups affected can vary between patients. Ocular weakness, involving weakness of the extraocular and eyelid muscles, is the most common initial presentation of MG, occurring in approximately 85% of patients[8]. Ocular weakness commonly presents as fluctuating ptosis (drooping of upper eyelids), diplopia (double vision), and ophthalmoplegia (paralysis of extraocular muscles)[9]. Bulbar weakness presents with dysphagia (difficulty with swallowing,

excessive clearing of throat), dysarthria (difficulty with articulation, nasal speech), dysphonia (eg. hoarseness), weakness of facial muscles such as masticatory weakness, and axial muscles weakness[7]. Bulbar weakness is the initial symptom in up to 15% of patients[7]. Weakness remains restricted to ocular and/or bulbar muscles in about 15% of patients[10], while in the majority of patients the disease progresses to generalized weakness, involving weakness of the upper and/or lower extremities, usually within two years of disease onset[7]. Difficulty with respiration (dyspnea and orthopnea) due to respiratory muscle weakness can also occur in MG. Respiratory muscles weakness is rarely the presenting feature of the disease, but can be life-threatening if it results in a myasthenic crisis, severe respiratory muscle weakness that necessitates intubation for ventilator support or airway protection[7]. Infection (usually pneumonia or an upper respiratory infection) is the most common trigger of a crisis (in 38% of cases), followed by no obvious reason (30%), and aspiration (10%)[11].

Thymic abnormalities in MG patients are also frequent. About 80% of early-onset AChR-MG patients have thymic lymphoid follicular hyperplasia (LFH), characterized by B lymphocyte infiltrates and germinal centers[12]. Around 10-15% of MG patients have a thymic epithelial tumour, or thymoma[7]. Thymic atrophy is common in late-onset patients.

MG patient with AChR antibodies (AChR-MG) and MuSK antibodies (MuSK-MG) are clinically distinct disease entities with different clinical presentation. MuSK-MG patients tend to have more bulbar, facial, and neck weakness, and are more likely to have respiratory difficulties and myasthenic crisis[13]. MuSK-MG also appears to affect almost exclusively (90%) females, and patients have a younger age of onset than AChR-MG patients[13-17]. In contrast with AChR-MG thymus histology is generally normal in MuSK-MG patients[18, 19].

1.4 Epidemiology

1.4.1 Worldwide epidemiology

MG is a relatively uncommon disease, however both prevalence and incidence have increased over time. Incidence and prevalence rates vary widely between the geographical regions that have been studied. In a recent systematic review of epidemiological studies performed between 1950 and 2007[20], incidence rates per year were found to range from 1.7 to 21.3 per million, while prevalence rates ranged from 15 to 170 per million. In addition, since the discovery of MuSK antibodies, a proportion of more recent studies have examined the two serological MG subgroups, AChR-MG and MuSK-MG, separately. In AChR-MG specific studies, incidence of AChR-MG has been found to range from 4.3 to 18 per million, and prevalence from 70.6 to 163.5 per million[20]. Epidemiology studies of MuSK-MG are limited to two regions of Europe, Holland and Greece, with incidence rates of 0.1 and 0.32 per million, and prevalence rates of 1.9 and 2.9, respectively[20]. Rates of MG do not appear to be related to latitude, unlike other autoimmune diseases like multiple sclerosis[21].

MG occurs in both sexes and at all ages, but there are sex- and age-specific epidemiological differences. The incidence of MG has a bimodal distribution, with one peak in early adulthood around age 30-40 where women are more likely affected (F:M ratio 3:1), and another peak of elderly onset around age 70 where there is a slight male predominance[8, 22, 23]. In general, the incidence of MG increases with age. Of most significance, multiple studies have also found that both the incidence and prevalence of MG have increased over the last couple decades among the elderly, with a bias towards men[24-31]. These increases are likely due to improved diagnosis, especially among elderly[30], and improved survival of MG patients due to better treatment.

Improved survival of MG patients and increasing longevity of the general population likely means that prevalence of MG will increase.

1.4.2 Incidence of MG in British Columbia, Canada

To determine whether a similar trend of increasing incidence is present in Canada, the author of this thesis and colleagues conducted a study of MG incidence in the province of British Columbia (BC)[32], of which an extended version is presented here.

We conducted a population-based study of the incidence of the AChR-MG serological subtype in BC for the 28-year period of January 1, 1984 to December 31, 2011. Incidence cases were ascertained by retrospectively identifying all first-time anti-AChR seropositive samples, measured by radioimmunoprecipitation testing, from the Neuroimmunology Laboratory database at the University of British Columbia, the sole laboratory to offer AChR antibody testing in BC. A positive test was necessary and sufficient for a patient to be included as a case as positivity for AChR antibodies is an excellent surrogate marker for AChR-MG diagnosis.

Incidence was defined as the annual number of first-time anti-AChR seropositive cases. Incidence rates (IRs) were calculated per 1 million inhabitants based on annual July population estimates (www.bcstats.gov.bc.ca). Cases were stratified into four age groups based on age at the first positive test: ≤19, 20-44, 45-64 and ≥65 years. Age- and sex-stratified IRs were calculated based on population estimates of the corresponding age and sex group.

Between January 1984 and December 2011, 1493 new anti-AChR seropositive individuals were identified (767 women, 718 men, 8 unknown). The age at the first positive serum sample in women had a bimodal distribution with peaks at 45–55 and 70–85 years, whereas in men the

distribution had a single peak at 70–80 years (Figure 1-1), resembling previously reported age at onset distributions[22, 30].

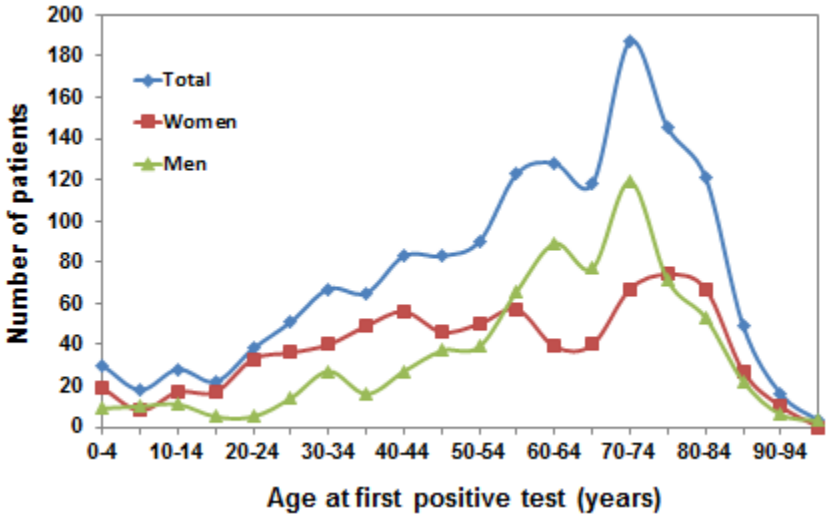

Figure 1-1 Age distribution of 1493 AChR-MG patients at first AChR seropositive test.

The average annual incidence of new AChR seropositivity significantly increased from 11.0 per million (1984-1988 average; 95% CI, 9.4-12.8) to 16.7 per million (2007-2011 average; 95% CI, 15.1-18.5). Mean annual IRs per million of the ≤19, 20-44 and 45-64 age groups remained relatively constant over the 28-year time period (Figure 1-2). In contrast, annual IRs of the ≥65 age group more than doubled. Sex-adjusted IRs ≥65 significantly increased for both men and women ≥65 (Figure 1-3).

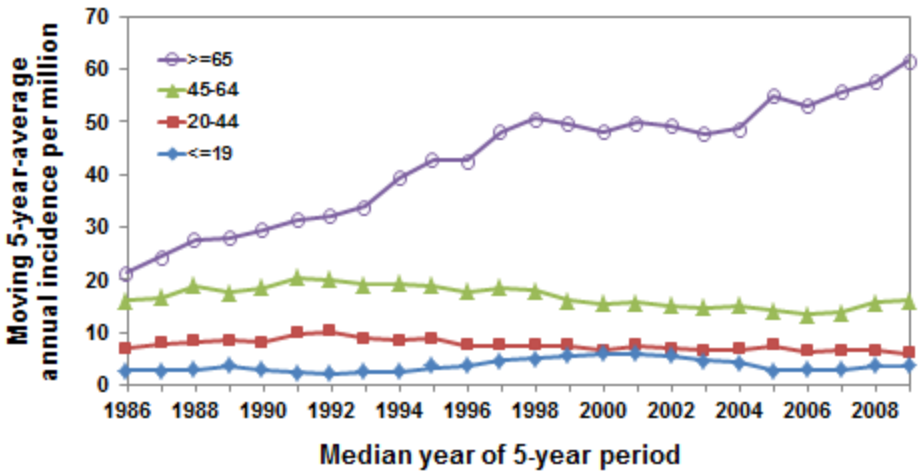

Figure 1-2 Age-specific incidence rates of AChR-MG in British Columbia from 1984-2011. The rates are age group adjusted and calculated per million population as 5-year simple moving averages. Modified from Pakzad *et al.*[32] with permission from Lippincott Williams & Wilkins, Inc.

The overall average anti-AChR incidence of first seropositivity of 16.7 per million (2007-2011 average) in BC is amongst the highest reported[20]. Our results indicate a continually increasing incidence of elderly-onset anti-AChR seropositive MG in BC. This trend cannot simply be attributed to demographic changes, such as increasing longevity and an aging population, since the incidence of anti-AChR seropositivity in the ≥65 age group increased at a significantly higher rate than the rate of increase in the proportion of people ≥65 in BC (Figure 1-3). One argument for an increasing incidence could be greater awareness of MG or increased AChR antibody testing, however, the IRs of the three younger age groups remained stable. Rather the trend is likely due to improved diagnosis of MG in elderly patients over the decades, or a true increase in incidence due to as yet undefined reasons. This study confirms the trend of increasing incidence of elderly-onset anti-AChR seropositive MG observed in previous studies and its results are important for future health care planning.

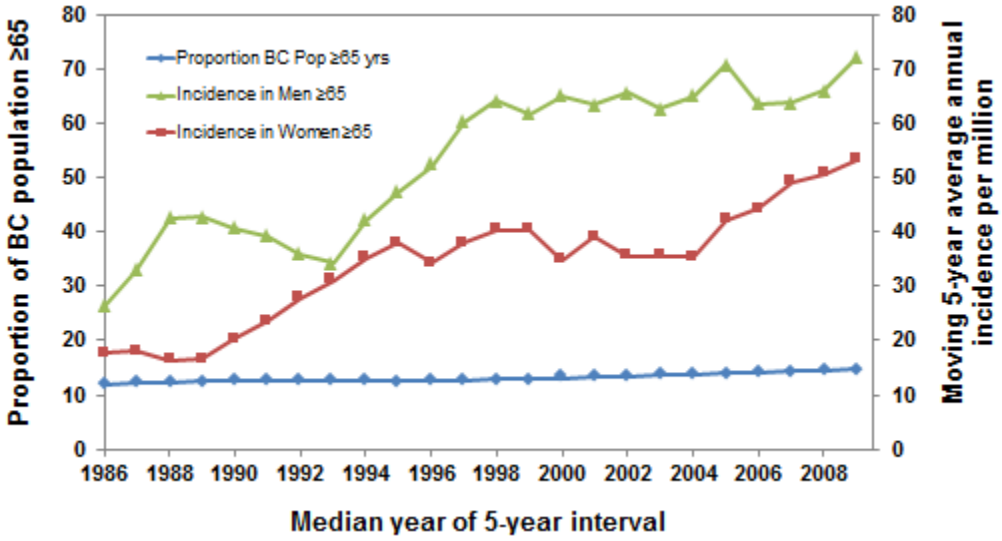

Figure 1-3 Sex-specific incidence of AChR-MG among elderly (≥65) in British Columbia from 1984-2011.

1.5 MG Pathophysiology

1.5.1 Structure and physiology of the neuromuscular junction

The muscle weakness and fatigue which are the clinical hallmarks of MG are a result of impairment in the physiology of the NMJ. The NMJ is the specialized synapse between a motor neuron and a skeletal muscle fiber where neuromuscular transmission takes place. It is comprised of the presynaptic motor nerve terminal (where the neurotransmitter acetylcholine is synthesized and stored in synaptic vesicles), the 20nm-thick synaptic cleft, and the post-synaptic muscle membrane[7] (Figure 1-4).

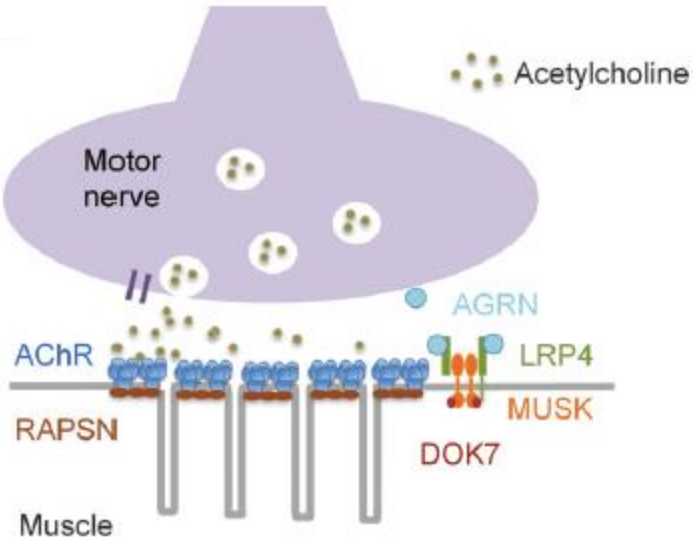

Figure 1-4 Structure of the neuromuscular junction, illustrating the high density of AChR at the tops of the postsynaptic membrane folds and the proteins involved in AChR clustering. Reprinted from Koneczny *et al.*[33] with permission from John Wiley and Sons.

The NMJ postsynaptic muscle membrane, or sarcolemma, is structurally characterized by many invaginations which increase the membrane surface area under the motor nerve terminal. These membrane folds contain a very high density of nicotinic acetylcholine receptors (AChRs), over 10,000 receptors/μm^2,[34]. AChR is a 290kDA pentameric transmembrane ligand-gated ion channel. It is comprised of 5 subunits, each with a large extracellular domain and 4 transmembrane domains (M1-M4), arranged around a central ion channel[35] (Figure 1-5A). There are two isotypes, fetal and adult, which differ in one subunit. The fetal AChR is composed of 2 α subunits and one each of β, γ, and δ, while in adult AChR the γ subunit is replaced by the ε subunit. Embryonic muscle expresses fetal AChR, while after innervation expression of the γ subunit is substituted by the ε subunit. Some adult muscle like the extraocular muscles continue to express fetal AChR[36]. AChR has two binding sites for acetylcholine, one located between the α and δ subunits, and the other between the second α subunit and the γ/ε subunit.

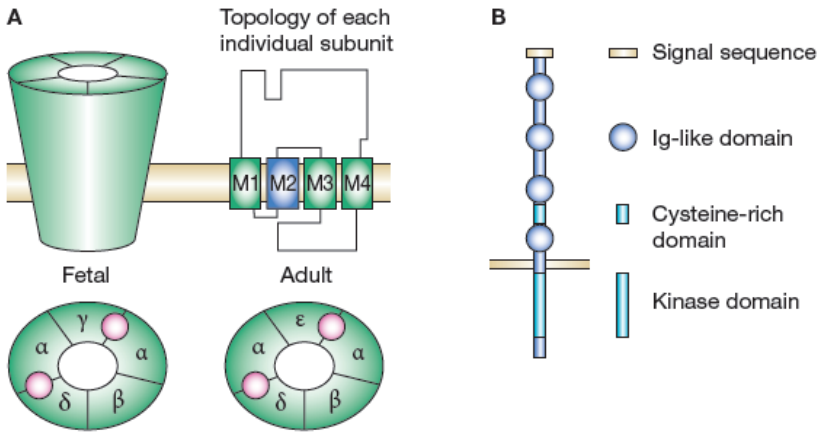

Figure 1-5 Structures of the acetylcholine receptor and muscle specific kinase. (A) The AChR is a 5-subunit transmembrane ion channel, with fetal and adult isotypes differing in one subunit. (B) MuSK has a single transmembrane domain with a large extracellular region of 4 Ig-like domains and an intracellular tyrosine kinase domain. Reprinted from Buckley and Vincent[35] with permission from Nature Publishing Group.

AChRs are densely clustered on the postsynaptic membrane folds through a pathway involving multiple proteins. During NMJ development, agrin released by the motor nerve terminal binds to low-density lipoprotein receptor-related protein-4 (LRP4), which then binds muscle specific kinase (MuSK) on the postsynaptic membrane[37, 38] (Figure 1-4). MuSK is a 110kDa postsynaptic single-pass transmembrane protein, with a large extracellular region consisting of four immunoglobulin-like domains and an intracellular tyrosine kinase domain[35] (Figure 1-5B). LRP4 binds to the first Ig-like domain of MuSK[39], leading to MuSK activation by dimerization and autophosphorylation[33]. This stimulates a signalling pathway involving Dok7[40], culminating in AChR-clustering by rapsyn. Rapsyn is a peripheral membrane protein expressed on the cytoplasmic side of the postsynaptic membrane and is required for anchoring and stabilizing the

AChRs at the postsynaptic membrane[41, 42]. Mice with MuSK, LRP4, or rapsyn knocked out fail to form AChR clusters during development[43, 44].

Neuromuscular transmission is initiated when an action potential travelling along the motor nerve axon reaches the nerve terminal and triggers the opening of voltage-gated calcium channels (VGCCs) on the presynaptic membrane. The influx of calcium ions triggers the release of acetylcholine stored in synaptic vesicles via exocytosis into the synaptic cleft[45]. The acetylcholine diffuses across the synaptic cleft and binds to the AChRs on the post-synaptic muscle membrane, opening the cation channels and causing an influx of sodium ions into the muscle fiber. This triggers a depolarization of the membrane called the endplate potential (EPP). The EPP activates voltage-gated sodium channels (VGSCs) in the muscle membrane, generating a muscle action potential. In normal NMJ transmission, the EPP is much larger than the threshold required for a muscle fibre action potential; this is referred to as the safety factor of neuromuscular transmission[46]. As the action potential spreads along the muscle, calcium channels are activated causing a rise in intracellular calcium concentration that leads to muscle contraction[7, 45]. The action of acetylcholine is terminated by being hydrolyzed by acetylcholinesterase within the synaptic cleft[7].

1.5.2 Pathophysiology of AChR antibodies in AChR-MG

The primary mechanism causing the clinical features of MG are pathogenic autoantibodies targeting the AChRs at the NMJ. About 85% of patients with generalized MG have detectable antibodies to AChR (AChR-MG)[47]. In MG patients who have purely ocular symptoms, the percentage who have detectable AChR-Abs is lower, at around 50%[48].

AChR-Abs are measured by radioimmunoprecipitation assay (RIPA) using solubilized human AChR labelled with ^{125}I-α-bungarotoxin (^{125}I-αBT). The AChR used is commonly extracted from the rhabdomyosarcoma cell lines TE671 (which expresses fetal AChR only)[49-51] and CN21 (a genetically modified cell line which expresses adult receptor)[52, 53]. This assay has proven to be highly specific and sensitive and of great diagnostic value. AChR-Ab positivity together with clinical symptoms can be considered a definite diagnosis of AChR-MG. In the absence of clinical signs, the presence of AChR-Abs indicates sub-clinical MG as in such cases the number of receptors at the NMJ is generally reduced and the NMJ safety margin can still be compromised.

The pathogenicity of AChR-Abs has been clearly demonstrated. Immunization of animals with AChR induces chronic experimental autoimmune myasthenia gravis (EAMG). This was first demonstrated by Patrick and Lindstrom[6], who induced MG in rabbits immunized with AChR from the electric organ of electric eels (*Electrophorus electricus*). EAMG has also been reproducibly induced in animals by injection of AChR antibodies, either of monoclonals (especially anti-MIR mAbs)[54] or passive transfer of purified IgG from patients' sera[48, 55]. Clinically, weakness in MG patients also improves following removal of circulating antibodies by plasmapheresis[56]..

A majority of AChR-Abs target a conformational-dependent extracellular epitope of the AChR alpha subunit, comprised of α67-76, called the main immunogenic region (MIR)[57, 58]. However they also bind to multiple other epitopes on all subunits, likely due to epitope spreading[59]. AChR-Abs induce a loss of functional AChR at the NMJ, leading to impaired neuromuscular transmission and muscle weakness and fatigue. There are three main mechanisms by which

AChR-Abs induce a loss of functional AChR: complement-mediated damage of the muscle endplate, antigenic modulation, and blocking of the acetylcholine binding site[60, 61].

Complement-mediated damage of the muscle endplate is probably the most important mechanism[62]. AChR-Abs are predominantly of the IgG1 and IgG3 isotype, and are therefore capable of activating complement[63, 64]. Triggering of the complement cascade results in lysis of the postsynaptic membrane by the membrane attack complex (MAC)[65]. This effect is intensified by AChR-Abs binding to AChR which is at high density on the postsynaptic muscle folds, which results in high density of Fc regions. Complement-mediated lysis by AChR-Abs results in morphological changes in the post-synaptic muscle membrane, most importantly a simplification of the folding pattern of the muscle membrane. This complement-mediated loss of endplate membrane not only results in a loss in the number of functional AChR, which decreases the EPP amplitude, but also in a loss of VGSCs which increases the threshold depolarization needed to produce a muscle fibre action potential, reducing the safety factor for neuromuscular transmission from both sides[66].

The second mechanism by which AChR-Abs induce a loss of AChR is antigenic modulation, whereby cross-linking of AChRs by the divalent antibodies (IgG1, IgG2, and IgG3) accelerates the internalization and degradation of AChRs[67, 68]. Membrane fragments containing AChR are internalized by endocytosis and degraded by lysosomal enzymes. Serum IgG from 90% of MG patients has been shown to increase the AChR degradation rate by 2-3 fold[69]. Antigenic modulation is also facilitated by the complement-mediated lysis that occurs as this alters the cytoskeletal structure of the postsynaptic membrane, facilitating AChR endocytosis[70]. This process results in a lowered density of AChR and lower sensitivity to ACh, thereby decreasing the amplitude of EPPs[71].

The third mechanism by which AChR-Abs impair the activity of AChRs is by directly blocking the ACh binding sites or the ion channel[72]. These type of blocking antibodies are usually present at low levels, however they may contribute to an acute myasthenia crisis[73], making them clinically important.

Reduction in the number of active AChR decreases the EPP, which although adequate at rest, when the release of ACh is reduced by repetitive activity of the muscle the EPP can fall below the threshold required to activate VGSCs and trigger an action potential (safety factor is reduced), resulting in neuromuscular transmission failure. This manifests clinically as muscle weakness and fatigue. Extraocular muscles are especially susceptible to myasthenic weakness because their NMJs have a lower degree of postsynaptic folding and therefore lower levels of AChR and VGSCs resulting a reduced safety factor, they have a higher neural firing frequency making them more fatiguable, and they are more susceptible to complement-mediated damage as they express lower levels of complement regulators[2]. This may explain why the majority of MG patients have ocular symptoms as their primary symptoms.

Titers of AChR-Abs are highly variable in MG patients and generally do not correlate well with disease severity[74-79]. However when examined within individual patients a decline in antibody titer is associated with clinical improvement in many cases, especially after immunosuppression and plasmapheresis[80-84]. Therefore, measuring AChR-Ab levels over the course of the disease may be useful as follow-up to treatment.

1.5.3 Pathophysiology of MuSK antibodies in MuSK-MG

Of the approximately 15% of generalized MG patients who do not have detectable AChR-Abs in their serum by RIPA, a variable proportion have antibodies to MuSK (MuSK-MG). Antibodies

against MuSK were first described in 2001 by Hoch *et al.*[85], who found MuSK-Abs in 70% of patients previously negative for AChR-Abs. Since then, MuSK-Abs have been reported worldwide in a variable proportion of AChR antibody-negative patients, with frequencies ranging from 0-64% depending on the ethnic group or geographic location[17, 86]. Like for AChR-Abs, the gold standard method for measuring MuSK-Abs is by RIPA, using ^{125}I-labelled MuSK.

Animals immunized with MuSK ectodomain have been shown to develop muscle weakness[87]. Passive transfer of IgG from MuSK-MG patients into mice also leads to muscle weakness in these animals[88], demonstrating their pathogenicity.

The mechanisms by which MuSK-Abs impair neuromuscular transmission, although not fully understood, appear to be quite different from AChR-Abs. Unlike AChR antibodies which are IgG1 and IgG3, MuSK antibodies are mainly of the IgG4 subclass which are functionally different as they are not complement activating[14, 89], suggesting MuSK-Abs have a different pathogenic mechanism than AChR-Abs. IgG4 antibodies also undergo a posttranslational Fab arm exchange, which produces an IgG4 molecule with two different antigen-binding sites, preventing the IgG4 from cross-linking identical antigens[90] and making them functionally monovalent. This suggests that the pathogenic mechanism of IgG4 MuSK-Abs is likely to be a direct effect on the function of MuSK, rather than the complement-mediated damage to the NMJ seen in AChR-MG. In fact, unlike in patients with AChR-Abs, studies of muscle biopsies in patients with MuSK-Abs have shown little loss of AChR density at the muscle endplate, and no substantial complement deposition or morphological damage[91]. This may however depend on the type of muscle biopsied, as MuSK-Abs appear to more commonly target facial and bulbar muscles, which cannot be biopsied. There was also no observed complement activation in both passive transfer and active immunization models of MuSK-MG in animals, and MuSK-MG still

developed in complement-deficient animals[92]. This evidence suggests that complement deposition is not a major pathogenic mechanism of MuSK-Abs, however in many patients MuSK-Abs of the IgG1 subclass are also found, which are capable of binding complement[93].

The pathogenic mechanisms of MuSK-MG may involve changes in the function and distribution of various elements of the NMJ. Cell culture experiments using the AChR-expressing rhabdomyosarcoma cell line TE671 found that some MuSK-Ab positive sera caused downregulation of AChR subunits and rapsyn, suggesting that MuSK-Abs may compromise AChR clustering, causing the NMJ to become structurally and functionally disorganized[94]. MuSK antibodies are specific for the extracellular domain, and *in vitro* studies have demonstrated that MuSK antibodies from MG patients inhibit agrin-induced AChR clustering in cultured myotubes[85], indicating MuSK-Abs may interfere with MuSK function.

Taken together, the many differences between MuSK-MG and AChR-MG suggest that MuSK-MG have different etiology and pathogenic mechanisms. Although the pathological mechanisms of MuSK-Abs at the mature NMJ have not yet been fully elucidated, it is clear that they are clinically relevant. Studies have shown that there is a correlation between MuSK-Ab levels and disease severity, both in individual patients and in the population as a whole[95]. Studies on the longitudinal relation between disease severity and titers of MuSK-Abs have also shown that MuSK-Abs IgG4 titers, and not IgG1, significantly correlated with disease severity, emphasizing the important role of IgG4 antibodies in the pathogenesis of MuSK-MG[96].

1.5.4 Seronegative MG

MG patients who do not appear to have anti-AChR or anti-MuSK antibodies by standard radioimmunoprecipitation assay are often referred to as having seronegative myasthenia gravis

(SNMG). Prior to the discovery of anti-MuSK antibodies SNMG was a term used for patients who had AChR antibody-negative MG, but will be used here to describe patients who are seronegative for both AChR and MuSK antibodies.

Despite not having detectable antibodies, the fact that SNMG patients respond to immunosuppressive treatment and plasma exchange show they have an antibody-mediated disease[97]. Increasing evidence shows that SNMG patients have more similarities to AChR-MG patients than MuSK-MG patients in terms of clinical features, thymic pathology, and response to immunosuppressive treatments and plasma exchange[13-15, 17-19, 93, 98, 99]. Thymic histology in these patients show lymph node type infiltrates similar to lymphoid follicular hyperplasia in AChR-MG[12, 19]. Muscle biopsies also show loss of AChR and complement deposition, similar to what is seen in AChR-MG and in contrast to MuSK-MG[91].

The similarities between SNMG patients and AChR-MG may be explained by these patients having very low affinity antibodies to AChR not picked up by conventional RIPAs which use solubilized AChR. Immunofluorescence and flow cytometry studies by Leite *et al.*[93] found low affinity antibodies that bound to AChRs when the receptors were clustered by rapsyn on the surface of transfected cell lines in 66% of sera from patients with MG who were previously antibody-negative on conventional RIPA. These antibodies were of the IgG1 subclass and induced complement deposition, supporting their pathogenic role. Furthermore, there was a correlation between antibodies binding to clustered AChR and thymic pathology[93]. This suggests that autoantibodies in SNMG patients do target AChR but bind only to AChR when it is densely clustered, explaining why they are antibody-negative by RIPA.

While low affinity antibodies explain many cases of apparent SNMG, there still appears to be a proportion of patients who remain seronegative. These patients could have antibodies targeting other NMJ components besides AChR and MuSK.

1.5.5 Other autoantibodies

Antibodies against other proteins at the NMJ and in muscle, as well as antigens outside of muscle, have been found in MG patient. However, whether these antibodies contribute to the pathogenesis of MG or are non-specific (as many of them are also found in other autoimmune disease) needs to be determined[100].

Most recently, a group of studies reported lipoprotein-related protein-4 (LRP4) to be a potential new autoantigen specific to MG[101-106]. As described above, LRP4 is a receptor for agrin, and is required for AChR clustering through its activation of MuSK during NMJ development. Three studies using various techniques found that the presence of anti-LRP4 antibodies in SNMG patients (negative for both AChR-Abs and MuSK-Abs) ranged from 3.3% to as high as 50%[101, 104, 106]. No AChR-MG patients were found to have LRP4 antibodies, however 2.8-10.7% of MuSK-MG patients had LRP4 antibodies of low titers[101, 106]. AChR antibodies and LRP4 antibodies therefore appear to be mutually exclusive, while a small proportion of MuSK-MG patients can also have LRP antibodies. LRP4 antibodies were found to inhibit binding of LRP4 to agrin and were predominantly of the IgG1 subclass, therefore able to activate complement[101]. Hence LRP4 antibodies could potentially exert a pathogenic effect at the NMJ. In the overall picture of MG, patients with LRP4 antibodies are rare, and their potential contribution to MG pathogenesis needs to be further studied, especially in patients with low titers.

In addition to LRP4 antibodies, there are also a range of antibodies found in MG patients against other muscle proteins, such as actin, myosin, α-actinin, titin, rapsyn, and ryanodine receptor[48]. Detection of some of these antibodies can be helpful in diagnosing paraneoplastic-associated MG, for example anti-titin and anti-ryanodine-receptor antibodies are detected in 95% and 70% of MG patients who have thymoma[107]. Combined testing of these antibodies gives the high sensitivity and specificity for detecting thymoma in MG patients.

1.6 Disease etiology

The precise etiology of the autoimmune response in MG is not known, but abnormalities of the thymus (hyperplasia and thymoma) likely play an important part, along with genetic predispositions.

1.6.1 Role of the thymus and thymic pathology in MG

About 80% of early-onset AChR-MG patients have thymic lymphoid follicular hyperplasia (LFH), characterized by B lymphocyte infiltrates and germinal centers, which are sites of intense B cell response typical of lymph nodes[12]. Thymoma is present in about 10% of MG patients, usually between the ages of 40-60, and 30-60% of thymomas are associated with MG[108]. There is increasing evidence for these pathological changes of thymus gland being are involved in the initiation of the autoimmune response in MG.

Hyperplastic thymuses from MG patients contain all the components necessary for developing an immune response to the AChR. They contain AChR-specific T cells[109], and AChR-Ab producing B cells and plasma cells in the lymphoid follicles and germinal centers[110]. In the thymic medulla there are also muscle-like myoid cells that express several muscle proteins, among them

AChR[111]. Besides muscle, myoid cells are the only cells known to express whole AChR in its native conformation, especially of the fetal isotype which is preferentially recognized by autoantibodies in many early-onset MG patients[111]. Myoid cells themselves are unable to present antigen to $CD4^+$ T cells, but they are surrounded by clusters of professional antigen-presenting cells (eg. dendritic cells) which can present AChR from myoid cells to the surrounding T cells[112]. Cultures of thymic lymphocytes also produce AChR-Abs[113, 114]. Also, transplantation of MG thymic tissue into mice with severe combined immunodeficiency (SCID) induces AChR-Ab production and deposition at the muscle end plate[115]. Together this evidence supports the theory of intrathymic pathogenesis and involvement of the hyperplastic thymus in the primary sensitization to muscle antigens in early-onset MG. Late-onset MG patients typically do not have thymic abnormalities, so the role of the thymus in these patients is not as clear[7].

In thymoma MG patients, epithelial cells of the thymoma express AChR subunit, titin-like, and ryanodine receptor-like epitopes, but not the intact proteins[116]. All thymoma MG patients have AChR-Abs, and frequently antibodies against titin[117] and the ryanodine receptor[118], supporting the role of thymoma in the pathogenicity of MG. Thymomas also have a large number of autoreactive T cells[119]. Negative selection of T cells within a thymoma appears to be defective, resulting in autoreactive T cells to be falsely selected for and sent to the periphery, where they are activated by an unknown mechanism and help stimulate antibody-producing B cells, even after thymectomy[120]. Destruction of the postsynaptic membrane, particularly complement-mediate damage, may provide a continuous source of antigen for the stimulation of the autoreactive T and B cells[48]. Deficiency in the expression of the autoimmune regulator gene (AIRE) and loss of regulatory T cells may contribute to the impairment of the negative selection process[121, 122].

MuSK-MG patients have minimal thymic histological changes[18, 19], arguing against intrathymic pathogenesis in these patients.

1.6.2 Genetic factors

MG is associated with several genes, the most important being the human leukocyte antigen (HLA) genes, which encode the major histocompatibility complex (MHC). Different HLA genes appear to correlate with the various MG subtypes, suggesting different genetic factors may be associated with the development of the different subtypes. Early-onset MG with thymic hyperplasia and AChR-Abs is strongly associated with the HLA-DR3 and HLA-B8 alleles[123, 124], while late-onset MG appears to be weakly associated HLA-DR2 and B7[124]. In Chinese and Japanese MG patients, there is a higher frequency of HLA-DR9 and HLA-DRw13[125, 126]. Ocular MG in Chinese patients is also associated with HLA-Bw46 and DR9[125], where up to 30% of patients in this population present during childhood[123]. In MuSK-MG patients, an associated is reported with HLA-DR14-DQ5[127]. There have also been several non-HLA genes found to be associated with MG, the most interesting being the *CHRNA1* gene, which encodes the AChR alpha subunit[128]. Monozygotic twins are also at increased risk of concordance[108], and there are cases where more than one family member has MG[129].

1.6.3 Other factors

Vitamin D deficiency may be a risk factor in MG, as seen in other autoimmune diseases like lupus and multiple sclerosis. One small pilot study found vitamin D deficiency in MG patients compared to controls, and that when supplemented with vitamin D there was a 38% improvement in MG composite scores used to assess fatigue[130]. However larger studies are needed as there could be confounding factors. There is also the theory that a viral infection

contributes to the pathogenesis of MG, particularly an intra-thymic infection of the Epstein-Barr virus, however the evidence so far is debatable[131, 132].

1.7 Diagnosis of MG

1.7.1 Edrophonium (Tensilon®) test

The edrophonium (or Tensilon®) test is a test that can be administered at the bedside for diagnosis of MG. Edrophonium is an effective short-acting acetylcholinesterase inhibitor, improving muscle weakness by blocking the enzymatic action of acetylcholinesterase at the NMJ. This prolongs the presence of acetylcholine in the synaptic cleft, helping to increase the amplitude and duration of the EPP[7]. During this test edrophonium is injected intravenously and the patient is observed for increased muscle strength, most reliably seen by improvement of ptosis or extraocular weakness[133]. This test is reported to have a sensitivity of 71.5-95% for generalized myasthenia gravis[133].

1.7.2 Ice pack test

The ice pack test is a non-pharmacological test that can also be administered at the bedside. This is a test that is used only when assessing ptosis, and is based on the principle that the optimal temperature at which acetylcholinesterase functions is 37^{o}C. In this test, an ice pack is placed over the affected eye for 2-5 minutes and the eye is then examined for improvement in ptosis[134, 135]. Improvement is due to the cold temperature increasing the amount of ACh at the NMJ by impairing the activity of acetylcholinesterase, providing evidence that the ptosis is due to a deficit of the NMJ.

1.7.3 Electrophysiological tests

1.7.3.1 Repetitive nerve stimulation

Repetitive nerve stimulation (RNS) is an electrophysiological test used to assess neuromuscular transmission. In disorders of the NMJ, repetitive electrical stimulation of the motor nerve (2-5 Hz) produces a decrease or decrement in the amplitude of the muscle action potential[7]. The quantal content of ACh decreases during repetitive stimulation, which is not a problem in normal NMJ due to the large safety factor, but because of the reduced sensitivity to ACh in AChR-MG this leads to a greater rate of neuromuscular transmission failure[45]. A decrement by at least 10% is characteristic of neuromuscular transmission deficit. RNS is abnormal in about 75% of patients with generalized MG and in <50% of patients with ocular MG. The choice of muscle tested is therefore critical for usefulness in diagnosis[135].

1.7.3.2 Single-fiber electromyography

Single-fiber electromyography (SFEMG) is an electrophysiological test that is used to measure neuromuscular jitter. A special needle electrode is used to identify action potentials from individual muscle fibers. The action potentials of two muscle fibers innervated by the same motor axon are simultaneously recorded. Jitter refers to the variability in time between the action potential of the first relative to the second. In MG, reduced sensitivity to ACh results in variations in the time between when a motor nerve is stimulation and the muscle action potential is generated, increasing jitter[45]. When the appropriate muscles are tested, SFEMG reveals abnormal jitter in 95-99% of MG patients[136, 137]. However, although SFEMG is highly sensitive, it is not specific for MG. It can also be abnormal in other disease of the NMJ, like Lambert-Eaton myasthenic syndrome, or other muscle diseases, like amyotrophic lateral sclerosis or polymyositis[138].

1.7.4 Immunological testing

Antibody testing is critical for the diagnosis of MG not only because the presence of antibodies (AChR-Abs or MuSK-Abs) is a diagnostic biomarker, but identifying the serological MG subtype can help tremendously with disease management and therapy. As mentioned throughout this thesis, the most common autoantibody MG patients have are anti-AChR antibodies, which are detected by radioimmunoprecipitation. Immunological testing for AChR-Abs is highly specific, with AChR-Ab positivity proving the diagnosis. However, AChR-Ab negativity does not rule out an MG diagnosis. The sensitivity of the test is approximately 85% in patients with generalized MG, and about 50% for ocular MG[47, 139]. Patients may also be falsely negative if they have had immunosuppression or if the test is done very early in the disease[140]. Patients may also have low affinity antibodies not detectable by RIPA, but only by binding to clustered AChR in a cell-based assay[93], however this is not a test that is currently available for diagnostic purposes. MG patients who are anti-AChR antibody negative should be tested for anti-MuSK antibodies. Also testing for other antibodies such as anti-titin or anti-ryanodine-receptor antibodies can help with the detection of a thymoma[141].

1.7.5 Imaging

In MG, abnormalities of the thymus (lymphoid follicular hyperplasia or thymoma) are frequent. Chest CT or MRI scans are performed in MG patients to evaluate the size of the thymus and detect if the patient has thymoma[7].

1.8 Management and treatment of MG

Management of MG depends in part on the clinical subtype of the patient, and is individualized according to the severity and characteristics of a patient's disease. There are two approaches to treating MG. The first is symptomatic therapy, which involves the use of acetylcholinesterase inhibitors. The second is treating the autoimmune process, using either short-term immune therapies (plasmapheresis or intravenous immunoglobulin therapy) or a variety of long-term immune therapies. Surgical intervention is also used in the form of thymectomy. Special attention is needed in the case of an acute attack (myasthenic crisis), as this is a life-threatening condition.

1.8.1 Acetylcholinesterase inhibitors

Acetylcholinesterase inhibitors are the first-line treatment for MG patients. Acetylcholinesterase inhibitors act by increasing the amount of acetylcholine available for binding at the NMJ by inhibiting the enzymatic action of acetylcholinesterase, thereby improving neuromuscular transmission[142]. They are used purely as symptomatic therapy and do not have an effect on disease progression. Acetylcholinesterase inhibitors rarely completely eliminate MG symptoms, however in milder cases, especially in patients presenting with only ocular symptoms, they may be used as long-term treatment[7]. Oral pyridostigmine bromide (Mestinon®) is the most widely used acetylcholinesterase inhibitor. Pyridostigmine has a rapid onset of action within 15-30 minutes, reaching peak within 2 hours[138]. The oral dose can be up to 60mg five times a day[143], but dosing can vary over time based on the patient's response and disease progression, and in an effort to maximize clinical improvement while minimizing side effects. Response to acetylcholinesterase inhibitors is poorer in patients with MuSK-MG[15, 144].

Acetylcholinesterase inhibitors can have a number of side effects due to the increased concentration of acetylcholine at both nicotinic and muscarinic synapses. Common muscarinic side effects are abdominal cramps, diarrhea, increased salivation and bronchial secretions, nausea, sweating, and bradycardia[143]. Nicotinic side effects include muscle fasciculation and cramping[138, 145]. Some caution is also needed when prescribing acetylcholinesterase inhibitors to MG patients with MuSK antibodies as some of these patients may have increased sensitivity to acetylcholine[146].

1.8.2 Short-term immune therapies

Two short-term immune therapies, plasmapheresis and intravenous immunoglobulin, are used more often for the treatment of acute symptoms and myasthenic crisis, where rapid improvement is necessary.

1.8.2.1 Plasmapheresis

Plasmapheresis, or plasma exchange (PLEX), is one of the short-term immune therapies, used to treat MG exacerbations and life-threatening myasthenic crises, situations where rapid clinical response is required[81, 147, 148]. PLEX improves weakness by directly reducing the concentration of pathogenic antibodies from the circulation. The procedure involves drawing blood, separating the components via centrifugation, and after discarding the serum containing the antibodies re-injecting the blood cells with human albumin. Typically an exchange is done every other day, up to 4-6 times[7]. Clinical response is rapid in most patients, usually occurring within 2-3 days. However improvement rarely persists for more than 4-10 weeks and de novo increase in antibody secretion is often seen; PLEX is therefore used together with immunosuppressive therapies[147]. In addition to treating an acute myasthenic crisis, the short-term benefits of plasmapheresis are also useful in strengthening patients pre-operatively before thymectomy or

other surgical procedures and during the post-operative period, and in cases of symptom worsening during tapering of immunosuppressive therapy[143, 147].

The effectiveness of plasmapheresis was not only shown with AChR antibody positive MG, but also in patients with no detectable AChR antibodies, indicating that a circulating serum component was also present in these cases (this was prior to discovery of anti-MuSK antibodies)[147]. It was therefore useful in diagnosis SNMG. Plasmapheresis is highly effective for MuSK-MG patients, with studies reporting improvement in up to 93% of these patients[16].

Side effects for plasmapheresis can include hypotension, paresthesias, infections or thrombotic complications from venous access, and bleeding tendencies due to removal of coagulation factors[7]. Continued development of this technique, particularly in the use of immunoadsorption columns with immobilized AChR for selective removal of anti-AChR antibodies[149, 150], may provide safer and more efficient apheresis therapies.

1.8.2.2 Intravenous immunoglobulin therapy (IVIg)

Several randomized clinical trials have provided evidence on the effectiveness of intravenous immunoglobulin (IVIg) in treating worsening MG symptoms[151-153]. IVIg involves administrating immunoglobulins isolated from pooled human plasma at doses up to 1-2g/kg over a period of days[138, 151]. A randomized study comparing IVIg to PLEX found IVIg and PLEX have comparable efficacy and are equally tolerated in adult patients with moderate to severe MG[154]. However, most studies report that in MuSK-MG PLEX is more effective than IVIg[144], with one study of two large cohorts showing 61% of MuSK-MG patients improving with IVIg compared to 93% improving with PLEX[16].

The mechanisms by which IVIg improves weakness are complex, likely involving competition with autoantibodies and interference with Fc-receptor binding on macrophages[155]. IVIg may also reduce the concentration of specific autoantibodies at the NMJ by increasing the total concentration of circulating IgG. Serious side effects of IVIg are rare, although some milder side effects do occur relating to the large volumes and viscosity of the infusions, including vasomotor symptoms, headache, allergic reactions, rash, and leukopenia (decrease in leukocyte number)[156].

1.8.3 Long-term immune therapies

Most patients whose symptoms are not being well controlled with acetylcholinesterase inhibitors alone or who are not in remission are usually treated using some form of long-term immune therapy[142]. The goal of long-term immune therapies is to induce remission or near remission and maintain it. Because of the limitations in designing clinical trials for an uncommon disease like MG, most of the therapeutic recommendations for MG are based on either small, randomized controlled trials, or anecdotal observations[7].

1.8.3.1 Corticosteroids

Corticosteroids are the most commonly used immunosuppressant medications in MG. Although no formal clinical trial has been conducted, prednisone has been the corticosteroid of choice for treating MG over many decades of clinical practice[148]. In four large studies of prednisone therapy, 73.8% of the total 422 patients with generalized MG patients that were studied were reported to have marked improvement or remission (ranging from 63.4%-81.7% in the individual studies)[157-160]. The mechanism of action of corticosteroids is complex and may include a reduction in lymphocyte proliferation and differentiation, changes to cytokine expression, and inhibition of macrophages or other antigen-presenting cells[2].

Prednisone is used when the symptoms of MG are not being adequately managed by acetylcholinesterase inhibitors alone. Prednisone is commonly administered starting at a high dose, followed by a gradual tapering down to the lowest dose that still maintains a positive response without use of acetylcholinesterase inhibitors[7]. However in many cases starting corticosteroid treatment rapidly at a high dose can induce a temporary exacerbation[160]. Plasmapheresis or IVIg are used to manage exacerbations, and in cases where the patients already have respiratory weakness plasmapheresis can be given before initiating steroid treatment[7]. Another option to lower the risk for exacerbations is starting at a low dose (eg. 10-25mg), then increasing the dose (eg. to 60-100mg) until maximum improvement is reached, and then tapering[161].

Although highly effective, treatment with chronic corticosteroids is often associated with significant side effects, including fluid (sodium) retention, hypertension, weight gain, potassium loss, osteoporosis, and impaired glucose tolerance[162].

1.8.3.2 Azathioprine (Imuran®)

Although corticosteroids such as prednisone form the foundation of MG treatment, their extensive list of side effects can limit their use. A variety of immunosuppressive therapies are therefore used as steroid-sparing medications, generally used alongside prednisone to limit the dose of prednisone a patient has to be on. These immunosuppressive therapies are generally started soon after corticosteroid therapy is initiated as their effect is delayed.

One of the well-established immunosuppressive therapies used in MG is azathioprine (Imuran®)[97, 163, 164]. Azathioprine, a purine analogue, inhibits DNA synthesis, thereby inhibiting T-cell and B-cell proliferation and suppressing autoimmunity[138]. Azathioprine is effective in 70-

90% of MG patients[7, 138, 165]. However the clinical effect of azathioprine is delayed until after 3-6 months, with maximum effect occurring after 1-2 years[148].

Azathioprine is often used in conjunction with prednisone, especially initially as it has a long onset of action[148]. Although no randomized placebo-controlled trial of azathioprine has been performed, a multicenter randomized double-blind study of 34 MG patients comparing prednisone (on alternate days) combined with azathioprine (2.5mg/kg) versus prednisone alone (on alternate days, combined with placebo), found treatment with prednisone plus azathioprine to be superior[166]. In the prednisone plus azathioprine group, the prednisone dose was lower after two and three years and incidence of side effects were lower, while higher AChR antibody levels, relapses and a failure of remission were more frequent in the prednisone plus placebo group[166]. Use of azathioprine alongside alternate day prednisone as a steroid-sparing agent allows for patients to be maintained on a lower dose of prednisone, which results in fewer side effects and longer remission periods. MG patients with MuSK antibodies are also generally well-controlled using azathioprine plus prednisone, but many can still be left with permanent facial or bulbar weakness[167].

Side effects of azathioprine include hepatotoxicity and leukopenia (decrease in blood leukocyte levels)[168], but these can be monitored for and are reversible[7]. Levels of lymphocytes and other leukocytes should be monitored regularly and dosage adjusted accordingly to reduce risk of infection, and liver enzymes can also be monitored for liver function[148]. Long-term use of azathioprine may also increase risk of certain cancers, such as lymphoma[169-171].

1.8.3.3 Mycophenolate mofetil (CellCept®)

Mycophenolate mofetil (CellCept®) is an immunosuppressive therapy which inhibits purine synthesis, thereby suppressing T-cell and B-cell proliferation.[172]. It is a prodrug of mycophenolic acid, an inhibitor of inosine monophosphate denydrogenase, an enzyme involved in purine synthesis[172].

Initial clinical efficacy of mycophenolate mofetil in MG was demonstrated in two case series of 32 and 12 MG patients[173, 174] and a retrospective analysis of 85 patients[175]. A double-blind placebo-controlled pilot study of suboptimally controlled stable MG also suggested greater improvement in patients treated with mycophenolate mofetil compared to placebo[176].

However, two clinical trials of mycophenolate mofetil failed to confirm a positive effect[177, 178]. One trial comparing treatment with mycophenolate mofetil plus 20mg/day of prednisone to 20mg/day prednisone alone as initial therapy did not find any difference after 12 weeks[177]. Another trial assessing mycophenolate mofetil as a steroid-sparing agent failed to show benefits over placebo in maintaining control on MG during 36 weeks of prednisone tapering[178]. These studies may have failed to show effect either due to their short duration, better than anticipated response to the low dosage of prednisone, or the mild disease status of the patient populations studied [179], or the therapy may be less effectively than previously thought. Even with these negative results, mycophenolate mofetil continues to be used in MG treatment, particularly of a mild form.

1.8.3.4 Cyclosporine A (Neoral®)

Cyclosporine inhibits the synthesis of interleukin 2 (IL-2) and other cytokines essential to helper $CD4^+$ T cell proliferation and activity[7]. A small, randomized, placebo-control trial showed

cyclosporine to be effective in improving strength and reducing antibody titer[180]. In another retrospective study clinical improvement on cyclosporine was reported in 96% of patients, and it was also shown to be an effective steroid-sparing agent[181]. Side effects are common, including hypertension, nephrotoxicity, gum hyperplasia, hirsutism, and increased risk of malignancy[7]. In one study, 35% of patients discontinued therapy within 18 months, 10% due to nephrotoxicity[180]. Due to the high rate of side effects cyclosporine is a second-choice immunotherapy, usually used if patients are not responding to or are having side effects with azathioprine[148].

1.8.3.5 Tacrolimus (FK506)

Tacrolimus has a similar mechanism of action as cyclosporine, inhibiting the proliferation of T cells, but it also appears to act on ryanodine receptors to modulate calcium release from the sarcoplasmic reticulum of muscle[148, 182]. Efficacy of tacrolimus is supported by several studies[183-185]. Tacrolimus also appears to have less nephrotoxicity than cyclosporine[7]. However, more controlled trial data is needed.

1.8.3.6 Rituximab

Rituximab is a monoclonal antibody against the CD20 B cell surface marker[186]. It was first approved for treatment of B-cell lymphoma (non-Hodgkin's lymphoma), but being an anti-B cell therapy it also began being used off-label in various autoimmune and immune-mediated diseases like systemic lupus erythematosus and rheumatoid arthritis[186].

Various studies have now also shown rituximab to be effective in treating refractory AChR-MG and MuSK-MG, particularly in patients that do not respond well to other immunosuppressive therapies. Rituximab appears to be most beneficial in treating MuSK-MG, bringing about

marked improvement of severe symptoms, and in many cases clinical remission, in treated patients[187-191].

Side effects of rituximab can include fever, rigours, nausea, and hypotension. The most severe risk is progressive multifocal leukoencephalopathy (PML), however the risk is low[191].

1.8.3.7 Cyclophosphamide (Cytoxan®, Procytox®)

Cyclophosphamide, administered either orally or intravenously, can be effective in treating MG [192]. However, it has a variety of potentially severe side effects, including bone marrow suppression, hair loss, nausea, vomiting, anorexia, and skin discoloration[2]. Cyclophosphamide is therefore usually only considered in patients with severe refractory MG or who develop strong side effects to treatment with corticosteroids or other immunosuppressants.

1.8.4 Thymectomy

Thymectomy has been used for the treatment of MG for over 75 years, its use starting based on empirical evidence of improvement in MG patients[193]. Its use as a therapy is supported by the frequent presence of thymic pathology in MG patients. However, there is a lack of randomized controlled trials on the efficacy of thymectomy. An analysis by the American Academy of Neurology of retrospective non-randomized studies concluded that while there generally were higher remission and improvement rates in thymectomy patients versus non-thymectomy patients, these studies were confounded by important baseline and other differences between the two groups of patients[194, 195]. Patients in the surgical groups were younger, more often women, and also more likely to have severe symptoms[195]. In addition the studies differed in patient selection, surgical approaches, how remission and improvement was defined, and what methods were used to analyze results[196].

Currently, clinical indication of a thymectomy is only absolute for patients who have a thymoma. For non-thymomatous patients, the benefit of thymectomy is not conclusive. However, thymectomy is still often used as a therapeutic option in non-thymomatous patients to increase the probability of remission, more frequently in those with AChR-Ab positive generalized MG with early-onset disease onset (below 50-60 years of age)[143]. Thymectomy appears to be less beneficial in MuSK-Ab positive MG patients[15, 17], likely due to these patients usually lacking the abnormal thymic histology that characterize AChR-Ab positive patients.

To try and solve some of the issues, a prospective, randomized, controlled clinical trial is currently underway, called the MGTX trial, to try to resolve whether thymectomy reduces corticosteroid requirements in patients with generalized AChR-Ab positive MG[197].

1.8.5 Management of myasthenic crisis

A myasthenic crisis is a life-threatening severe respiratory muscle weakness that necessitates intubation for ventilator support or airway protection[11]. Plasmapheresis is the therapy of choice for a crisis due to its rapid onset of action. High dose prednisone is also included to maintain a longer therapeutic effect as plasmapheresis is not long-acting[7]. The length of intubation time varies and there are some predictors of prolonged incubation; mortality is often due to medical comorbidities[11].

1.9 Study objectives and rationale

In this chapter we've shown that MG patients are a very heterogenic population in terms of clinical presentation, antibody profile, severity, disease progression, treatment regimen and response to treatment. The most complex part of this illness seems to be the variety of

immunosuppressive therapies that are prescribed and the equal variety in the clinical response and side effect profile of these patients. There is a need for clinical biomarkers that could be used alongside clinical evaluations in predicting treatment response and clinical outcome, in order to help with a patient-specific approach to disease management[198].

What is common among MG patients is that they have a disease mediated by pathogenic autoantibodies. The measurement of AChR-Abs and MuSK-Abs already serves as an excellent diagnostic biomarker for MG. It is known that over the course of an immune response, antibody parameters like titer, isotype/subclass, and affinity change, and that these parameters influence the pathogenicity of autoantibodies. Autoantibodies in serum are a heterogeneous mix comprised of different isotypes and affinities, and from one patient to the next the antibody types that are dominant will differ and likely influence disease severity. Although studies have been done to characterize AChR-Ab and MuSK-Ab isotypes and determine if correlations exist between antibody titer to disease severity, they have not addressed the temporal changes in these characteristics, especially with regards to antibody affinity. The hypothesis of this thesis is that tracking changes in titer, affinity, and IgG subclass of autoantibodies in MG may help in predicting disease exacerbations, treatment response, and therefore prognosis.

In order to measure these temporal changes in antibody characteristics we needed a robust assay system that we could use to easily and rapidly measure these characteristics. Previous studies have typically used RIPA and ELISA to measure antibody titer and evaluate isotype, however these types of immunoassays are limited to detecting antibodies of high affinity and using them to measure antibody affinity is cumbersome and impractical. We therefore elected to use the Biacore™ biosensor system, which can be used to monitor antibody-antigen interactions in real-time, to develop assays to characterize autoantibodies in MG.

In this thesis, the focus is on characterizing MuSK antibodies, but preliminary studies with AChR antibodies are also presented. The primary objectives of my thesis were to (1) develop a Biacore™ assay to measure and characterize MuSK antibodies in serum, and (2) use this assay system to evaluate temporal changes of MuSK-Ab titer, isotype/subclass, and affinity in serial serum samples from a series of MuSK-MG patients. The secondary objective was to conduct preliminary studies in developing a Biacore™ assay for detecting AChR antibodies in serum, specifically how AChR may be immobilized onto a sensor chip in its membrane-bound native conformation.

Chapter 2: A biosensor-based assay for measurement and characterization of MuSK antibodies in myasthenia gravis patients

2.1 Introduction

2.1.1 Chapter Introduction

Antibodies against muscle specific kinase (MuSK) were first identified in 2001 in a proportion of MG patients who were previously identified as having "seronegative" MG, or no detectable AChR antibodies[85]. MuSK is a 110kDa single-pass transmembrane protein expressed at the post-synaptic membrane of the neuromuscular junction, where it co-localizes with and is essential for AChR clustering[199]. MG patients with MuSK antibodies (MuSK-MG) have emerged as a distinct clinical entity from patients with AChR antibodies (AChR-MG), with differences in clinical presentation and response to treatment.

Measurement of MuSK antibodies is a critical diagnostic test for separating MuSK-MG from AChR-MG. The current gold-standard method for measuring MuSK antibodies is by radioimmunoprecipitation (RIPA), using ^{125}I-labelled MuSK. Serum is incubated with ^{125}I-MuSK, followed by precipitation of MuSK antibodies with anti-human IgG. Precipitates are centrifuged, washed and counted using a gamma counter. While measurement of MuSK antibodies is an excellent diagnostic biomarker for MuSK-MG, a more in depth profiling of MuSK antibodies in MG patients could aid in better understanding of the pathophysiology of these antibodies. For example, it is already known that MuSK antibodies are predominantly of the IgG4 subclass, in contrast to AChR antibodies which are predominantly IgG3 and IgG1, indicating a different pathogenic mechanism[96].

The hypothesis of this thesis is that in the titer, isotype/IgG subclass, and affinity of autoantibodies in MG (both anti-AChR and anti-MuSK) change over the course of the disease, due to processes like affinity maturation, and that tracking these parameters may be useful as biomarkers for predicting disease exacerbations and treatment response. The goal of this chapter was to measure these variables in serial serum samples from MuSK-MG patients, and examine how they change over the course of the disease.

To measure and characterize MuSK antibodies, a suitable method was needed. Although typical immunoassay methods like RIPA and ELISA have been used for characterization of MuSK antibody IgG isotype[14, 96] and affinity[14], these assays are time-consuming and have limitations. Due to the multiple incubation and washing steps only antibodies of high affinity are measured. Also with RIPA usually only antibodies of the IgG isotype can be detected due to the use of secondary anti-IgG for immunoprecipitation.

In this chapter, we present the development and optimization of a novel biosensor (Biacore™) assay for measuring MuSK antibodies in serum and characterizing them in terms of isotype, IgG subclass, and dissociation rate (as an indicator of binding affinity). Biacore technology uses the principle of surface plasmon resonance (SPR) to monitor biomolecular interactions in real-time (for more detail see section 2.1.2). This type of assay platform was chosen because it enables monitoring of the entire antibody-antigen interaction, something not provided by typical end-point immunoassays. Biacore assays can be used to more easily analyze a full scope of immune response parameters, including binding, concentration, specificity, kinetics, affinity, binding epitope, and immunoglobulin class and subclass. Furthermore, Biacore assays detect and characterize all types of immune responses, including transient ones producing low-affinity antibodies with fast off-rates which are usually missed by typical immunoassays, providing a

more thorough characterization of the entire immune response, not only of stable high affinity antibody responses.

In this chapter we start out by presenting the development and optimization of this assay. Briefly, the assay involves immobilization of MuSK onto a sensor chip surface, over which diluted serum is injected and binding of MuSK antibodies detected. An analysis of MuSK antibody binding levels, isotype and subclass determination, and dissociation rate measurements of serial samples of 19 MuSK-MG patients is subsequently presented. Finally, we present a case study of one MuSK-MG patient treated with the anti-CD20 therapy rituximab, to demonstrate how monitoring antibody parameters over the disease course can help in a clinical setting with assessing clinical outcome of patients.

2.1.2 Biacore™ technology

Biacore instruments are biosensors that utilize the optical phenomenon of surface plasmon resonance (SPR) to monitor biomolecular interactions in real-time. In Biacore systems, molecular interactions are monitored on a removable sensor chip. The basic principle is that one of the binding partners is attached (immobilized) to the surface of the sensor chip, while the other partner is injected in a continuous flow of solution over the sensor chip surface. The binding partner immobilized on the chip is called the ligand, and the partner in solution is called the analyte. Unlike other immunoassays the Biacore SPR system is label-free, not requiring the use of enzymatic, fluorescent, or radioactive labelling of the binding partners or any secondary detector molecules. Biacore experiments can be designed to measure a range of interaction

characteristics, such as binding (yes/no), kinetics, affinity, specificity, and sample analyte concentration, thereby helping to understand the entire dynamics of an interaction.

Biacore system

There are three main components to a Biacore system: the sensor chip, the optical system, and the microfluidic and liquid handling system. The sensor chip surface is the site of the biomolecular interactions, while the optical system detects the changes in SPR signal brought about by binding events. A series of pumps and an integrated microfluidic cartridge (IFC) precisely deliver buffer and samples to the sensor surface, at volumes as low as a few microliters. The IFC consists of a series of micro-channels which form flow cells on the sensor surface when pressed against it (in the Biacore 3000^{TM} series, there are four flow cells per chip). The Biacore is a continuous flow system, when sample is not being injected a running buffer is continuously flowing over the sensor surface.

SPR phenomenon and sensorgrams

Biacore uses SPR to detect biomolecular interactions in real-time. SPR is an optical phenomenon that occurs on a thin conducting film at the interface between two mediums of different refractive indexes. In Biacore systems, the conducting film is a thin gold coating on the sensor chip surface, sandwiched between the glass layer of the chip and the solution flowing through the IFC.

Light of a fixed wavelength is focused on the back of the sensor chip, as shown in Figure 2-1. At a certain angle of incidence, electrons in the gold film are excited, resulting in the formation of electron charge density waves (surface plasmons), and a drop in the intensity of reflected light. As analyte binds to the ligand, the increase in mass results in a change in the refractive index

close to the sensor chip surface, altering the reflected SPR angle. The change in SPR angle is reported in response (or resonance) units (RU) and is directly proportional to the mass of material bound on the surface, with 1 RU corresponding approximately to 1 pg/mm^2 of bound analyte (for proteins), or to a 0.0001^o shift in SPR angle[200].

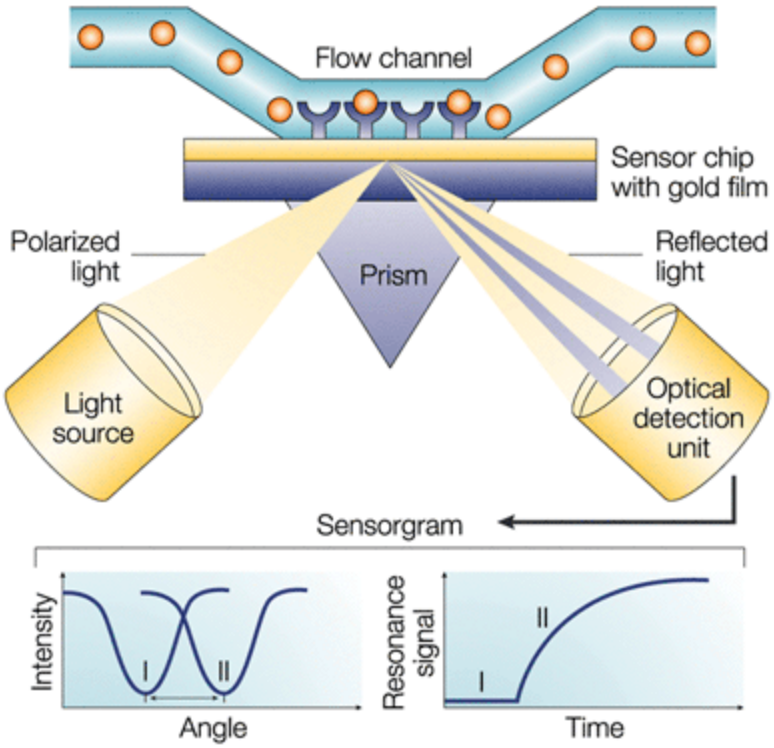

Figure 2-1 Principle of surface plasmon resonance. SPR detects changes in the refractive index close to the sensor chip surface. Binding of molecules to the surface causes a change in refractive index which results in a shift in the SPR angle, monitored in real-time. Reprinted from Cooper[201] with permission from Nature Publishing Group.

The change in binding response (RU) over time (seconds) is displayed as a sensorgram, which provides real-time monitoring of the binding kinetics. An example of a typical sensorgram is shown in Figure 2-2. Prior to analyte injection, running buffer flows through the IFC and over the sensor chip surface, producing a baseline response. Upon analyte injection, if binding to the

immobilized ligand occurs, an increase in binding response occurs (association phase). After a period of time (2-3 minutes), sample injection is stopped and the system returned to running buffer flow. The bound analyte then begins to dissociate from the ligand, causing a decrease in the binding response (dissociation phase). Most biomolecular complexes have long half-lives, so the surface is regenerated by injecting a regeneration solution (eg. low pH, high salt, or detergent) to remove any remaining bound analyte, making the ligand surface ready for a new binding cycle. The same surface can be re-used for as many cycles as the activity of the immobilized ligand is maintained.

The sensorgram provides information on whether binding has occurred, and binding levels which can be used for semi-quantitative or quantitative determination of analyte concentration in a sample. Curve-fitting software also allows for calculation of kinetic rate constants, such as rates of association (k_a or k_{on}) and dissociation (k_d or k_{off}), and affinity (K_D).

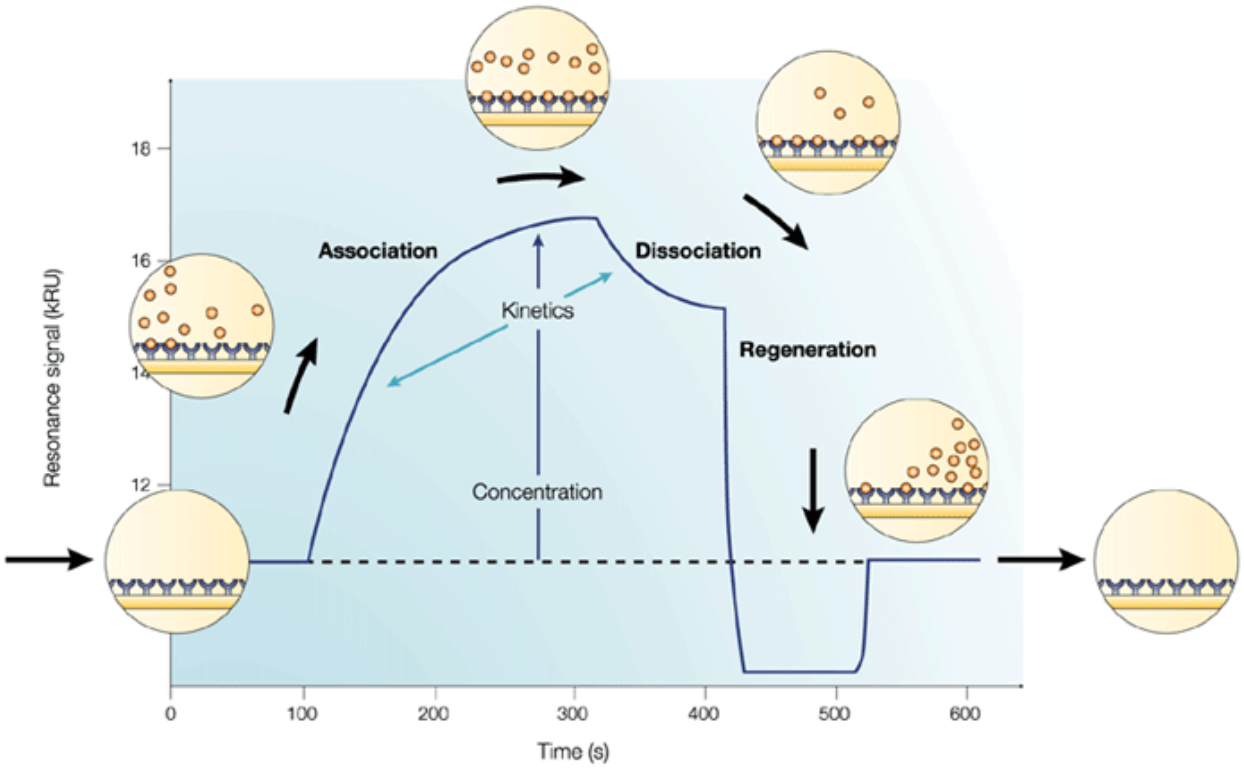

Figure 2-2 A typical binding sensorgram. A sensorgram is a plot of the resonance signal (binding response) in resonance units (RU) over time in seconds. Prior to sample injection, running buffer flow over the immobilized ligand gives a baseline response. Upon injection of analyte (t = 100s), if binding occurs, an increase in mass on the sensor chip results in an increase in binding response and association rate can be measured (k_{on}). At the end of analyte injection (t = 320s), running buffer flow restarts and the complex is allowed to dissociate, where the dissociation rate can be measured (k_{off}). A pulse of regeneration solution (t = 420s) removes remaining bound analyte for a new binding cycle. Reprinted from Cooper[201] with permission from Nature Publishing Group.

Sensor Chip & Immobilization Chemistries

There are a variety of different sensor chip types available for the Biacore system, each designed with slightly different modifications for analyzing different types of interactions. The most versatile and commonly used sensor chip is the CM5, which is also used in the experiments in

this chapter. The CM5 chip can be used in the analysis of a wide range of molecules, including proteins, lipids, carbohydrates, and nucleic acids[202]. To the 50nm gold film of the CM5 chip is attached a layer of carboxymethylated dextran (CMD), which acts as a matrix to which the ligand is attached (immobilized). The dextran matrix provides a fluid hydrophilic environment favourable to solution-based molecular interactions, a three dimensional space which increases the surface capacity for ligand immobilization, and the negatively charged carboxyl groups allow for efficient immobilization of positively charged ligands in dilute solutions[202].

Ligands can be attached onto the dextran surface via a range of immobilization chemistries. The most common technique for covalent immobilization is via amine coupling, illustrated in Figure 2-3. The carboxyl groups on the sensor chip surface are first activated with a mixture of N-hydroxysuccinimide (NHS) and 1-ethyl-3-(3-dimethylaminopropyl)-carbodiimide (EDC) to produce reactive succinimide esters. These esters then react with primary amines or other nucleophilic groups of the ligand to covalently couple the ligand to the dextran matrix. Remaining reactive groups are deactivated with ethanolamine.

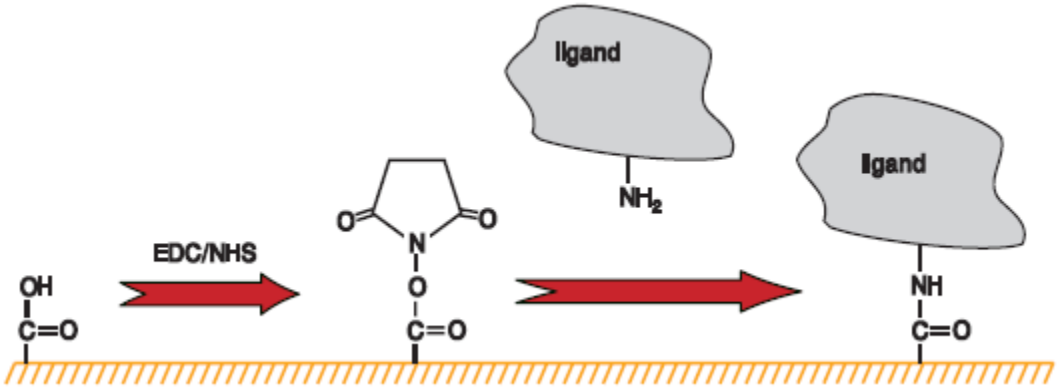

Figure 2-3 Amine coupling of ligand to sensor chip surface. The sensor chip surface is activated with a mixture of EDC/NHS to form reactive succinimide esters, which react with primary amine groups on the ligand to form covalent bonds. Reprinted from GE Healthcare [202] with permission from GE Healthcare.

2.2 Methods

2.2.1 Patient sera

For the development and validation of the MuSK-Ab Biacore assay, a series of healthy control, MuSK-Ab negative, and MuSK-Ab positive serum samples were utilized. The MuSK-Ab negative and MuSK-Ab positive sera had been previously tested for MuSK antibodies using a RIPA technique at the Institute of Molecular Medicine, Oxford, UK (Prof. Angela Vincent). Normal healthy pooled serum (NHPS) was also used as an antibody negative and matrix control.

For the MuSK-Ab characterization studies, serial serum samples from MuSK-MG patients were selected from the UBC Neuroimmunology Laboratory MG serum bank based on the following criteria: a) serum from at least two time points were available, and b) at least one sample had tested positive at Oxford for anti-MuSK antibodies. Sex, age and clinical features were also obtained from records of physician-filled clinical information sheets accompanying samples.

Serum samples were stored at -70^{o}C before assaying. The samples were prepared for analysis by centrifuging at 16,000xg for 12 minutes at 4^{o}C, in order to pellet any aggregates present and, in lipemic samples, to float the fat to the top. The less lipemic serum below was aliquoted for analysis in order to prevent clogging of the Biacore IFC and microfluidic system.

2.2.2 Instrumentation and data analysis software

Interaction analyses experiments were carried out using a Biacore™ 3000 biosensor instrument (Biacore™, GE Healthcare) using Biacore control software v4.1.2. For assays with a large number of samples, a 96-well plate format was used. All analyses were carried out at 25.0^{o}C with a data collection rate of 1.0 Hz. For longer experiments (>8 hours) the sample compartment temperature was decreased to 4^{o}C using a water cooling system, but the analysis temperature

remained at 25^{o}C. Sensorgrams were evaluated using Scrubber v2.0 (BioLogic Software, Campbell, Australia).

2.2.3 Running and sample buffers

The general purpose buffer HBS-EP (0.01M HEPES pH 7.4, 0.15M NaCl, 3mM EDTA, and 0.005% v/v surfactant P20) (GE Healthcare) was used in all interaction analyses, with modifications as indicated. In preliminary assays using serum, HBS-EP was used as running buffer while HBS-EP with 1mg/mL soluble carboxymethyl dextran (NSB reducer, GE Healthcare) was used as the sample buffer to dilute the serum (HBS-EP-CMD). In subsequent assays a switch was made to using HBS-EP with 0.2mg/mL (0.02% w/v) bovine serum albumin as both running buffer and sample buffer (HBS-EP-BSA), as it was found to be better suited to limit non-specific binding to the BSA reference surface (see section 2.2.7).

Buffers were prepared fresh each day using Milli-Q water and fully degassed before use. The Biacore system was primed with newly prepared running buffer a minimum of five times before starting an experiment.

2.2.4 Preparation of MuSK antigen

Recombinant human MuSK extracellular domain (aa 1-490), with a molecular weight of 62kDa, was used as ligand (RSR Limited, Cardiff, UK). The MuSK was provided in a buffer of 10mM Tris-HCl pH 8.0, 0.5mM EDTA, and 50mM NaCl, at a concentration of 1.1mg/mL (by Bradford assay), with a purity >95%. Since Tris contains primary amines, a buffer exchange into HBS buffer (10mM HEPES pH 7.4, 150mM NaCl) was performed to avoid having Tris in the immobilization buffer which would compete with the ligand during amine coupling. Buffer

exchange was performed using Vivaspin™ 2 10kDa MWCO sample concentrators (GE Healthcare), according to the manufacturer's instructions.

2.2.5 Immobilization pH scouting

To determine the appropriate immobilization pH, a pH scouting procedure was performed. The MuSK ligand was diluted in buffers of different pH to a final concentration of 50μg/mL and injected over an unmodified research-grade CM5 biosensor chip (GE Healthcare) flowcell surface at a flow rate of 20μL/min for 2 minutes. The buffers tested were HBS-EP (pH 7.4), 10mM maleate (pH 6.0), and 10mM sodium acetate (pH 5.5, 5.0, 4.5, and 4.0). The most neutral pH was injected first followed by the more acidic injections. After the last ligand injection, a 30s pulse of 50mM NaOH wash solution was injected to remove any remaining ligand molecules.

2.2.6 Immobilization of MuSK ligand and verification of surface activity

Under conditions of continuous flow of HBS-EP running buffer, MuSK was covalently immobilized on research-grade CM5 biosensor chips (GE Healthcare) using standard amine-coupling chemistry. Using an amine coupling kit (GE Healthcare), the surface of the flow cells were activated with a 7-minute injection of a 1:1 mixture of 0.1M NHS (N-hydroxysuccinimide) and 0.1M EDC (1-ethyl-3-(3-dimethylaminopropyl)-carbodiimide), according to the manufacturer's instructions, to form activated succinimide esters. MuSK ligand diluted in 10mM sodium acetate pH 4.5 at concentrations of 10-100μg/mL, depending on the desired immobilization level, was subsequently injected. The target immobilization level was specified using the Biacore™ immobilization wizard, with the "Aim for Immobilized Level" procedure. To serve as a reference surface, BSA (in 10mM sodium acetate pH 4.5, at concentrations of 2.5-10μg/mL) was immobilized at a similar level as the active MuSK surface. BSA was used as the reference surface ligand as it is a relatively inert protein and its molecular weight of 66kDa was

similar to the molecular weight of the MuSK ligand (62kDA). Following immobilization, unreacted esters were blocked with a 7-minute injection of 1M ethanolamine-HCl (pH 8.5).

The surface activity of a newly immobilized MuSK surface was tested with a 3-minute injection (10μL/min) of a 1/10 dilution of a MuSK-Ab negative and a MuSK-Ab positive control serum sample.

2.2.7 Regeneration scouting and surface performance

To determine the optimal regeneration buffer that will remove all of the bound analyte while maintaining the MuSK ligand activity, a regeneration scouting was performed. Chemicals from the regeneration scouting kit (GE Healthcare) were used under conditions of continuous flow of HBS-EP running buffer. Six different regeneration solutions were tested using a freshly immobilized and previously unused MuSK surface (~4500RU): a) 100% ethylene glycol, b) 10mM glycine-HCl pH 2.5, c) 10mM glycine-HCl pH 1.7, d) 60mM phosphoric acid (pH 1.75), e) 50mM NaOH (pH 12.7), and f) 4M $MgCl_2$. A high titer MuSK-Ab positive serum sample was used as the analyte, diluted 1/10 in HBS-EP-CMD. Each regeneration solution was tested with two repeated cycles of a 2-minute analyte injection followed by a 30-second injection of regeneration solution, at a flow rate of 20μL/min. The conditions that gave the best regeneration during scouting were verified by performing five cycles of repeated analyte binding and regeneration, in order to evaluate the stability of the baseline and analyte binding capacity.

2.2.8 Optimization and evaluation of assay specificity

To optimize assay conditions and evaluate assay specificity, 20 healthy control, 10 MuSK-Ab negative, and 10 MuSK-Ab positive sera were assayed. Three MuSK immobilization densities were tested: ~300RU (low density), ~1600RU (medium density), and ~4500RU (high density).

The MuSK active surfaces had matched reference surfaces with similar immobilization levels of BSA. Serum samples were diluted 1/10 and 1/100, initially in HBS-EP-CMD (with HBS-EP running buffer), and in subsequent assays switched to HBS-EP-BSA as both sample and running buffer.

A 96-well microtiter plate format was used to perform the assays, and all samples were run together in duplicate. Each sample was sequentially injected over the active MuSK and reference surface BSA surfaces for 3 minutes (association phase) at a flow rate of 10μL/min. After sample injection was stopped, dissociation was allowed for 2.5 minutes (running buffer flow only). At the end of each cycle, the sensor chip surface was regenerated with a 30-second pulse of 60mM phosphoric acid at 20μL/min. Each assay began with a duplicate run of diluted NHPS as a matrix control and to prime the system, and also included a blank control consisting of sample diluent and a positive control placed at intervals throughout the assay.

Binding on the reference surface was subtracted from binding on active surface. Relative sample binding response was found by subtracting the baseline response, before injection, from the response after injection. The assay positivity cut-off was taken as the mean + 3SD of the 20 healthy control samples, with borderline samples falling between mean + 2SD and mean + 3SD.

2.2.9 Inter- and intra-assay variability

Inter- and intra-assay variation were evaluated by assaying three MuSK-Ab positive serum samples of high, medium, and low titers, based on response rankings from the screening assays. Intra-assay variability was evaluated by assaying the three sera in 12 replicates in the same assay. Inter-assay variability was evaluated by assaying the three sera in 3 replicates in three assays on separate days. Samples were diluted 1/10 in HBS-EP-BSA and assayed on a high MuSK density

surface (~4500RU), with assay parameters as described in section 2.2.8. Percent coefficient of variation (%CV) was calculated according to the formula %CV = (SD replicates / mean replicates) * 100%.

2.2.10 Biacore analysis of antibody binding levels of serial sera

All serum samples were assayed at the same time in duplicate under conditions of continuous HBS-EP-BSA running buffer flow. Sera were diluted 1/10 in HBS-EP-BSA. Each sample was sequentially injected over the active MuSK surface (~6000RU) and reference BSA surface at a flow rate of 10μL/min for a 3 minute association phase and 2.5 minute dissociation phase. Regeneration was performed with a 30-second pulse of 60mM phosphoric acid at 30μL/min. The assay included 20 healthy control sera and began with a duplicate run of diluted NHPS, and also included a positive and negative control, and a blank control consisting of sample diluent. The sensorgrams were normalized by subtracting binding on reference surface from binding on active surface. The assay positivity cut-off was taken as the mean + 3SD of the 20 healthy control samples. For positive samples, the antibody binding levels were measured as the increase in SPR response (RU) from the baseline response, before injection, to after injection.

2.2.11 Biacore analysis of antibody isotype and IgG subclasses of serial sera

To evaluate antibody isotypes and IgG subclass specificities, injection of diluted serum was followed by the sequential injection of mouse antiserum against human IgM, IgG, IgG1, IgG2, IgG3, and IgG4 (see Figure 2-11 in results for a representative sensorgram).

Serum samples diluted 1/5 in HBS-EP-BSA were injected over the MuSK active surface (~6000RU) and BSA reference surface for 5 minutes at a flow rate of 10μL/min. This was followed by 2-minute sequential injections of purified monoclonal mouse anti-human IgM (clone

UHB), anti-human IgG (Fc-specific, clone JDC-10), anti-human IgG1 (hinge-specific, clone 4E3), anti-human IgG2 (Fc-specific, clone 31-7-4), anti-human IgG3 (hinge-specific, clone HP6050), and anti-human IgG4 (pFC'-specific, clone HP6023) (all antisera from SouthernBiotech), at concentrations of 100μg/mL in HBS-EP-BSA. At the end of each cycle, the sensor chip surface was regenerated by a 30-second injection of 60mM phosphoric acid at 30μL/min.

Sensorgrams were analyzed by subtracting binding on the reference surface from the active surface, followed by subtracting of the NHPS curves to normalize for non-specific binding of antiserum. The binding levels of each of the antisera were measured as the increase in binding response from the level before each injection to after the end of injection.

2.2.12 Biacore analysis of antibody dissociation rates of serial sera

For antibody dissociation rate (relative binding affinity) determinations, sera were diluted 1/10 in HBS-EP-BSA and injected over a low MuSK density surface (~300RU) and matched BSA reference surface at a flow rate of 60μL/min for 2 minutes, followed by a dissociation phase of 10 minutes during which only HBS-EP-BSA running buffer was injected. A longer dissociation phase was used compared to the binding level assays to get a better curve fit and increase the resolution between low and high dissociation rates. Following dissociation, the sensor surface was regenerated with a 30-second injection of 60mM phosphoric acid. These kinetic assays also included a series of 12 start-up cycles of buffer and 5 cycles of diluted NHPS to equilibrate the surface and for the purposes of referencing.

For the analysis of the antibody dissociation rates (k_d), sensorgrams were processed using Scrubber v2.0 software (BioLogic Software, Campbell, Australia). All of the curves were

overlaid and the sensorgrams y-transformed to zero the baseline, followed by x-transformations to align the sample injection start points. Data was double-referenced by subtracting out binding on the BSA reference surface and blank buffer injections. The dissociation phases of the sensorgrams were then fitted to a 1:1 (Langmuir) binding model, starting at 30 seconds post the end of sample injection to the end of the 10 minute dissociation phase. The fit of the curves was assessed by examination of the residuals for any systematic deviations of fit. The resulting dissociation rates (k_d), with units of $second^{-1}$, are an approximate indicator of the antibody binding affinity, with antibodies of a higher affinity having a slower dissociation rate, and antibodies of a lower affinity having a faster dissociation rate.

2.2.13 Statistical analysis

Statistical analysis was performed using SPSS Statistics version 22 (IBM Corporation). The relationship between antibody dissociation rates (k_d) and antibody binding response was determined by Spearman's correlation test.

2.3 Results

2.3.1 Immobilization pH scouting

During immobilization, in order to effectively attract the MuSK ligand to the sensor chip surface, the protein has to be attracted by electrostatic forces during a pre-concentration step. This electrostatic attraction is affected by the pH of the buffer the ligand is dissolved in. To determine the optimal immobilization buffer pH, a pH scouting procedure was performed by diluting the MuSK ligand in buffers of a range of pHs, as described in section 2.2.5. The aim was to obtain a

sufficiently high increase in pre-concentration response, but with the most neutral pH possible to maintain the native state of the ligand.

As shown in Figure 2-4, the attraction of the MuSK ligand to the dextran matrix of the sensor chip surface increased with decreasing pH of the buffers. This is explained by the fact that the protein is more positively charged at a lower pH (when buffer pH < protein pI), which effects the attraction to the negatively charged dextran matrix. Based on the response levels reached, 10mM sodium acetate buffers of pH 4.0, 4.5 and 5.0 gave suitable pre-concentration effects, with pH 4.0 and 4.5 giving the highest response. At pH 4.0, a plateau was reached at the end of injection, which indicates that the maximum level of attraction was reached at that pH. Based on these results, 10mM sodium acetate pH 4.5 was chosen as the immobilization buffer, as a milder pH gives a more efficient amine coupling. The buffer of pH 5.0 could also have been used in the event that the lower buffer pH buffer was still too harsh (i.e. was found to inactivate the MuSK), as a more neutral pH would give a milder treatment to the ligand.

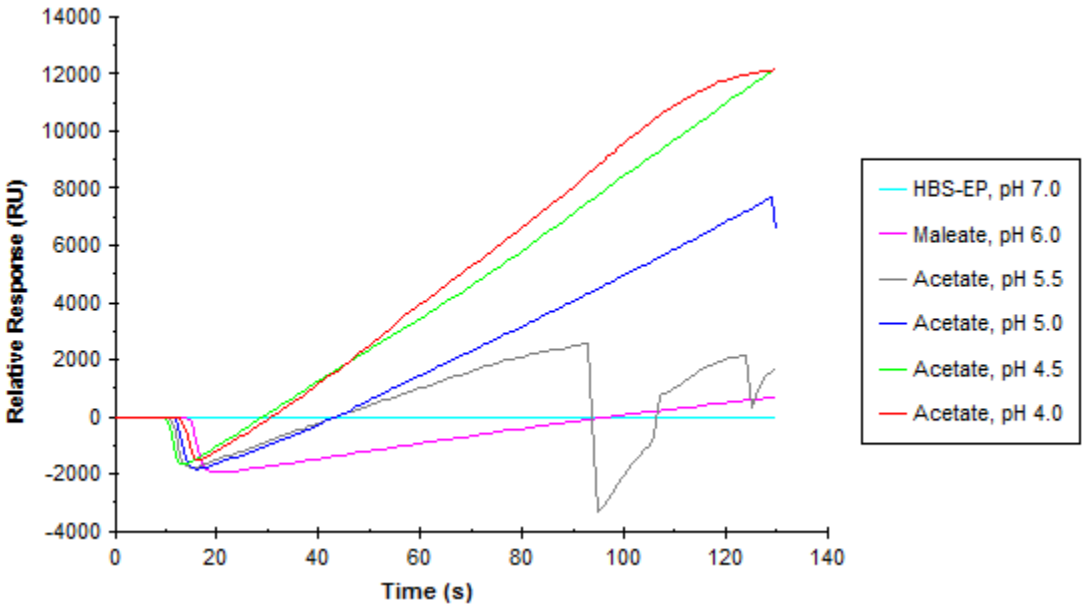

Figure 2-4 pH scouting for MuSK immobilization.

2.3.2 MuSK immobilization and verification of activity

MuSK antigen was immobilized onto CM5 sensor chips using amine coupling chemistry, as described in section 2.2.6. The sensor chip was activated with equimolar amounts of NHS and EDC, followed by coupling of the MuSK to the activated succinimide esters. Uncoupled esters were then blocked with ethanolamine. Between 300RU and 6000RU of MuSK was immobilized, depending on the application. BSA surfaces of approximately equal immobilization density were used as a reference surface. Representative immobilization sensorgrams of MuSK and BSA immobilization of equal surface density (~4500RU ligand bound) are shown in Figure 2-5.

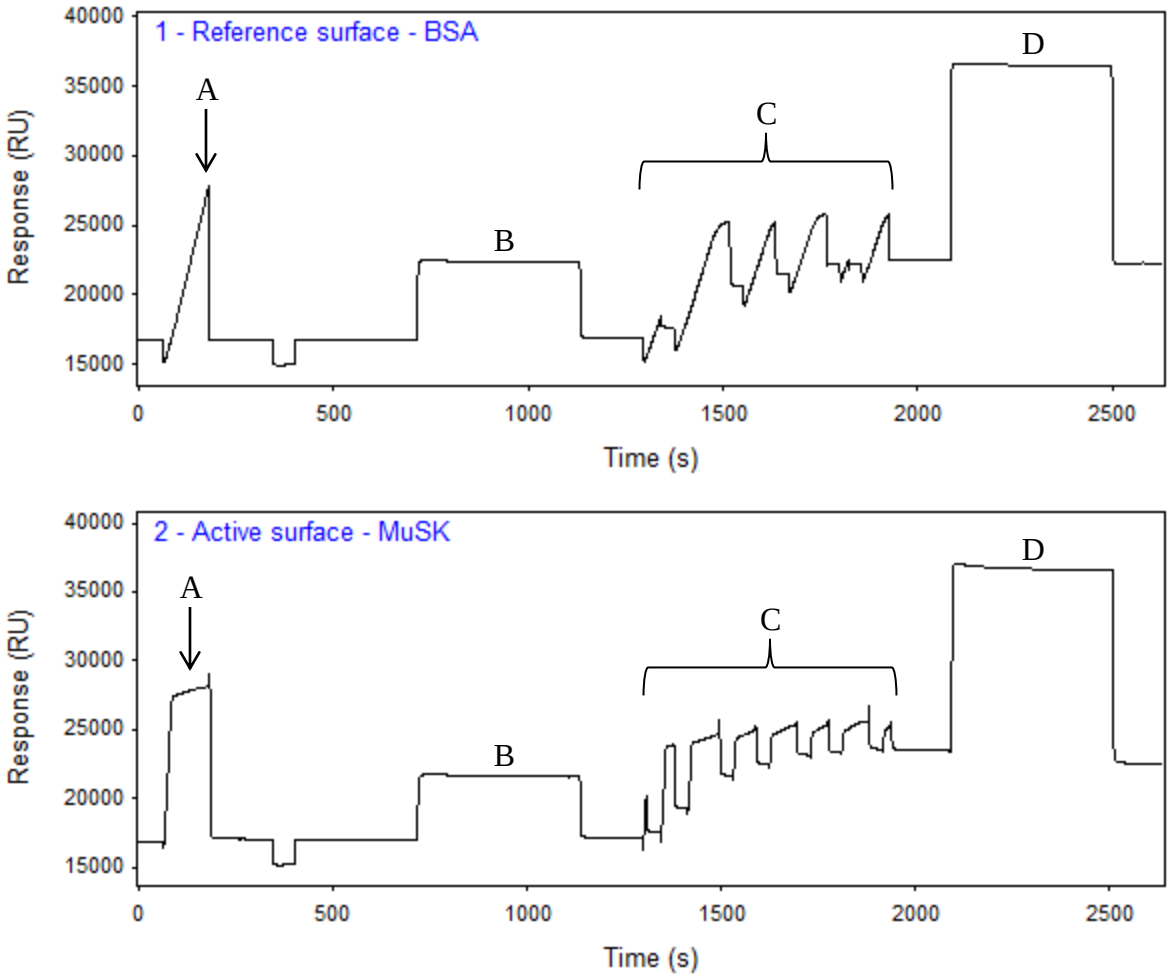

Figure 2-5 Representative immobilization sensorgrams of MuSK active surface and BSA reference surface. (A) Preconcentration of ligand, a process by which the ligand is electrostatically attracted to the negatively charged dextran matrix, and the target level of immobilization is tested. (B) Activation of surface with 1:1 mixture of 0.1M NHS and 0.1M EDC to create reactive succinimide esters. (C) Injection of ligand diluted in immobilization buffer. Primary amine groups of ligand couple with reactive succinimide groups to form covalent bonds. (D) 1M ethanolamine is used to block the uncoupled succinimide groups.

To confirm ligand activity of a newly immobilized MuSK surface, a test of analyte binding capacity was performed by assessing binding of control MuSK-Ab positive and MuSK-Ab negative sera. Figure 2-6A clearly shows binding of the MuSK-Ab positive serum to the active

MuSK surface and not to the BSA reference surface, while there is no binding of the MuSK-Ab negative serum to either surfaces, demonstrating the specificity of the MuSK surface and the minimal to no non-specific binding to the BSA reference surface. The square-shaped response of the sensorgrams is the bulk response due to differences in the refractive index between the sample buffer containing the analyte and the running buffer. Although the sample and running buffers are matched to help reduce the bulk effect, exact matching is not possible because of the complex matrix of the analyte[200]. This is where normalization of the sensorgrams comes in, shown in Figure 2-6B, where the reference surface is subtracted from the active surface in order to subtract the bulk refractive index response from the specific binding signal. A slight bulk effect can still remain post-normalization if there is a difference in the bulk response between the reference and active surfaces. These tests indicated that the immobilized MuSK ligand is active and there is sufficient analyte binding capacity for an assay to measure anti-MuSK antibodies in serum.

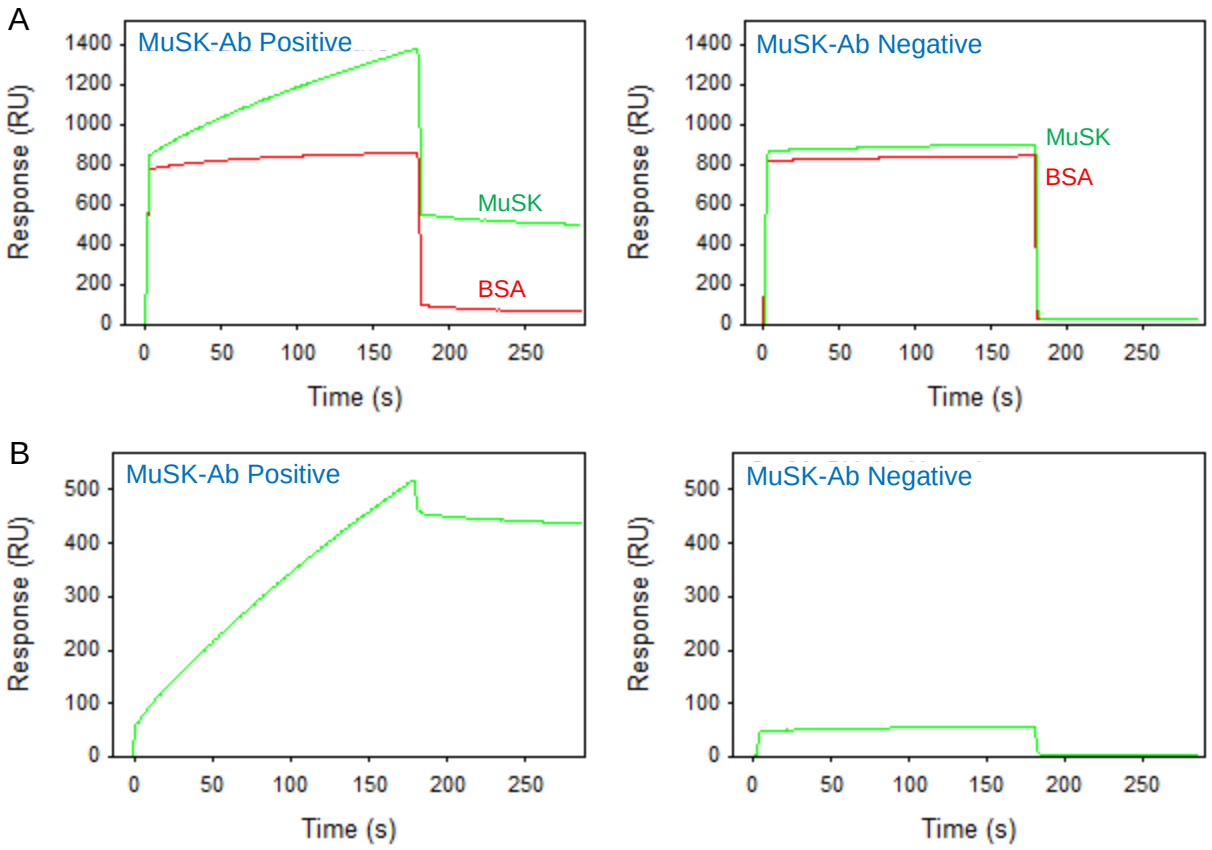

Figure 2-6 Representative binding sensorgrams of MuSK-Ab positive and negative sera. (A) Binding of MuSK-Ab positive and negative sera to MuSK active and BSA reference surfaces. (B) Normalized sensorgrams, obtained by subtracting reference sensorgram from active surface.

2.3.3 Regeneration scouting and surface performance

The goal of regeneration is to completely remove the bound analyte without disrupting ligand activity. Incomplete regeneration can result in loss of binding capacity and shorten the lifespan of the immobilized surface. Exploratory tests with a range of different regeneration solutions were first performed to establish which regeneration conditions were worth pursuing. In these tests, consecutive cycles of analyte and regeneration were performed on a freshly immobilized high density (~4500RU) MuSK surface, using a MuSK-Ab positive serum sample as analyte, as

described in section 2.2.7. Six different regeneration solutions were tested, for two cycles each. Between 250-300RU of analyte was bound each cycle, as shown in Table 2-1. The analyte binding was relatively constant even though the regeneration was incomplete during many of the cycles, indicating that the immobilized MuSK surface had a high binding capacity. The regeneration solutions that had the best performance in terms of % analyte removed were 10mM glycine pH 1.7, and 60mM phosphoric acid, both removing >100% of the amount of analyte bound during the indicated cycle.

Table 2-1 Regeneration scouting results

		In Current Cycle		Total	
Cycle	Solution	Change in Response (RU)	Analyte Removed (%)	Binding Remaining (RU)	Remaining Analyte (%)
1	MuSK-Ab positive analyte	+ 299.7		299.7	
	100% Ethylene glycol	- 85.1	28	214.6	72
2	MuSK-Ab positive analyte	+ 253.9		468.5	
	100% Ethylene glycol	- 102.7	40	365.8	78
3	MuSK-Ab positive analyte	+ 246.0		611.8	
	10mM Glycine-HCl, pH 2.5	- 195.4	79	416.4	68
4	MuSK-Ab positive analyte	+ 255.1		671.5	
	10mM Glycine-HCl, pH 2.5	- 170.7	67	500.9	75
5	MuSK-Ab positive analyte	+ 250.2		751.0	
	10mM Glycine-HCl, pH 1.7	- 526.4	210	224.7	30
6	MuSK-Ab positive analyte	+ 281.3		506.0	
	10mM Glycine-HCl, pH 1.7	- 300.5	107	205.5	41
7	MuSK-Ab positive analyte	+ 281.5		487.0	
	60mM Phosphoric acid	- 338.8	120	148.2	30
8	MuSK-Ab positive analyte	+ 285.1		433.2	
	60mM Phosphoric acid	- 295.6	104	137.6	32
9	MuSK-Ab positive analyte	+ 283.5		421.1	
	50mM NaOH	- 239.1	84	182.0	43
10	MuSK-Ab positive analyte	+ 290.1		472.1	
	50mM NaOH	- 209.1	72	263.0	56

		In Current Cycle		Total	
Cycle	Solution	Change in Response (RU)	Analyte Removed (%)	Binding Remaining (RU)	Remaining Analyte (%)
11	MuSK-Ab positive analyte	+ 276.6		539.7	
	4M $MgCl_2$	- 175.5	63	364.2	67
12	MuSK-Ab positive analyte	+ 261.4		625.5	
	4M $MgCl_2$	- 159.7	61	465.9	74

To further establish the reliability of the two best regeneration conditions, a longer series of five repeated cycles of analyte injection and regeneration were performed in order to reveal trends in regeneration efficiency and ligand activity by examining changes in baseline levels and analyte binding response following regeneration. An increase in baseline could indicate material accumulating on the surface (too mild a regeneration), while a decrease could indicate loss of ligand from the surface (too harsh a regeneration). Similarly, a decrease in sample binding response could indicate either loss of ligand activity or accumulation of matter on the surface. A small constant decrease in baseline may be acceptable as long as the analyte response is repeatable.

Figure 2-7 shows the trends of the sample response and baseline over 5 cycles for the two regeneration solutions. When using the glycine-HCl pH 1.7, the baseline dropped after the first cycle, however this can happen when using a newly prepared surface. However, the baseline continued to drop slightly with every following cycle, and along with a falling trend in the sample binding response this indicated a possible loss of ligand activity as a result of too harsh a regeneration. When using the 60mM phosphoric acid, the baseline appeared to be more stable, with only a slight decrease over the 5 cycles, however this was acceptable as the sample response appeared to be more stable compared to using the glycine-HCl, indicating that surface activity

was maintained following regeneration. The 60mM phosphoric acid solution was therefore selected as the regeneration solution for all follow up assays.

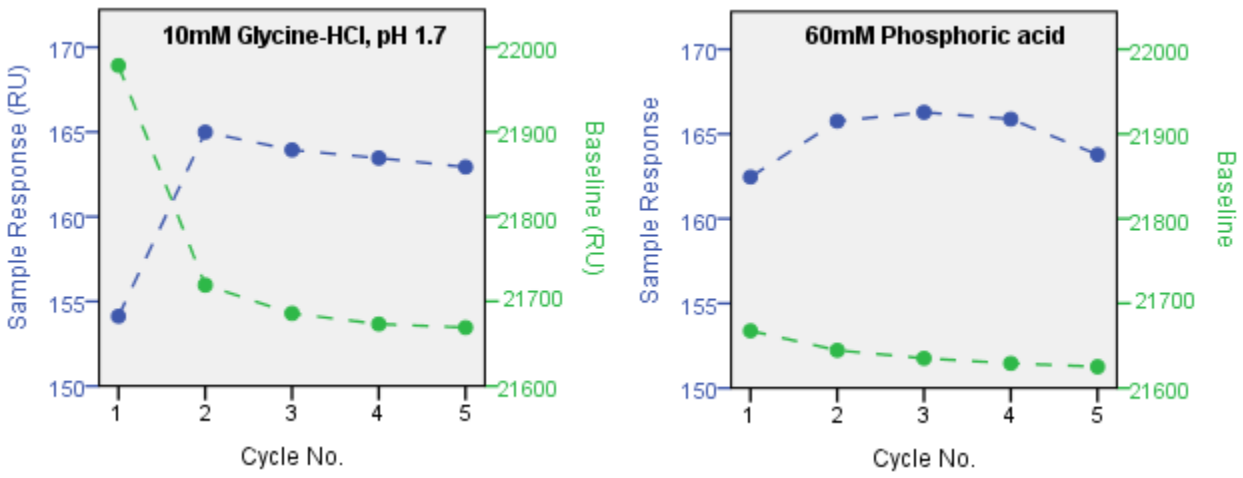

Figure 2-7 Regeneration performance of MuSK-Ab positive sample. Five regeneration cycles of a MuSK-Ab positive sample using 10mM glycine-HCl pH 1.7 and 60mM phosphoric acid were performed on a high density MuSK surface to assess surface performance.

2.3.4 Optimization and evaluation of assay specificity

To assess the specificity of the Biacore assay to detect antibodies against MuSK, samples from 20 healthy controls, 10 MuSK-Ab negative, and 10 MuSK-Ab positive individuals were assayed. To determine what MuSK immobilization density best discriminates between MuSK-Ab positive and MuSK-Ab negative serum samples, three MuSK immobilization densities were tested: high density (~4500 RU), medium density (~1600 RU), and low density (~300 RU), as described in section 2.2.8. Serum dilutions of 1/10 and 1/100 were tested.

Initially, HBS-EP-CMD was used as sample buffer, with HBS-EP as running buffer. The addition of soluble carboxymethyl-dextran to the sample buffer is commonly used in Biacore

assays to reduce non-specific binding of components in complex sample matrices, such as serum, to the dextran on the sensor chip surface by competition[202]. Figure 2-8 shows the results of a screening assay on the high density MuSK surface. For both 1/10 and 1/100 serum dilutions, while all of the healthy controls and MuSK-Ab negative samples had binding responses below the assay cut-off (mean + 3SD of healthy controls), only 4 out of the 10 MuSK-Ab positive samples tested had binding responses above the cut-off. Many of the healthy control samples had large negative binding response values, indicating that these samples were binding more to the BSA reference surface than to the MuSK active surface, resulting in the large negative values upon sensorgram normalization. This was also the case for one of the MuSK-Ab negative samples (sample #26). This effect caused the artificial inflation of the healthy control binding response standard deviations (SDs), especially with the 1/10 dilution, thereby also inflating the assay cut-off. As a result, although there did appear to be a distinct separation between the negative and positive samples, the high cut-off resulted in 6/10 positive samples having a borderline or negative result.

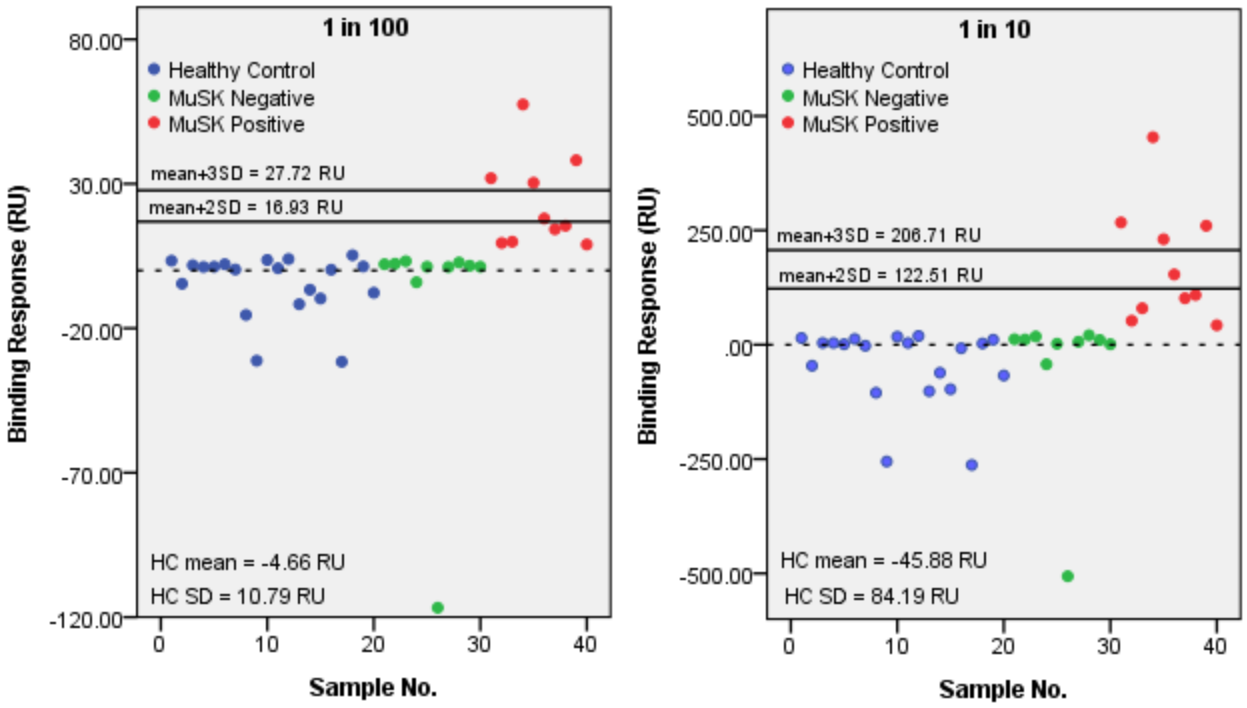

Figure 2-8 Screening assays using HBS-EP-CMD sample buffer. Twenty healthy control, 10 MuSK-Ab negative, and 10 MuSK-Ab positive samples assayed on a high density MuSK surface at 1/100 and 1/10 dilutions in HBS-EP-CMD.

The high degree of binding to the BSA reference surface observed with some of the samples was hypothesized to be due to anti-BSA antibodies or other components of the serum matrix binding non-specifically to BSA. To counteract this, BSA was added to the sample and running buffers (HBS-EP-0.02% BSA), replacing the CMD, to inhibit the non-specific binding. The running and sample buffers were matched to minimize bulk shifts seen in sensorgrams when running and sample buffers with different refractive indexes are used[203]. Figure 2-9 shows the results of binding assays of the three groups of sera, diluted 1/10 and 1/100 in HBS-EP-BSA, on the three immobilization densities.

The large negative binding response values post-normalization, seen previously with some of the sera when using HBS-EP-CMD sample buffer, were no longer present. The binding responses of the healthy controls were much tighter, with smaller SDs. This resulted in the assay cut-offs (mean + 3SD) being significantly smaller. With the high density surface, for example, the cut-offs when using HBS-EP-CMD were 27.72 RU and 206.71 RU for the 1/100 and 1/10 dilutions, respectively (Figure 2-8), compared to 5.32 RU and 33.48 RU when using HBS-EP-BSA buffer (Figure 2-9A). This indicated that adding BSA to the sample and running buffers inhibited the non-specific binding to the reference surface seen previously.

Using the high density surface (~4500 RU), all 10 MuSK-Ab positive samples were found positive, and all 10 MuSK-Ab negative and 20 healthy control samples were found negative, at both 1/100 and 1/10 dilutions. This was also the case when using the medium density surface (~1600 RU), with only one healthy control sample having a borderline result at the 1/10 dilution. However, once the surface density was decreased to a low density (~300 RU), the sensitivity decreased, with 4/10 MuSK-Ab positive samples at the 1/10 dilution having binding responses below cut-off. In all cases, the binding responses for the MuSK-Ab positive samples using a 1/100 dilution were found to be about 10-fold lower than those obtained using a 1/10 dilution. This corresponds with the fact that Biacore is an SPR-based technique where the response generated by binding of molecule to the sensor surface is directly proportional to the bound mass.

The optimal assay conditions for measuring MuSK antibodies therefore include using a high immobilization surface density (>4500RU MuSK) for the best sensitivity, a 1/10 serum dilution for higher binding responses and sensitivity (although a 1/100 dilution also discriminated well between positive and negative samples), and adding 0.02% BSA to the sample and running

buffers to inhibit non-specific binding of anti-BSA antibodies or other serum matrix components to the BSA reference surface. Using these conditions, the Biacore assay developed was found to have high specificity and sensitivity in detecting anti-MuSK antibodies in serum.

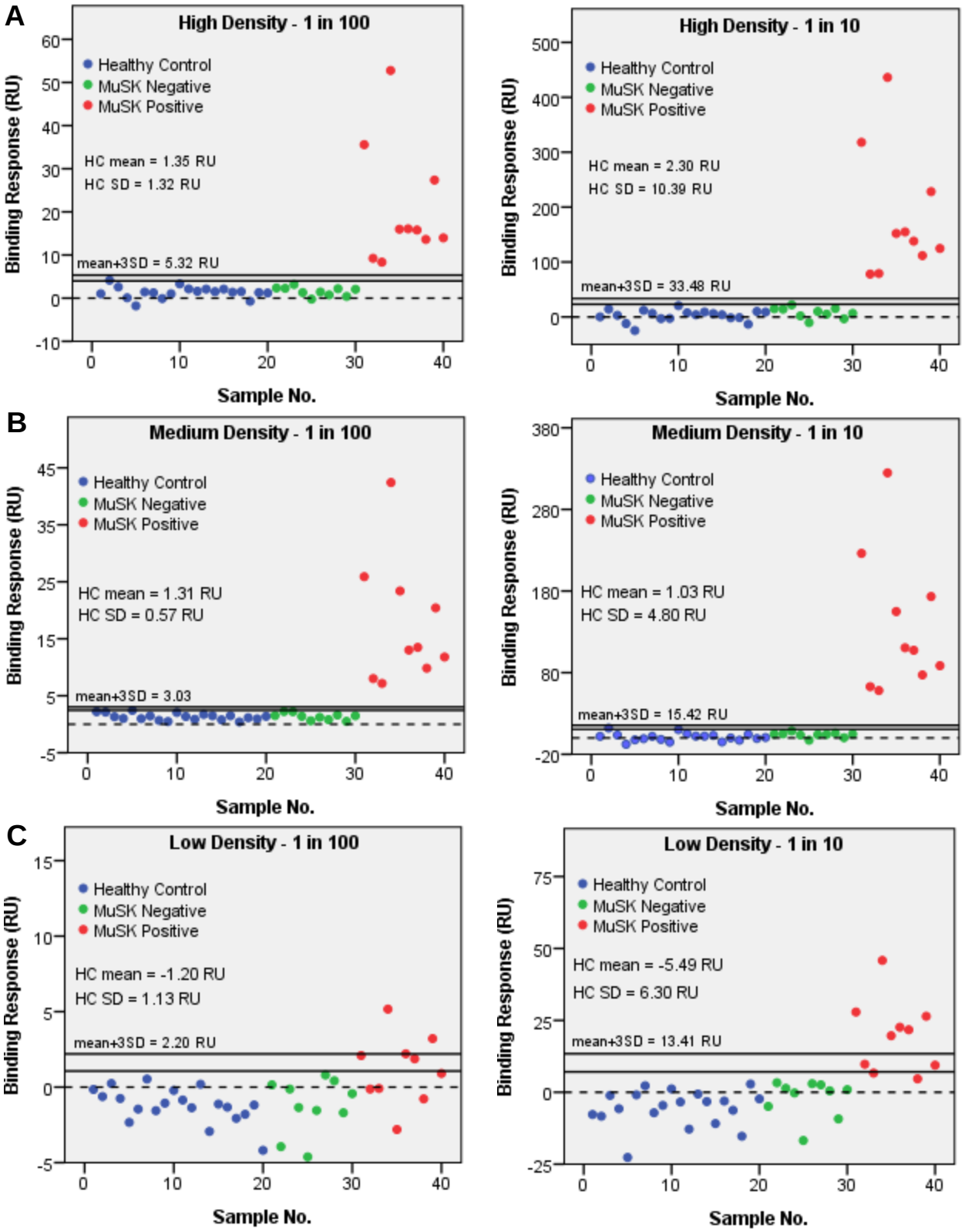

Figure 2-9 Screening assays using HBS-EP-BSA sample buffer. (A) High (~4500RU), (B) medium (~1600RU), and (C) low (~300RU) MuSK densities, at 1/100 and 1/10 dilutions in HBS-EP-BSA.

2.3.5 Inter-assay and intra-assay variability

Intra-assay and inter-assay variations were evaluated by assaying 3 sera, chosen to represent a range of binding response values, which were designated as having a low, medium, and high titer. These samples were chosen from the MuSK-Ab positive samples assayed in section 2.3.4.

Intra-assay variability was evaluated by assaying the three sera 12 times in the same assay. The coefficients of variation for the intra-assay variability were 7.3%, 6.6%, and 8.1% for the low, medium, and high titer respectively (Table 2-2). Inter-assay variability was evaluated by assaying the three sera in triplicate on three separate days. The coefficients of variation for the inter-assay variability were 14.0%, 4.6%, and 5.0% for the low, medium, and high titer respectively (Table 2-3). The method was found to be robust, with variability not exceeding a coefficient of variation of 15%, well within acceptable limits for a biological immunoassay[204].

Table 2-2 Intra-assay variability

Sample	Mean Binding Response (RU)	SD	% CV
Positive Low	61.76	4.48	7.3
Positive Medium	127.49	8.47	6.6
Positive High	228.12	18.55	8.1

Table 2-3 Inter-assay variability

Sample	Mean Binding Response (RU)	SD	% CV
Positive Low	61.25	8.60	14.0
Positive Medium	110.17	5.09	4.6
Positive High	226.63	11.30	5.0

2.3.6 Clinical features of MuSK-MG patients

The Biacore assay developed for detecting anti-MuSK antibodies in serum was used to characterize the changes in binding levels (titers), antibody isotype and IgG subclass, and dissociation rate of anti-MuSK antibodies in serial serum samples of MuSK-MG patients.

A retrospective analysis of serum samples referred to the UBC Neuroimmunology Laboratory for anti-MuSK antibody testing to the Institute of Molecular Medicine (Oxford, UK) was performed. A total of 19 patients were identified who had MuSK-Ab positive MG, for whom a total of 65 serial serum samples were available (between 2 and 7 samples per patient), taken over a period of 1 to 189 months (15.75 years) (Table 2-4). The first sample date for each patient was designated as month 0, with the draw dates of all follow-up samples adjusted to the number of months after the first sample. For all of the patients the sample designated month 0 was drawn around the time of disease onset, except for patient 2 which was drawn approximately 10 years after onset. 7 out of 19 patients had only two serial samples, and for all of these cases the samples were drawn over a period of less than one year, likely because MuSK antibody testing was being done at disease onset for diagnostic purposes only. Some of the patients had many more samples over a long duration as they had repeatedly tested negative for AChR antibodies before being tested for MuSK antibodies, in some cases this was before the characterization of MuSK antibodies in 2001.

The clinical features of these patients are described in Table 2-4. Notably, all of the MuSK-MG patients in this cohort were female, in agreement with previous studies finding that patients with MuSK-MG are predominantly female[13-17, 205, 206]. The age of onset ranged from 12 to 59 years of age, with a mean of 39.6 ± 13 years, and 78.9% of patients presenting under 50 years of age.

This is also in agreement with epidemiological data that MuSK-MG is more frequent in younger individuals than AChR-MG[13-17, 205, 206].

Based on the physician-reported clinical information accompanying serum samples, 12/19 patients (63.2%) had ocular symptoms, 9/19 (47.4%) had bulbar symptoms, and 14/19 (73.7%) had generalized MG. For the other clinical parameters, a complete set of information was not available for all patients. 13/14 patients (92.9%) had clinical fatiguability, and 11/16 patients (68.8%) had a positive tensilon test and 1 had an equivocal response. In terms of electrical tests, out of 12 patients who had repetitive nerve stimulation done (RNS), 8/12 (66.7%) had a decrementing response, while out of 7 patients who had single fibre electromyography performed (SFEMG), 5/7 (71.4%) had an increased response, and 1 had an equivocal result. The one patient (patient 6) who had a normal SFEMG also had a no decrement in RNS.

Table 2-4 Clinical features of 19 MuSK-Ab positive MG patients[a]

Patient No.	No. Samples	Sampling Period (months)	Sex	Age at Onset	Type of muscular deficit	Clinical Fatiguability	Effect of Tensilon	RNS	SFEMG
1	3	66	F	12	Ocular & bulbar	Yes	Negative	Mild decrement	NA
2	3	133	F	20	Generalized	NA	Modest	Decrement	Increased
3	2	7	F	54	Generalized	Yes	Equivocal	NA	NA
4	2	1	F	22	Ocular, bulbar, generalized	Yes	Positive	Decrement	NA
5	2	2	F	30	Bulbar	No	Negative	No decrement	NA
6	4	60	F	46	Bulbar & generalized	Yes	Positive	No decrement	Normal
7	3	22	F	48	Ocular & generalized	Yes	Negative	No decrement	Increased
8	3	161	F	42	Generalized	Yes	Positive	Decrement	Increased
9	2	2	F	30	Ocular, bulbar, generalized	Yes	Positive	Decrement	NA
10	6	189	F	53[b]	Ocular and bulbar	NA	NA	NA	NA
11	7	44	F	31[b]	Generalized	NA	NA	NA	NA
12	7	157	F	44	Ocular, bulbar, generalized	Yes	Negative	Decrement	NA
13	3	14	F	41	Generalized	Yes	Positive	No decrement	Increased
14	3	128	F	37[b]	Ocular	NA	NA	NA	NA
15	2	3	F	34	Ocular, bulbar, generalized	Yes	Positive	Decrement	NA
16	4	15	F	56	Ocular & generalized	Yes	Positive	Decrement	Increased
17	2	1	F	49	Ocular, bulbar, generalized	Yes	Positive	NA	NA
18	5	20	F	44	Ocular & bulbar	NA	Positive	NA	Equivocal
19	2	1	F	59	Ocular, bulbar, generalized	Yes	Positive	NA	NA

[a]If characteristic not available, indicated as NA.

[b]Age of onset estimated from difference between date of birth and date of first serum sample.

2.3.7 Serial profiles of anti-MuSK antibody binding levels

The 19 MuSK-MG patients identified had between 2 and 7 serial samples each, which were drawn over a period of between 1 and 189 months (15 years 9 months). Figure 2-10 shows the change in MuSK antibody binding levels (RU) of the serial samples over time. The serial serum samples were diluted 1/10 in HBS-EP-BSA and run in duplicate in the same assay, along with 20 healthy control serum samples. The assay cut-off was calculated as the mean+3SD of the healthy controls. The antibody binding values for all of the patients, along with corresponding sample dates, are shown in Table A1 of the appendix.

The results show that the magnitude of the antibody binding levels clearly changes over the course of the disease. The highest binding level of MuSK antibodies attained in this group of patients was 346.44 RU, observed with patient 6 at month 2. The serial antibody profiles are patient-specific, but a few general trends can be observed.

For 7/19 patients (patients 1, 5, 7, 8, 9, 15, 17), antibody profiles consisted of an overall decrease in antibody levels over a period ranging from 1 month to 161 months (13.4 years). For one of these patients (patient 8) antibody levels declined to negative. The antibody level in patient 17 decreased by 76% after only one month, from a high level of 312.60 RU at month 0 down to 75.54 RU at month 1, suggesting an effect of treatment, possibly plasmapheresis.

For 4/19 patients (patients 3, 4, 10, 19), antibody profiles consisted of an overall increase in antibody levels over a period of 1 month for patients 4 and 19 to 189 months (15.8 years) for patient 10. However, all of these patients except for patient 10 had two serum samples over a course of only 1 to 7 months, making it difficult to draw conclusions about what their antibody levels might be like over the duration of their disease. It was however interesting to see in patient

10 that at disease onset this patient had no detectable MuSK antibodies, and appeared to continue to not have any detectable antibody levels until at least 72 months (6 years), where her antibody levels were at borderline levels. A next serum sample for this patient was not available until month 189 (year 15.8), where her antibody levels continued to be at low levels (44.93 RU).

For the remaining 8/19 patients (patients 2, 6, 11, 12, 13, 14, 16, 18), their antibody levels fluctuated over the course of their disease, ranging over a period of 14 months (1.2 years) for patient 13 to 157 months (13.1 years) for patient 12. In one of these patients (patient 18), antibody levels increased at month 11, but then declined to negative after 16 months (1.3 years), and continued to remain negative until month 20 (1.7 years). In another patient (patient 16), levels increased to 154.47 RU for the first 14 months (1.2 years), and then decreased at month 15 to a borderline level of 38.06 RU, again likely due to effect of treatment.

Overall, from the results of such a retrospective look at the changes in antibody levels in this group of MuSK-MG patients, we can see that there are clearly patient-specific changes to antibody levels of the course of disease that can be measured by the Biacore assay developed. If these changes correlate with clinical status, this assay could easily be used to measure antibody levels continuously in a clinical setting, instead of only at disease onset for diagnostic purposes.

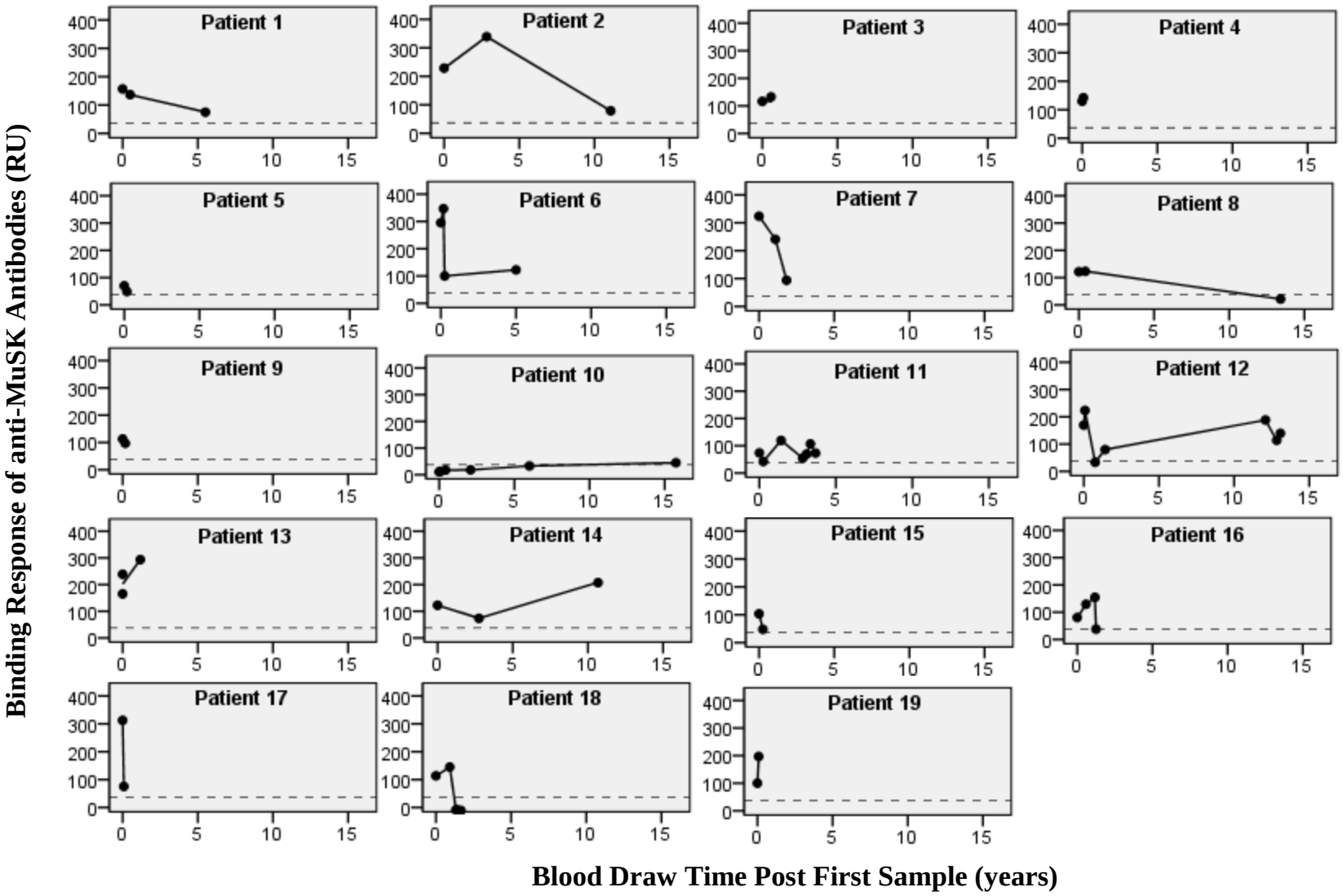

Figure 2-10 Serial MuSK antibody binding levels of 19 MuSK-MG patients. Serum samples were assayed in duplicate and each plotted point represents the mean anti-MuSK antibody binding response. The assay cut-off of 36.96RU, depicted as a dotted line, is the mean+3SD of 20 healthy controls.

2.3.8 Serial analysis of anti-MuSK antibody isotype and IgG subclass

The antibody isotype and IgG subclass specificity of the 55 samples that tested positive for MuSK antibodies in the serial binding analysis were determined. Sera diluted 1/5 were injected over a high surface density MuSK surface, followed by sequential injections of mouse antiserum against human IgM, IgG, IgG1, IgG2, IgG3, and IgG4. A 1/5 serum dilution was used to increase the MuSK-Ab binding levels, especially for low titer samples, thereby increasing the sensitivity of the binding of subsequent secondary antibodies.

When analyzing the results, the curves obtained from injection of diluted NHPS were subtracted to normalize for non-specific binding of the antiserum, particularly anti-IgG, to the MuSK antigen. Such binding was not observed on the BSA reference surface, suggesting it was specific to the MuSK antigen, possibly due to MuSK having Ig-like domains[35]. This binding therefore needed to be subtracted in order to accurately measure binding of the antisera to bound anti-MuSK antibodies in the tested serum samples.

Figure 2-11 shows a representative sensorgram depicting the sequential injection of diluted serum and mouse antisera. The amount of antibody and antisera bound is taken as the difference between the level pre-sample injection ("baseline") to the level post-sample injection, which is subsequently the baseline for the next sample injection.

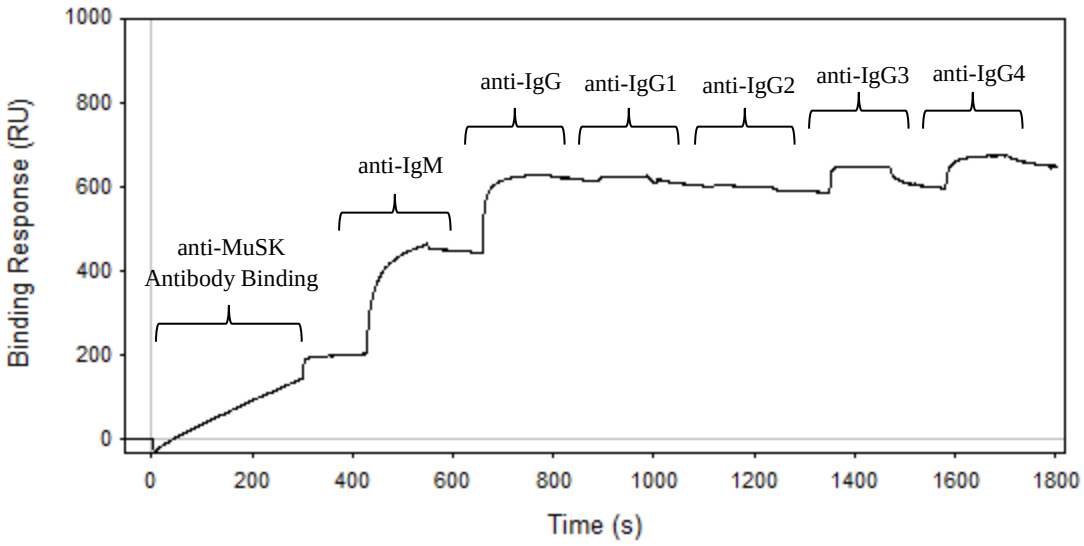

Figure 2-11 Representative sensorgram depicting the sequential injection of diluted serum and mouse anti-human IgM, IgG, IgG1, IgG2, IgG3, and IgG4. This particular sample was positive for antibodies of both IgM and IgG isotypes, with the IgG being of the IgG3 and IgG4 subclasses.

The serial analyses of anti-MuSK antibody isotype and IgG subclass for the 19 MuSK-MG patients are depicted in Table 2-5. The patients are separated into groups according to the isotypes and subclasses expressed.

11/19 patients had IgM antibodies, with 4 patients having continuous levels of IgM (patients 6, 14, 15, 16). Notably, patient 6 was the only patient who had very high continuous binding levels of IgM until month 60, ranging from 91.18 to 415.30 RU. Other patients had sporadic expression of IgM antibodies, and in these cases anti-IgM binding levels were lower, ranging from 2.44 to 21.03 RU. Some of the patients had IgM antibodies at month 0 that then disappeared, such as patients 8 and 19 who no longer had IgM antibodies at months 5 and 1 respectively. Conversely, other patients did not have IgM antibodies at month 0 but did so later at low levels, such as patients 5 (borderline level at month 2), 7 (month 22), and 13. Patient 13 did not appear to have

IgM antibodies for the first serum sample, but did so for a sample drawn only 9 days after and continued to have IgM at month 14. The presence of IgM antibodies in over half the patients, particularly the high levels in patient 6, points to a lack of antibody maturation or continuous antigen exposure generating IgM-producing plasma cells.

All 19 patients expressed MuSK antibodies of the IgG isotype. The predominant IgG subclass expressed was IgG4, with all 19 patients expressing IgG4 antibodies continuously over the course of their disease, in agreement with results of previous studies[14, 96, 206, 207]. This was followed by IgG1, continuously expressed by 13/19 patients, except for patient 18 where there was a class switch from IgG1 at month 0 to IgG2 at month 11. IgG3 was also expressed continuously by 13/19 patients (except for patient 6 which started at month 3), but only at very low levels, so their expression is likely negligible compared to IgG4 and IgG1 expression. MuSK antibodies do not appear to frequently be of the IgG2 subtype, there were only negligible levels of IgG2 expressed by patients 11 and 12. Only patient 18 expressed IgG2 at month 11, which appeared to be a class switch from IgG1.

Table 2-5 Summary of the MuSK antibody isotypes and IgG subclasses in 19 MuSK-MG patients. Isotype analysis was performed on 55 serum samples positive for anti-MuSK binding antibodies from 19 MuSK-MG patients. The sample binding response and confirmatory binding of each anti-human immunoglobulin reagent to each bound sample are summarized. Patients are shown grouped by antibody isotype/subclass profile.

			Anti-human Immunoglobulin Responses (RU)					
Patient	**Sample Month**	**Sample Response (RU)**	**IgM**	**IgG**	**IgG1**	**IgG2**	**IgG3**	**IgG4**
Group 1a - Isotype: IgM, IgG and Subclass: IgG3, IgG4								
6	0	489.56	415.30	316.13	-	-	-	49.10
	2	555.67	402.51	391.73	-	-	-	67.35
	3	147.14	91.18	218.91	-	-	1.82	69.03
	60	134.88	234.51	147.81	-	-	9.56	38.24

			Anti-human Immunoglobulin Responses (RU)					
Patient	**Sample Month**	**Sample Response (RU)**	**IgM**	**IgG**	**IgG1**	**IgG2**	**IgG3**	**IgG4**
7	0	550.90	-	546.99	-	-	3.63	89.80
	13	423.96	-	467.92	-	-	2.45	87.40
	22	99.09	15.46	222.55	-	-	3.03	74.07
8	0	171.31	9.32	237.63	-	-	3.00	61.21
	5	144.67	-	250.09	-	-	3.71	64.24
10	189	34.76	18.32	93.45	-	-	3.57	30.81
Group 1b - Isotype: IgG and Subclass: IgG3, IgG4								
1	0	250.15	-	215.63	-	-	2.66	28.79
	6	236.95	-	245.45	-	-	3.54	29.30
	66	57.93	-	134.04	-	-	1.01	43.59
12	0	122.10	-	262.67	-	1.15	2.83	87.70
	1	279.89	-	366.34	-	1.17	2.28	79.08
	17	47.21	-	213.73	-	1.37	1.93	63.04
	145	200.84	-	310.09	-	0.50	3.28	74.77
	154	139.59	-	235.80	-	0.53	1.14	65.30
	157	111.60	-	206.92	-	0.72	2.89	86.93
Group 2a - Isotype: IgM, IgG and Subclass: IgG1, IgG4								
14	0	198.92	32.93	271.71	27.69	-	-	81.87
	33	107.71	55.36	182.88	23.69	-	-	74.88
	128	304.29	49.14	319.07	65.64	-	-	99.56
15	0	139.75	43.44	273.93	28.89	-	-	97.53
	3	77.32	56.02	183.07	18.99	-	-	87.17
16	0	124.62	33.89	272.92	54.08	-	-	81.53
	7	173.54	43.83	335.83	59.65	-	-	91.28
	14	124.40	29.57	383.94	65.05	-	-	118.75
	15	31.94	56.12	232.29	38.54	-	-	108.31
19	0	129.11	21.03	191.68	82.83	-	-	106.76
	1	247.10	-	418.31	31.05	-	-	129.20
Group 2b – Isotype: IgG and Subclass: IgG1, IgG4								
17	0	458.16	-	685.09	45.67	-	-	177.01
	1	83.45	-	332.03	31.25	-	-	147.26
Group 3a – Isotype: IgM, IgG and Subclass: IgG1, IgG3, IgG4								
11	0	72.22	-	128.14	2.45	-	5.51	40.06
	3	54.78	11.12	100.14	0.71	-	4.02	34.80
	17	189.80	-	200.58	8.27	-	3.24	40.07
	34	38.61	-	109.11	6.11	0.80	5.42	31.61
	37	118.51	-	128.94	3.65	0.54	4.07	35.19
	40	100.19	-	175.97	9.93	-	4.79	48.35
	44	13.01	7.73	83.67	-	-	4.04	48.44
13	0	332.92	-	365.79	4.83	-	2.47	77.34
	0.3 *(9 days)*	325.30	18.00	309.36	-	-	1.97	80.31
	14	345.96	11.53	359.87	2.41	-	1.11	138.71
Group 3b – Isotype: IgG and Subclass: IgG1, IgG3, IgG4								
2	0	395.76	-	353.25	25.63	-	10.35	33.84
	34	528.21	-	500.30	21.46	-	18.91	81.36
	133	71.37	-	160.93	28.70	-	9.83	18.47

			Anti-human Immunoglobulin Responses (RU)					
Patient	**Sample Month**	**Sample Response (RU)**	**IgM**	**IgG**	**IgG1**	**IgG2**	**IgG3**	**IgG4**
3	0	313.95	-	375.21	15.01	-	3.52	73.10
	7	142.15	-	258.15	5.12	-	4.47	51.17
4	0	154.47	-	271.50	40.33	-	8.68	42.00
	1	196.15	-	283.01	51.92	-	17.41	44.91
5	0	88.24	-	187.96	8.49	-	4.82	44.36
	2	36.29	2.44	145.21	6.78	-	4.33	37.23
9	0	141.67	-	249.77	6.66	-	7.33	55.57
	2	91.93	-	232.81	1.06	-	4.48	58.08
Isotype: IgG and Subclass IgG4 with switch from IgG1 → IgG2								
18	0	103.42	-	362.30	36.73	-	-	144.24
	11	153.64	-	414.11	-	19.49	-	149.87

2.3.9 Serial analysis of relative antibody dissociation rates

Antibody dissociation rates (k_d) were determined for the 55 serum samples positive for MuSK antibodies. Diluted sera were injected over a low MuSK surface density (~300RU) at a high flow rate of 60µL/min. A low surface density was used to minimize mass transport limitations and to reduce avidity effects due to the bivalent nature of antibodies. Similarly, a high flow rate was also used to minimize mass transport limitations and minimize rebinding of antibodies during dissociation. The resulting dissociation phases of the sensorgrams were fitted to a 1:1 (Langmuir) binding model to obtain antibody dissociation rates (s^{-1}). The antibody dissociation rates for all of the samples analyzed are shown in Table A1 of the appendix. Figure 2-12 shows a representative plot of sensorgrams from serial samples of one patient (patient 12), with the corresponding dissociation rates.

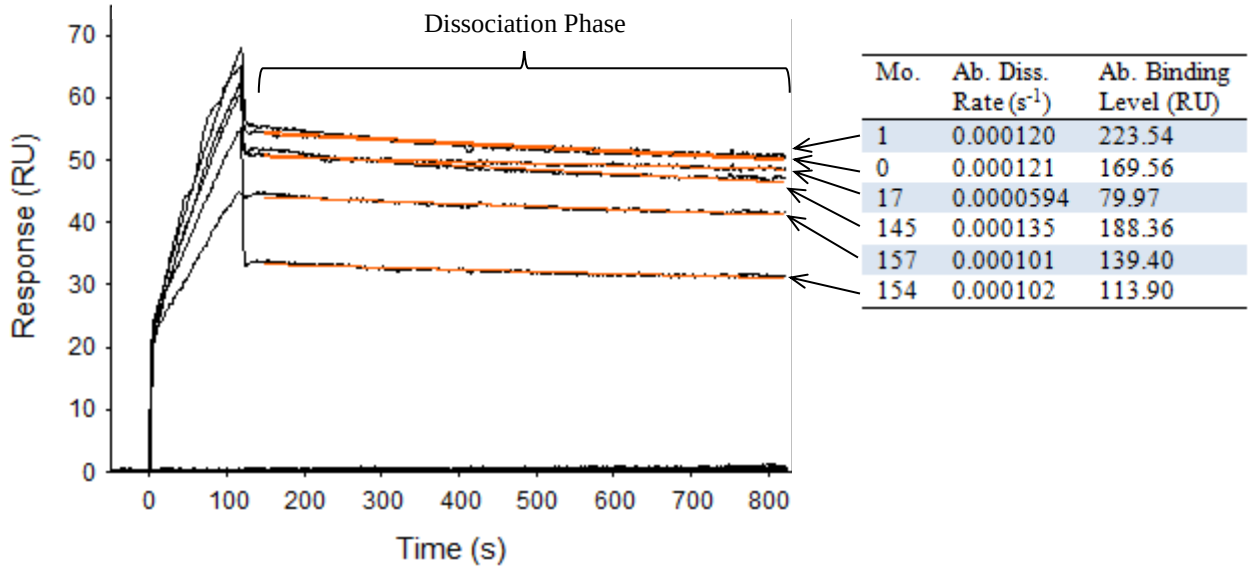

Mo.	Ab. Diss. Rate (s^{-1})	Ab. Binding Level (RU)
1	0.000120	223.54
0	0.000121	169.56
17	0.0000594	79.97
145	0.000135	188.36
157	0.000101	139.40
154	0.000102	113.90

Figure 2-12 A representative plot of sensorgrams from serial samples of one patient. Diluted sera were injected over a low density (~300RU) MuSK active surface and BSA reference surface at a flow rate of 60µL/min, with a 10-minute dissociation phase. The sensorgram dissociation phases were fit to a 1:1 binding model, shown by the orange fit lines, to obtain dissociation rates (s^{-1}). The sensorgrams, with corresponding dissociation rates, of serial samples from patient 12 are shown here.

Dissociation rates are an approximate indicator of relative binding affinity, with antibodies of a higher affinity often having a slower dissociation rate, and antibodies of a lower affinity having a faster dissociation rate[208]. Antibody maturation is often reflected in slower dissociation rates. Since the antibody population in serum is of a polyclonal nature, the dissociation rates calculated represent a weighted average of the dissociation rates of the different populations of antibody clones[209]. The calculated dissociation rates can therefore be called "apparent dissociation rates", which are indicators of apparent affinity.

The dissociation rates for the 55 samples assayed from the 19 MuSK-MG patients ranged in magnitude from 2.67×10^{-5} to 6.69×10^{-4} s^{-1}, a 25-fold difference. To examine trends in the serial

samples, dissociation rates were plotted against the antibody binding levels for each patient, as shown in Figure 2-13. Patient 10 was not included as 5 out of 6 samples had negative or borderline levels of antibodies, therefore a trend in dissociation rate could not be determined for this patient. As with the antibody binding levels (section 2.3.7), the serial profiles are patient-specific but a few general trends were observed.

In 11/18 patients, dissociation rate and binding response had a linear monotonic relationship ($R^2 > 0.90$). In 3 out of these 11 patients (patients 1, 8, and 18) the relationship was positive, as binding response increased so did the dissociation rate (i.e. relative affinity decreased). In the other 8 patients (patients 2, 3, 4, 5, 9, 16, 17, and 19), the relationship between binding response and dissociation rate was negative, as binding response increased dissociation rate decreased (i.e. relative affinity increased). However, all but 3/11 of these patients (patients 1, 2, 16) had only two serial samples, making it difficult to make any conclusions on whether these trends were sustained throughout the course of the disease. There was no consistent relationship between antibody dissociation rates and binding levels in the remaining 7/18 patients.

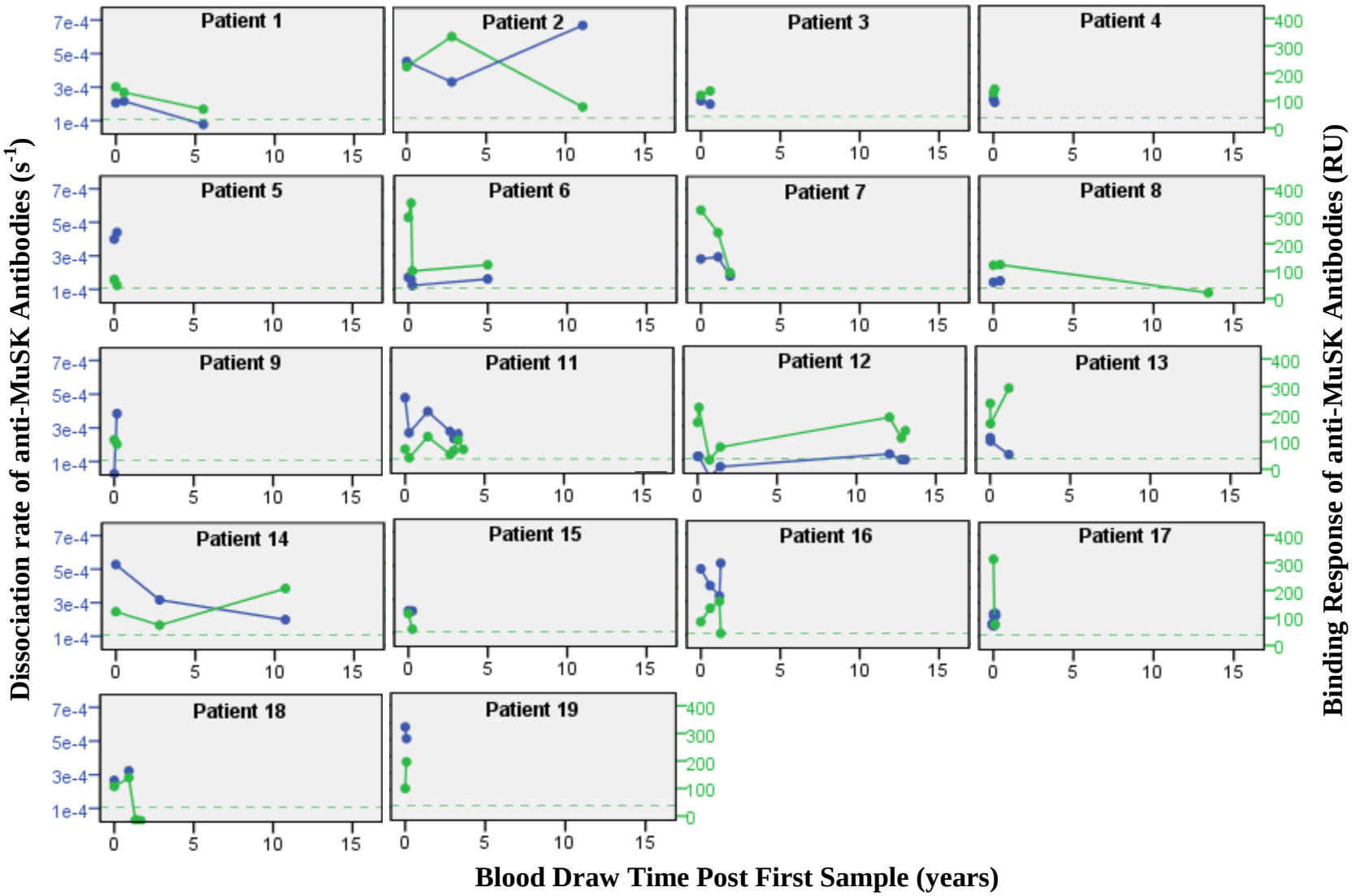

Figure 2-13 Serial MuSK antibody dissociaton rates. Antibody dissociation rates (k_d) are plotted together with binding responses for 18 MuSK-MG patients. The dotted line represents the cut-of for MuSK-Ab positivity. Patient 10 is not depicted here as 5/6 samples were negative or borderline for MuSK-Abs, therefore k_d trends could not be determined.

To determine if overall there is a relationship between changes in antibody binding levels and dissociation rates, a Spearman's correlation was performed. There was no significant correlation between binding response and dissociation rate (r_s = -0.240, p = 0.084), as seen in Figure 2-13. Even when the 11 patients who had a monotonic relationship were divided into groups based on whether the relationship between the two variables was positive or negative, there was still no significant correlation.

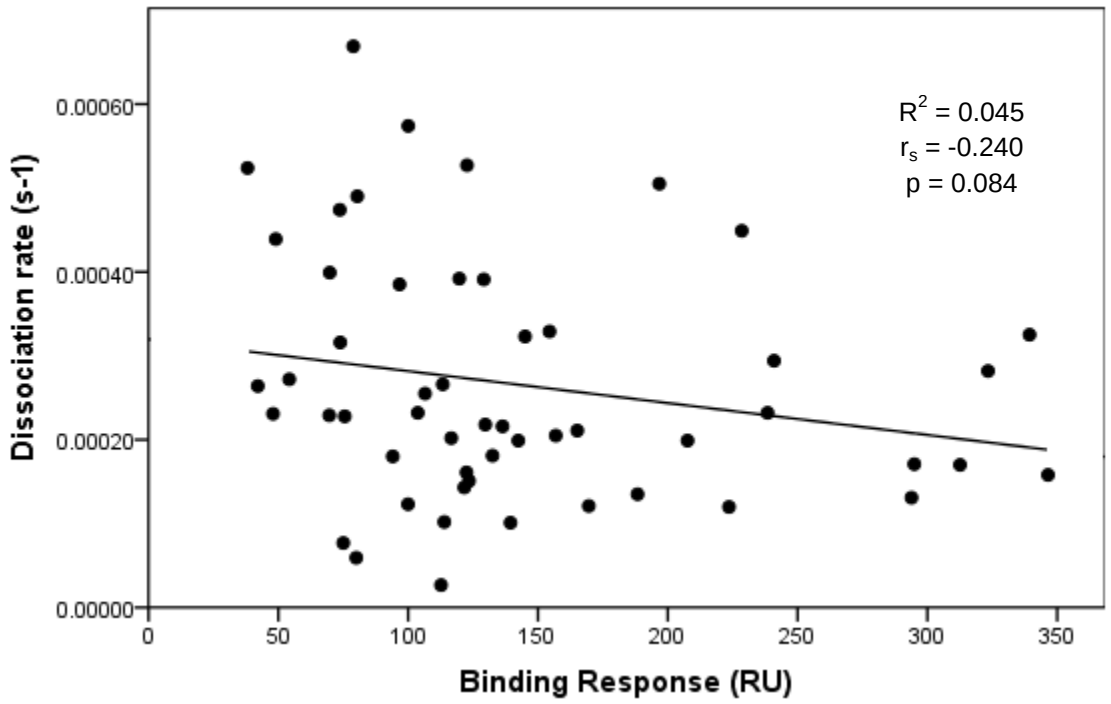

Figure 2-14 Correlation between antibody binding response and dissociation rate of MuSK antibodies. R^2, Spearman's correlation coefficient (r_s), and p-value are shown (p-value < 0.05 is significant).

2.3.10 A clinical case study: Rituximab treatment of a MuSK-MG patient

Changes in antibody levels, dissociation rates, and isotype and subclass specificities over time may correlate with clinical progression of MG. Here, a clinical case study is presented of one of

the MuSK-Ab positive MG patients studied (patient 18). A review of the patient's clinical chart was performed, with information collected on progression of symptoms and treatment over approximately a 2-year period after onset. The patient gave written consent to participate.

This case is of a 44-year-old woman who presented in November 2011 with diplopia. She was first seen at the UBC Hospital MG Clinic four months later in March 2012, at which time her diplopia was still ongoing and she was taking prednisone at 25mg daily. Her activities of daily living (MG-ADL) score [210] upon examination was 5. SFEMG was equivocal, but she had a positive edrophonium chloride (Tensilon) test. Chest computerized tomography (CT) was normal. Serological testing for AChR antibodies was negative (UBC Neuroimmunology Lab). She was treated with pulse steroids (IV methylprednisolone) over a period of two weeks in April 2012. She continued to have diplopia as her only symptom until the end of 2012, just over one year post-onset. In February 2013, she was seen with increasing symptoms of severe diplopia, now accompanied by facial and bulbar weakness, with weakness of the tongue and perioral muscles manifesting as fatigued chewing, intermittent dysphagia, and slurring of speech with prolonged conversation. Her MG-ADL score was now 8. Testing for MuSK antibodies was found positive (A. Vincent, Oxford, UK). Retrospective measurement performed by us in assays presented in this chapter showed that her MuSK antibody levels were higher than her first visit in March 2012 (Figure 2-15). As seen previously, her antibodies were predominantly IgG4, however there appeared to be a class switch from IgG1 to IgG2, which was unusual in the patients studied here (shown previously in Table 2-5).

In March 2013, she received three rounds of plasmapheresis with dramatic resolution of her facial and oral weakness, including resolution of her diplopia, with a concomitant decrease in MG-ADL score from 7 pre-plasmapheresis to 0 post-plasmapheresis. Her symptoms soon

returned however, including the dysphagia, so she was subsequently treated with two infusions of rituximab at 1000mg IV over a period of two weeks in late April to early May 2013. Rituximab, a monoclonal antibody specific for cell surface CD20 on B lymphocytes, is primarily used in the treatment of B-cell non-Hodgkin lymphoma[211] but has also been found successful in treating a variety of autoimmune diseases, including MG. There is accumulating evidence that rituximab is particularly effective in the treatment of MuSK-MG[187-190, 212, 213].

Upon examination two days after the second infusion of rituximab, the patient's MG-ADL score was 8. By July 2013, only two months after her second rituximab infusion, she was in complete remission with an MG-ADL score reduced to 0. All of her symptoms had resolved, she had no ptosis, diplopia, no problems with speech, swallowing or chewing, had strong neck flexors and no weakness in arms and legs. Remarkably, her MuSK antibody levels had also now become negative (Figure 2-15). At this point she was on prednisone 40mg every other day, on a tapering schedule of 5mg every month. She was seen again in August 2013, three months post-rituximab, in continued remission of her MG with an MG-ADL score of 0, an MG quality-of-life 15 (MG-QOL15)[214] score of 0, and a quantitative MG (QMG)[215] score of 2 (one point each for right hand grip and head lift). In November 2013, over 6 months post-rituximab treatment, she continued to be in remission with MG-ADL of 0, MG-QOL15 of 0, and QMG of 2 (right hand grip and head lift). At this point her prednisone was down to 5mg, and her MuSK antibody levels continued to be negative.

In this case study we see that parallel to clinical improvement following rituximab treatment this patient's antibody titers became negative, and remained consistent for at least 6 months following end of treatment, with a minimal dose of prednisone. This case study resembles the many others reported in the literature on the successful treatment of refractory MuSK-MG with

rituximab[187-191, 212, 213, 216]. This case demonstrates that serial testing of MuSK-Ab titers after therapy therefore aids in the monitoring of therapeutic response.

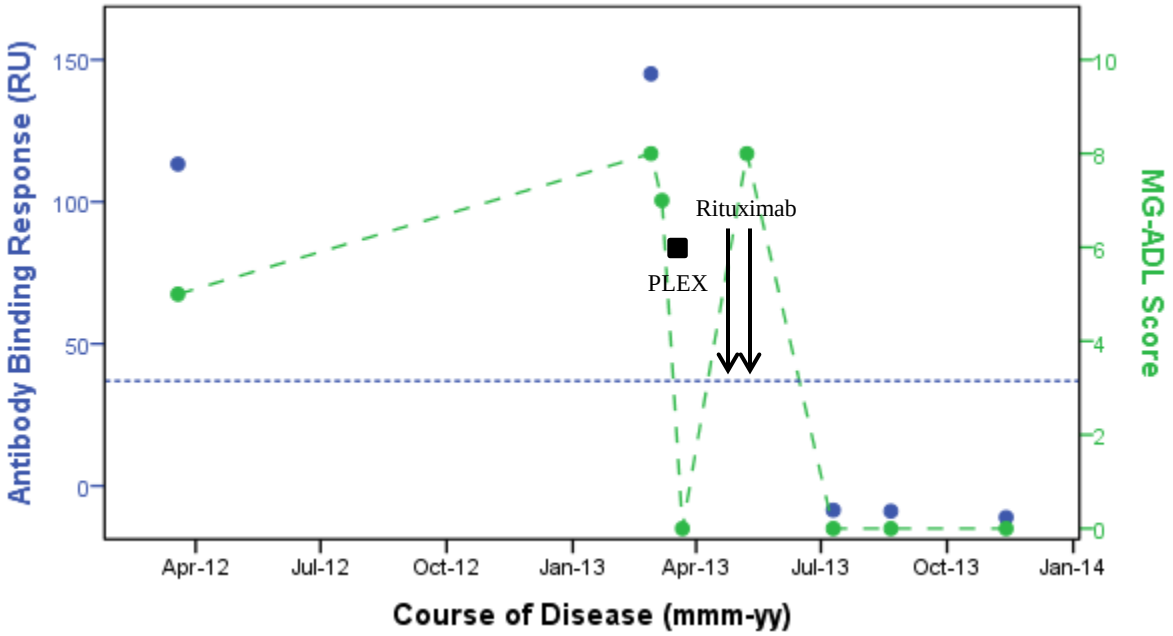

Figure 2-15 Clinical response to rituximab treatment. MuSK antibody levels (binding response) and ADL scores shown over course of 20 months for patient 18. *Plex*: square indicates a 3-day course of plasma exchange. *Rituximab*: each arrow indicates an intravenous administration of 1000mg. Dotted line represents cut-off for antibody positivity.

Chapter 3: Preliminary studies in the immobilization of membrane-bound human acetylcholine receptor

3.1 Introduction

Functional immobilization of transmembrane proteins requires consideration of their structural and physiological need of remaining in a membrane-bound form[217]. This potentially makes the development of biosensor assays for membrane-bound proteins more complex. This is particularly true for proteins with a complex structure and conformationally-dependent epitopes, like the AChR.

Previous attempts have been made to functionally immobilize AChR onto sensor surfaces through techniques like using AChR-rich tethered lipid membranes[218] or using biotinylated bungarotoxin to capture AChR reconstituted into lipid vesicles[219]. However, these techniques are quite complex and time-consuming, and have used AChR extracted from *Torpedo* eel electric organs. We sought to develop a method for immobilizing human AChR onto a sensor chip in its membrane-bound native and functional conformation which would be simpler and potentially applicable to detecting anti-AChR antibodies.

An interesting study by Pick *et al.*[220] has demonstrated a simple technique for producing native vesicles straight from the membrane of mammalian cells in culture. Formation of these vesicles uses a simple process whereby cells are incubated with cytochalasin B, a toxin known for destabilizing cytoskeleton-membrane interactions. This causes cells to produce tubular extensions which bud off as native vesicles when agitated. In this study specifically, the authors produced vesicles from adherent human embryonic HEK293 cells expressing the ion channel 5-HT_3, a receptor part of a family of ligand-gated ion channels which also includes the AChR. The

5-HT_3 receptor has a similar structure as AChR, with 5 subunits arranged around a central ion pore. This study showed that vesicles produced in this way maintained the cell-surface receptors in their native orientation and function.

Based on the success reported in this study, we took as an aim of our study to determine if similar vesicles could be produced from AChR-expressing cells and immobilized onto a sensor chip. The cells used were the human AChR-expressing rhabdomyosarcoma cell lines TE671 and CN21. TE671 cells express the fetal isoform of AChR, while the CN21 cells are TE671 cells which have been transfected with cDNA encoding the ε subunit to express high levels of adult AChR[53]. These cell lines are used as a source of AChR for the RIPA diagnostic assay for MG. Vesicles produced from these cells would be immobilized onto a Biacore L1 sensor chip, a chip specifically made for the direct capture of lipid vesicles and membranes. The L1 sensor surface consists of a dextran matrix modified with lipophilic residues (alkyl chains) which directly insert into the membrane, retaining its bilayer structure[202].

The specific aims of the studies presented in this chapter were to confirm AChR expression on the TE671 and CN21 cells, produce native vesicles via the cytochalasin vesiculation method, and test the immobilization and activity of these vesicles on an L1 sensor surface.

3.2 Methods

3.2.1 Cell lines, media, and growth conditions

The rhabdomyosarcoma cell lines TE671 and CN21 (kindly gifted by Drs. D. Beeson and A. Vincent, Weatherall Institute of Molecular Medicine, Oxford, UK) were maintained in Dulbecco's Modified Eagle's Medium (DMEM) supplemented with 10% fetal bovine serum

(FBS), 2mM L-glutamine, 0.075% sodium bicarbonate, 100U/mL penicillin, 100ug/mL streptomycin, and 0.25ug/mL amphotericin B, at 37^{o}C and an atmosphere of 5% CO_2. Cells were passaged twice weekly at 1:12 - 1:18 dilution with a limit of 25 passages.

In some instances, cells were cultured with 1 or 5mM nicotine during the proliferative growth phase to increase AChR expression. L-Nicotine (Sigma) solutions of 500mM were prepared in serum-free medium DMEM, neutralized with 6M HCl, and filtered using a 0.22μm filter. After passaging, cells were left to adhere and proliferate for 18h before the nicotine solution, freshly diluted in culture media, was added. Cells were cultured with nicotine-containing media for a further 2 days.

3.2.2 Immunofluorescence

TE671 and CN21 cells were cultured overnight (to reach 50-70% confluency) on 12mm coverslips placed in 24-well cell culture plates, at 37^{o}C and 5% CO_2. The following day, coverslips where gently rinsed with 4^{o}C phosphate buffered saline (PBS) and immediately fixed with 4% paraformaldehyde for 15 min at room temperature (RT). After rinsing with PBS, cells were labelled with anti-AChR monoclonal antibodies [mAb; anti-α-subunit (D6) and anti-ε-subunit (B-11), Santa Cruz Biotechnology], or with isotype control mAbs (normal mouse IgG_{2b} and mouse IgG_1, Santa Cruz Biotechnology), at 4μg/mL in PBS + 2% normal goat serum (NGS) buffer, for 1hr at RT in a humidified chamber. Cells were washed three times with PBS and incubated with anti-mouse-Alexa Fluor 488-conjugated secondary antibody (Invitrogen-Molecular Probes) at 1:1000 in PBS + 2% NGS buffer, for 1hr at RT in the dark. Cells were washed three times in PBS, and nuclei counterstained with Hoescht 33342 stain. Coverslips were mounted on slides in fluorescence mounting medium (SouthernBiotech), at stored at 4^{o}C protected from light before imaging.

3.2.3 Radioligand binding assays

Radioligand binding assays were performed to measure AChR expression on the cell surface. Confluent cells, cultured without and with nicotine added to growth media for (1mM and 5mM), were harvested using 0.5mM EDTA, washed with media to neutralize EDTA, and spun at 1500rpm for 5min to pellet cells. Cells were washed, resuspended in assay buffer (PBS, 1% FBS, 0.1% NaN_3) and 10^6 cells added to round bottom tubes. Cells were incubated with 0-50nM of alpha-bungarotoxin-I^{125} (αBT-I^{125}) for 1hr on ice, in a total reaction volume of 200μL. To determine non-specific binding, cells were pre-incubated for 1hr on ice with 10μM of non-labelled αBT prior to adding αBT-I^{125}. Cells with bound αBT-I^{125} were separated from free toxin with three washes of centrifugation at 500g for 5min, followed by aspiration of supernatant and resuspended in assay buffer as above. Following the last wash, supernatant was aspirated and cell pellets counted using a gamma counter. To analyze results, non-specific binding values (in counts per minute, CPM) were subtracted from total binding values to determine specific binding. CPM values were converted to disintegrations per minute (DPM) by dividing by the detector efficiency.

3.2.4 Flow cytometry

Flow cytometry was used to detect antibody binding of patient serum IgG to the surface of TE671 cells. Both AChR-Ab positive and MuSK-Ab positive samples (previously tested by standard radioimmunoprecipitation assay) were tested. In brief, the cells were detached using 0.5mM EDTA, washed with media to neutralize the EDTA, and spun at 1500rpm for 5min. Cells were washed twice and resuspended in ice cold FACS buffer (PBS, 1% FBS, 0.1% NaN_3), and 10^6 cells added to round bottom tubes for staining. Cells were incubated with for 1hr on ice with human sera diluted to a final dilution of 1:10 once added to the cells. The cells were then washed

twice with FACS buffer and incubated with fluorescein isothiocyanate (FITC)-conjugated rabbit anti-human-IgG secondary antibody (Pierce-Thermo Scientific), diluted 1:50 in FACS buffer, for 45min at 4^{o}C in the dark. The cells were washed again as above, suspended FACS buffer, and immediately analyzed using an LSR II flow cytometer (Becton Dickinson). A population of 10^4 cells were gated based on side scatter and forward scatter, excluding cell fragments or dead cells.

3.2.5 Cell membrane vesicle preparation

Vesicles were prepared by cell membrane blebbing according to methods in Pick, H *et al*.[220], with some modifications. Briefly, vesiculation was induced by incubating an 80% confluent cell layer at 37^{o}C for 40-60min with 10µg/mL cytochalasin B (Sigma) in pre-warmed serum-free DMEM medium. Following incubation, the culture flasks were agitated on an orbital shaker to help dissociate vesicles from cell bodies. The media was removed and centrifuged at 500g for 5min to pellet any cellular debris. To pellet the vesicles, the supernatant was removed and centrifuged at 15 000g for 30min. The supernatant was discarded and vesicles resuspended in PBS for storage at 4^{o}C up to one week.

3.2.6 Membrane vesicle immobilization and testing of AChR activity

The prepared cell membrane vesicles were immobilized onto a L1 sensor chip (GE Healthcare) using a Biacore™ 3000 system. The sensor surface was conditioned with two 60-second injections of 20mM CHAPS detergent (3-[(3-cholamidopropyl)-dimethylammonia]-1-propan-sulfonate) at 20µL/min. Detergent-free HBS-N buffer (0.01M HEPES pH 7.4, 0.15M NaCl, GE Healthcare), filtered and degassed, was used as running buffer.

Vesicles suspended in HBS-N were immobilized by injection over the sensor chip surface at a low flow rate of 1-2uL/min until the binding response on the sensorgram reached a plateau,

indicating complete surface coverage. Complete surface coverage at this flow rate typically took about 60-90min. The surface was washed with 50mM NaOH to remove unbound vesicles. Non-specific binding was tested with a pulse of BSA (0.1mg/mL in running buffer). A fully covered surface had only a minor binding of BSA (<50RU). This step also served as a blocking step to prevent non-specific binding of analyte.

The presence and activity of AChR on the immobilized vesicles was probed using anti-AChR mAbs [anti-α-subunit (D6) and anti-ε-subunit (B-11), Santa Cruz Biotechnology] and high affinity αBT. Analytes were diluted in running buffer and injected over the immobilized surface at 10μL/min for 2.5min. Regeneration of the vesicle surface was performed by selective dissociation of the bound analyte using 10mM glycine-HCl at 30μL/min.

3.3 Results

3.3.1 AChR expression on TE671 & CN21 cells using immunofluorescence

Immunofluorescence was used to confirm expression of AChR on the TE671 and CN21 cell lines. A mAb against the AChR alpha subunit was used to detect expression on both cell lines, while a mAb against the AChR epsilon subunit, specific for the adult AChR isotype only, was used to detect the expression of adult AChR on the CN21 cell line. Results are shown in Figure 3-1.

Binding of anti-AChRα mAb confirmed AChR expression on both TE671 and CN21 cells, with some cells appearing more densely stained than others. The staining pattern differed between the two cell lines, with staining on TE671 cells extending along the entire plasma membrane while staining on CN21 cells was more localized close to the nucleus. A much stronger signal was seen

with the adult-specific anti-AChRε mAb on the CN21 cell lines, which is expected as expression of the adult AChR subtype is high in the CN21 cell line[53]. There was limited binding with the anti-mouse IgG isotype controls, showing the specificity of the secondary antibody.

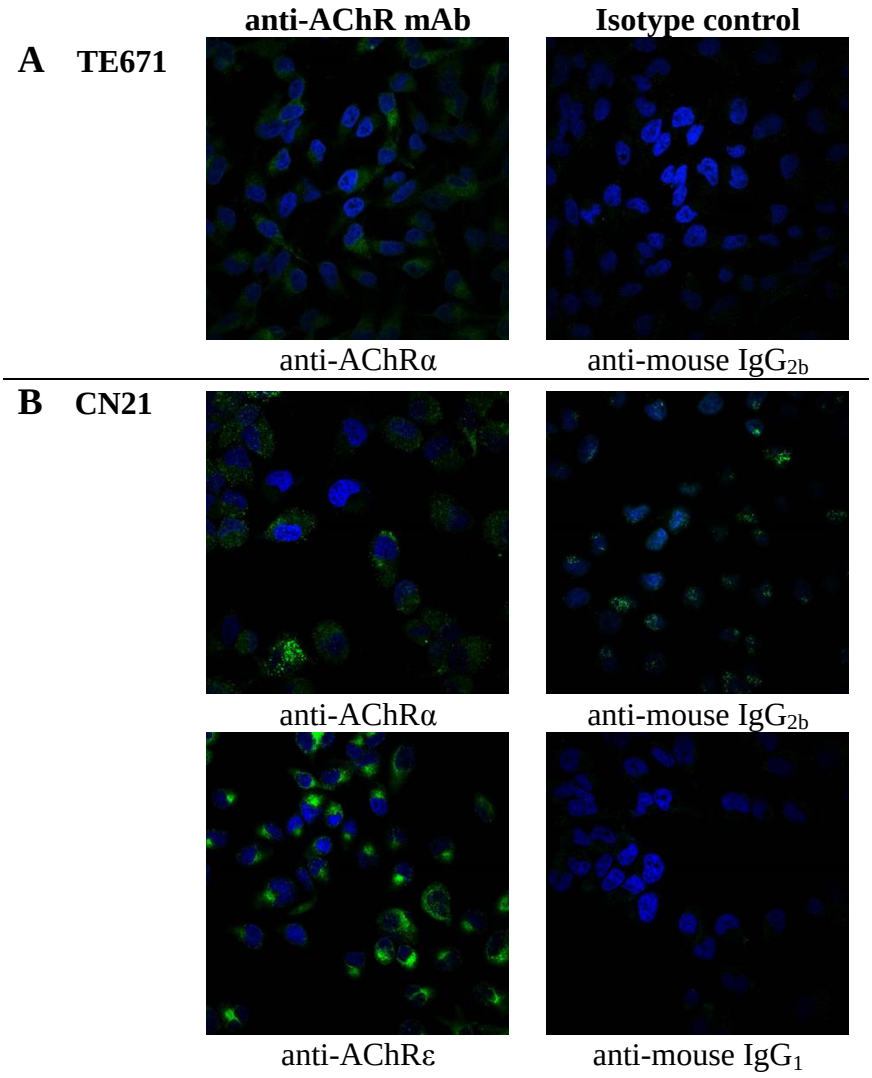

Figure 3-1 Expression of cell-surface AChR expression on TE671 and CN21. (A) Binding of anti-AChRα mAb and isotype control to TE671 cells. (B) Binding of anti-AChRα and adult-AChR-specific anti-AChRε mAbs to CN21 cells, with respective isotype controls.

3.3.2 Dose-dependent effect of nicotine on αBT-I^{125} binding

To confirm AChR expression on the cell lines, radioligand binding assays were performed using high affinity αBT-I^{125}. Specific binding levels of αBT-I^{125} were examined not only in cells cultured as usual, but also in cells cultured with 1mM and 5mM nicotine for 2 days, as nicotine has been shown to induce up-regulation of nicotinic AChR on TE671 and other AChR-expressing cells[221-223]. Increased binding levels of toxin would therefore be specific for AChR expression. Binding of increasing concentrations of αBT-I^{125} to TE671 cells cultured with 1mM and 5mM nicotine compared to no nicotine (control) are shown in Figure 3-2.

There was a dose-related increase in specific binding of toxin with increased nicotine concentration. Compared to control cells, 1mM nicotine increased specific binding of αBT-I^{125} by an average of 148.3 ± 9.0%, while 5mM nicotine increased specific binding by an average of 236.1 ± 15.1%. The increase in toxin binding suggests an apparent increase binding site density, and therefore an increase in AChR number on the cell surface. The increases in binding were statistically significant as the 95% confidence intervals (95% CI) do not overlap.

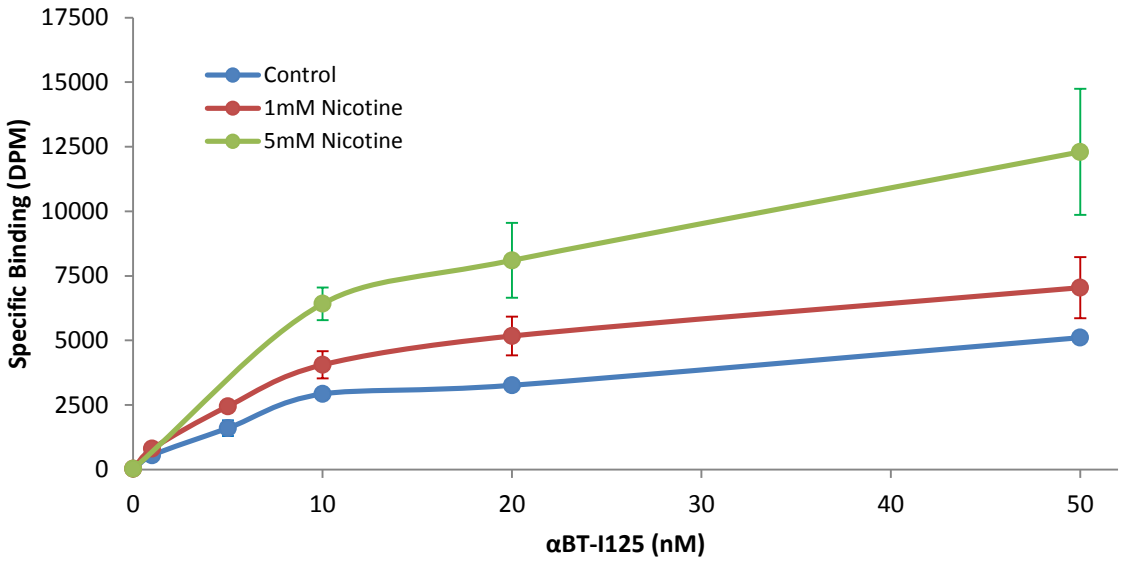

Figure 3-2 The effect of nicotine on αBT-I^{125-} binding to TE671 cells. Specific binding curves of 0-50nM of αBT-I^{125} to cells cultured without and with 1mM and 5mM nicotine. Each point represents the mean binding to 10^6 cells. Toxin binding is significantly elevated over control levels by 1 and 5mM nicotine (mean values ± 95% CI from duplicate determinations).

3.3.3 Binding of MG serum IgG to muscle-like cell line

Flow cytometry was used to detect binding of antibodies in serum from MG patients to the muscle-like TE671 cell line. Not only was serum from AChR-MG patients tested, but as the TE671 cell line is also known to express MuSK[224], serum from MuSK-MG patients was also tested to see if there was a difference in sensitivity. In all, 5 AChR-Ab positive (AChR1-5, in order of decreasing antibody titer as determined by radioimmunoprecipitation) and 3 MuSK-Ab positive samples (MuSK1-3, in order of decreasing antibody titer as determined by Biacore assay) were tested and results compared with 5 healthy control sera (Figure 3-3).

The healthy controls bound quite variably to the TE671 cells, with a median fluorescence intensity (MFI) value of 1198.8 ± 251.3. There appeared to be a high degree of non-specific binding with the healthy control sera, which can be seen when comparing MFI values of the

individual samples to cells incubated without antibody (MFI = 405.0) or with secondary antibody alone (MFI = 472.0). This is likely why only 2 of the 5 AChR-Ab positive samples (AChR1 and AChR2), which were the samples with the highest titers as determined previously by radioimmunoprecipitation, showed binding of IgG greater than that of the mean MFI ± 3SD (1922.8) of control values. While the MFI values did appear to correlate with antibody titers, the binding sensitivity appeared to be low. Interestingly, the MuSK-Ab positive samples showed stronger binding than the AChR-Ab positive samples, and MFI levels also correlated with antibody titers. Two of the 3 MuSK-Ab positive samples showed binding greater than the mean ± 3SD of control values, and the third which was of a very low titer by Biacore assay (sample 33, Figure 2-9, Chapter 2) was close to borderline.

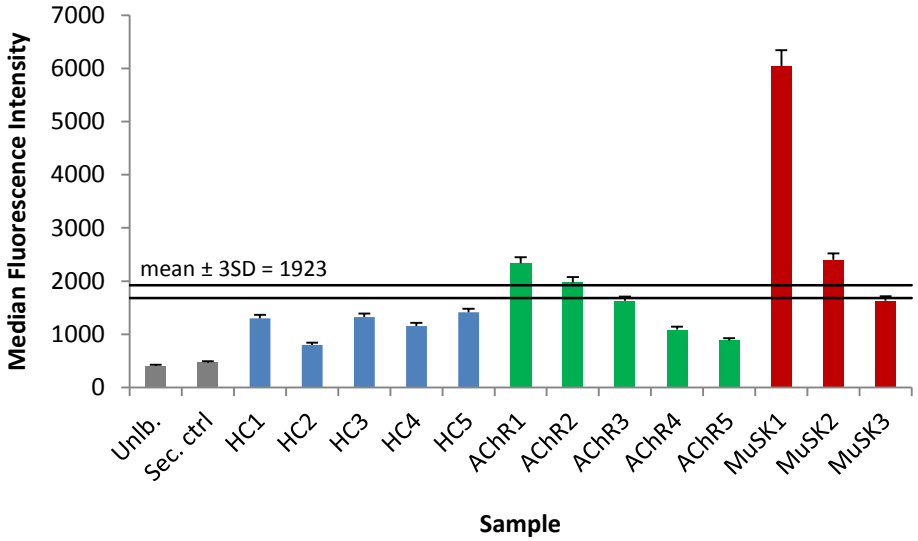

Figure 3-3 Binding of IgG from MG patients to TE671 cells. Cutoff value is mean ± 3SD of 5 healthy control samples (mean ± 2SD also shown). Unlb. = unlabelled cells, sec. ctrl = cells labelled with secondary antibody only (data are mean ± SEM of duplicate values).

3.3.4 Membrane vesicle immobilization onto L1 chip and testing of surface activity

To determine whether membrane vesicles produced from AChR-expressing TE671 or CN21 cells could be immobilized onto Biacore L1 chips and the surface subsequently used to detect binding of ant-AChR analytes, vesicles were prepared and immobilized onto L1 chips. Membrane vesicles were produced through a membrane-blebbing procedure involving the cytoskeleton-destabilizing toxin cytochalasin B, as described above. Figure 3-4 shows a typical immobilization sensorgram of membrane vesicles.

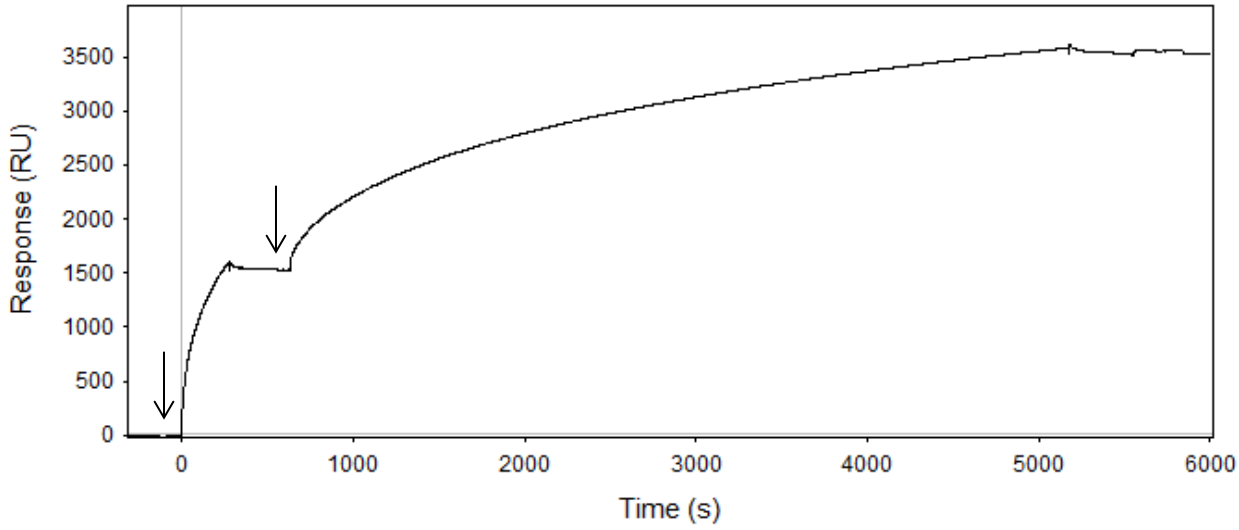

Figure 3-4 Typical immobilization sensorgram of cell membrane vesicles on L1 chip. In this example, a binding response of ~3400RU was reached following immobilization of TE671 membrane vesicles in a 2-step injection (shown by arrows) over a course of about 1.5hrs, until a plateau was reached demonstrating surface coverage.

To confirm the presence and activity of AChR on the immobilized vesicles, binding of anti-AChR mAbs and the high affinity analyte alpha-bungarotoxin was assessed. These tests were found to be inconclusive of AChR activity as there was no binding detected to the immobilized

surface, indicating either the vesicles did not contain AChR, either at all or at a high enough density to be detected, or the AChRs were not in their native conformational state.

Chapter 4: Discussion and Conclusion

4.1 Summaries and Discussion

Characterizing antibodies helps with understanding the underlying immunological process and, in the case of autoimmune diseases like MG, the pathogenic mechanisms whereby autoantibodies cause disease. The Biacore™ biosensor is an ideal system for the detection and characterization of antibody-antigen interactions as it provides a real-time picture of the entire interaction, from association to dissociation, unlike more commonly used immunoassays which are end-point assays. Biacore systems generate unique data on molecular interactions, including yes/no binding, measurement of concentration, binding stability, immunoglobulin isotype and subclass, and binding affinity and kinetics, to provide a comprehensive characterization of the immune response.

In this thesis, the main focus was the development and optimization of a Biacore assay for measuring and characterizing MuSK autoantibodies in serum of MuSK-MG patients. We demonstrate the use of this assay in analyzing the temporal changes in antibody levels, dissociation rate, and isotype and subclass distributions in serial serum samples from MuSK-MG patients (presented in chapter 2). Preliminary studies were also conducted in the immobilization of membrane-bound human AChR onto a sensor surface (presented in chapter 3).

4.1.1 Summary and Discussion of Chapter 2

Currently, MuSK antibodies are measured using a radioimmunoprecipitation assay (RIPA), and the test is generally requested by clinicians for diagnostic purposes only. Although RIPA is proven to be a very robust method for antibody detection, the test is limited to a qualitative to semi-quantitative measurement. Furthermore, this type of immunoassay is also limited to

detecting antibodies of moderate to high affinity, since only end-point measurements are captured following multiple incubation and wash steps.

In chapter 2, we presented the development and optimization of a novel assay using the Biacore™ platform for detecting MuSK antibodies in serum from MG patients. This type of assay platform was chosen because it enables the monitoring of the entire antibody-antigen interaction, something not provided by typical end-point immunoassays. We showed that this assay can be used not only to detect MuSK antibodies in serum, but also quantify their levels and characterize them in terms of antibody isotype, IgG subclass, and dissociation rate, an indicator of apparent binding affinity. An analysis of these parameters in serial samples of 19 MuSK-MG patients has been presented. Most importantly, we presented a case study of one of these patients who had been undergoing treatment with the anti-CD20 monoclonal antibody therapy rituximab, to demonstrate how monitoring antibody parameters over the disease course can help in a clinical setting with assessing therapeutic effect.

4.1.1.1 Assay optimization, measurement of antibody levels and dissociation rates

First, we optimized a Biacore assay for the detection of anti-MuSK antibodies in human serum. In this assay, MuSK antigen is immobilized onto CM5 sensor chips using amine-coupling chemistry, over which diluted serum is injected and binding of MuSK-Abs measured. We found that the parameters that optimize assay sensitivity and reproducibility include using a high immobilization surface density (>4500RU MuSK) to allows for high sensitivity, using BSA at an equal surface density for a reference surface, diluting pre-spun serum samples 1/10 prior to injection, and using a sample and running buffer comprised of HBS-EP with 0.02% BSA added to inhibit non-specific binding of anti-BSA antibodies or other serum matrix components to the

BSA reference surface. Using these conditions, the assay was found to have high specificity and sensitivity in detecting anti-MuSK antibodies in serum, and it was also robust, with inter- and intra-assay variability coefficients of variation not exceeding 15%.

Using this assay system, we were able to measure changes in antibody levels and dissociation rate (as a measure of binding affinity), over the disease course in a series of MuSK-MG patients. Serial analyses of 65 serum samples from 19 MuSK-MG patients, taken over a period of 1 month to 15.8 years, were presented. A dynamic temporal variability in MuSK antibody levels and dissociation rates were seen, suggesting changes in the underlying pathophysiology throughout the course of the disease. There was no correlation found between these two parameters, suggesting antibody titer and dissociation rate are regulated by different mechanisms.

4.1.1.2 MuSK-Abs are predominantly IgG4, but also IgG1 and IgM

We also showed the use of the Biacore assay in the determination of antibody isotype and IgG subclass. Following antibody binding to the immobilized MuSK, a secondary step involving binding of anti-human-Ig antibodies, targeting a specific isotype and subclass, was used to characterize isotype and subclass. The IgG subclass of an autoantibody contributes to its biological activity, and therefore the pathogenic mechanisms at play in an autoimmune disease.

The rearrangement of DNA in B cells generates an enormous diversity of different antibody molecules. Following exposure to antigen and B cell activation, class switching and somatic mutations of the Ig variable region resulting in affinity maturation occur. The first antibodies to appear in response to initial exposure to antigen early in the course of an immune response are of the IgM isotype. Class switching to IgG occurs after B cells receive further signalling in the form

of CD40 binding and exposure to cytokines, mediated by $CD4^+$ T helper cells, causing B cell activation and proliferation.

All IgGs are 150kDa Y-shaped structures comprised of two heavy chain/light chain pairs, connected by disulfide bonds in the hinge region and non-covalent bonds between the third constant domain[45]. The heavy and light chain variable regions form two antigen binding sites (Fab) and the constant regions of the heavy chain form the Fc region, which binds to Fc cell surface receptors on immune cells and to proteins of the complement system. There are four different IgG subclasses in humans, IgG1, IgG2, IgG3, and IgG4, which are named in order of their abundance in serum. In healthy individuals, the proportion of each subclass in serum is maintained within narrow ranges; IgG1 within 60-65%, IgG2 within 20-25%, IgG3 within 5-10%, and IgG4 within 3-6%[225]. The four IgG subclasses differ in their biological activity. Their main effector function difference lies in their ability to activate complement, due to differences in the amino acid sequence of their Fc region. The most effective complement activators are IgG1 and IgG3 antibodies, IgG2 antibodies are poor activators of complement, while IgG4 antibodies are deficient in the ability to activate complement[226]. Following an antigenic response, the distribution of IgG subclasses can change. The IgG subclasses that are made depend in part on the type of the antigen, with IgG1 and IgG3 antibodies predominating in response to a protein antigen, while IgG2 predominates in response to carbohydrates[227, 228]. The IgG subclasses profile is also dependent on the cytokine milieu, secreted by $CD4^+$ T helper cells with interact with and stimulate antibody-producing B cells. Th1 cells, which secrete pro-inflammatory cytokines like interleukin-2 (IL-2), interferon-gamma (IFN-γ), and tumor necrosis factor alpha (TNF-α), induce expression of complement-activating IgG1 and IgG3 subclasses in humans[229]. Th2 cells on the other hand, which secrete anti-inflammatory cytokines like interleukin-4 (IL-4), interleukin-6

(IL-6) and interleukin-10 (IL-10), induce expression of non-complement activating IgG4 antibodies in humans[229].

Due to their differences in biological activity, the antibody subclass generated in an autoimmune disease like MG plays a key role in the pathogenic mechanisms of the disease. Through analysis of the MuSK antibody isotypes and subclasses we were able to confirm that MuSK antibodies are predominantly of the IgG4 subclass, as has been described in literature[14, 89, 96, 206, 207]. In the group of 19 patients analyzed we found that all expressed IgG4 antibodies continuously over the course of their disease. Unlike in AChR-MG where IgG1 and IgG3 antibodies predominate, MuSK-MG is therefore an IgG4-mediated autoimmune disease, indicating different pathogenic mechanisms are at play in MuSK-MG compared to AChR-MG.

While normally IgG4 antibodies make up the lowest percentage of total IgG in serum (3-6%), prolonged antigenic stimulation causes significant increase in IgG4 titers[230]. IgG4 antibodies also have some unique properties. While the other IgG subclasses are pro-inflammatory, IgG4 antibodies appear to have anti-inflammatory activity[45]. Part of their anti-inflammatory activity is due to their poor ability to activate complement and immune cells due to low affinity in binding complement and Fc receptors. In addition, IgG4 antibodies undergo a posttranslational modification called Fab arm exchange, where one heavy chain/light chain half-molecule is exchanged with one from another antibody, producing IgG4 antibodies with two different antigen-binding sites. This makes them unable to cross-link two identical antigens, and therefore functionally monovalent[90]. Due to their anti-inflammatory properties, IgG4 antibodies appear to protect tissue against damage produced by the complement-fixing IgG subclasses[90]. However, there is much evidence that IgG4 antibodies are pathogenic in MuSK-MG. MuSK-MG also often

has a more severe course than AChR-MG, with patients having more bulbar symptoms and a risk for respiratory difficulties and myasthenic crisis.

While our study confirms with literature that MuSK-Abs are predominantly IgG4, we also found that a significant proportion of MuSK-MG patients also expressed IgG1 and/or IgG3 antibodies. IgG1 and IgG3 antibodies were both expressed by 13/19 patients, with 7 patients expressing both. In the patients with IgG1 antibodies, the levels of anti-human IgG1 binding were significant in most patients. This suggests that the expression of IgG1 antibodies, which are complement activators, may play a role in the pathogenicity of autoantibodies in some MuSK-MG patients. How important a role they play in relation to disease severity however needs further study, as in one study clinical fluctuations in MuSK-MG patients were found to correlate with IgG4 titers only and not IgG1[96]. In the case of IgG3 expression, we found that the levels of anti-human IgG3 binding seen was low in all patients, so their expression is likely negligible compared to IgG4 and IgG1 expression. Interestingly, we also found that 11/19 patients expressed IgM continuously, most at low levels, but in one patient the binding levels of anti-human IgM were as high as the anti-human IgG levels. The presence of continuous levels of IgM could indicate lack of affinity maturation or continuous re-induction of the disease process.

4.1.1.3 Monitoring antibody status as indicator of therapeutic response: a case of rituximab therapy for IgG4-mediated MuSK-MG

Previous studies have already shown evidence that disease severity in MuSK-MG patients correlates with antibody levels[95] and is also dependent on IgG isotype, with IgG4 titers also correlating with disease severity[96]. In this chapter, we showed a similar association between

antibody status and clinical status in the case study of patient 18, where antibody levels became negative following treatment with rituximab and the patient entering remission.

This patient initially presented with diplopia, which over a period of a year led to more severe bulbar symptoms. Early on she was treated with prednisone and a few rounds of plasmapheresis, but nothing brought about dramatic improvement of her symptoms until she was treated with two infusions of the anti-CD20 monoclonal antibody therapy rituximab. Her MuSK-Abs were IgG4, and we found that, following rituximab therapy, her antibody levels became negative, with a concordant decrease in clinical severity of MG-ADL levels. This case study showed that following antibody levels throughout the course of disease may allow for better monitoring of disease progression and response to treatment in MuSK-MG patients.

This case study also confirmed the increasing trend seen in literature with MuSK-MG patients having dramatic responses to rituximab therapy[187-191, 212, 213, 216]. Rituximab, a chimeric monoclonal antibody therapy targeting the B-cell specific surface antigen CD20, is being increasingly used in the treatment of various autoimmune diseases. By binding CD20, rituximab induces a sustained depletion in the number of circulating B cells[231]. In one case study, a MuSK-MG patient continued to have prolonged B cell depletion 3 years post-rituximab treatment[212].

The dramatic improvements seen in MuSK-MG patients appear to be related to MuSK-MG being an IgG4-mediated disease. Rituximab has been found to be effective in treating other IgG4-mediated diseases like pemphigus vulgaris and IgG4-related systemic disease[232]. A rapid decrease in IgG4 antibody concentrations, relative to the other IgG subclasses or total IgG, has been demonstrated in IgG4-related systemic disease[232]. CD20 is first expressed during B cell development at the pre-B cell stage, and continues to be expressed at all stages except for after

maturation of B cells into plasma cells. The rapid decrease in IgG4 antibodies following rituximab treatment relative to other subclasses suggests that IgG4-producing plasma cells are shorter-lived, and that rituximab acts by disrupting the generation of these short-lived IgG4-producing plasma cells[232].

Another aspect of the mechanism behind the response to rituximab appears to be expansion of $CD4^+$ regulatory T cells (Tregs)[233, 234], which are involved in maintaining tolerance to self-antigens. Depletion of B cells has been shown to influence the induction, maintenance, and reactivation of $CD4^+$ T cells[235]. MG is a T cell-dependent antibody mediated disease in which decreased frequency and functional impairment of Tregs has been reported[236-238]. An increase in the frequency of circulating Tregs following rituximab therapy has been reported in some MuSK-MG patients, with levels sustained even after B cell counts returned to pre-treatment levels[239].

Rituximab is currently more often used in cases of refractory MG, both of MuSK-MG and AChR-MG, but the increasing evidence of dramatic improvements seen in MuSK-MG patients suggests that rituximab could be used as an early therapeutic option in these patients, and not only in cases of non-responders to other immunomodulatory medications.

4.1.2 Summary and Discussion of Chapter 3

In chapter 3, we described preliminary studies conducted in the immobilization of membrane-bound human AChR onto a sensor surface. Our strategy involved producing membrane vesicles from the AChR-expressing rhabdomyosarcoma cell lines TE671 and CN21, using a method involving the cytoskeleton-destabilizing toxin cytochalasin B described by Pick *et al.*[220]. These

vesicles were immobilized onto the Biacore L1 sensor chip, made specifically for capturing lipid vesicles and membranes.

Our first aim was to confirm AChR expression on the rhabdomyosarcoma cell lines. We were able to demonstrate AChR expression through immunofluorescence and radioligand binding assays. Radioligand binding assays were also used to demonstrate that culturing these cells with nicotine increased αBT-I^{125} binding levels, suggesting increased AChR density. Binding of serum IgG from both AChR-MG and MuSK-MG patients to TE671 cells was also demonstrated using flow cytometry, however the sensitivity for positivity was low. There was a high degree of non-specific binding seen with healthy control samples, which likely inflated the cut-off for positivity, making sera positive by standard radioimmunoprecipitation assays appear negative by flow cytometry. This is effect was likely compounded in TE671 cells by the fact that these cells only express fetal AChR, and at lower levels than CN21 cells which express both isotypes[224].

Membrane vesicles from these cells were prepared using the cytochalasin B vesiculation method, and we were able to demonstrate immobilization of these vesicles onto an L1 sensor surface. However, when testing for the presence of AChR by assessing binding of anti-AChR mAbs and alpha-bungarotoxin, there was no conclusive binding of these analytes. This could either be due to the vesiculation procedure having produced vesicles with no AChR or at too low a density to detect binding, or the AChR may not be in their native conformation.

These preliminary studies in immobilizing AChR in its membrane-bound conformation demonstrate that immobilization of transmembrane proteins in their native membrane-bound conformation is more complex compared to immobilization of proteins using the amine-coupling method. This is due to difficulties in maintaining transmembrane proteins in a native

conformation within the membrane. In the case of AChR, this is made all the more difficult with the complex structure of this ion channel, consisting of 5 subunits, each with four transmembrane domains, and a main immunogenic region with a specific conformational epitope.

4.2 Future Directions

4.2.1 Measuring and characterizing MuSK antibodies

The assay developed here to measure MuSK antibodies is semi-quantitative; antibody levels are reported in response units (RU) which, although directly proportional to the amount of mass bound, is not a quantitative measure. Future directions include making this assay quantitative. This requires a standard curve, which could either be established from an anti-MuSK monoclonal antibody, or to make it more representative of polyclonal serum being tested, a dilution series of an antibody-positive reference pool with designated arbitrary lab units.

Limitations of our study include that the number of patients studied were modest. We also did not have access to clinical data on changes in disease severity to demonstrate that the changes in antibody parameters measured correlated with clinical status, except for in the case study for patient 18. Future work should focus on determining correlations antibody status to clinical status in a larger group of patients, although this is made difficult by MuSK-MG being a rare clinical subtype of an already uncommon disease. It would also be interesting to see if there are clinical differences between patients expressing different IgG subclasses.

The mechanisms behind the effect of rituximab treatment in MuSK-MG also warrant further study. A long-term follow up of the effect of rituximab in patient 18 could be performed to

ascertain how long this patient's MuSK-Ab status remains negative, and, if her antibody titers do increase, whether there are any changes in IgG subclass distribution.

4.2.2 Immobilization of membrane-bound AChR

The studies presented in chapter 3 were preliminary studies aimed at developing a method to immobilize the AChR in its native membrane-bound conformation onto a sensor chip, which could be applied to studying the interaction between anti-AChR antibodies and the AChR autoantigen in MG. Further work is needed to determine if the vesiculation and immobilization process proposed is a good method for immobilizing AChR in its membrane-bound form. Specifically, the lack of analyte binding to the immobilized vesicles suggested there might be a lack of AChR on the vesicles or that they are not in their native conformational state. In depth characterization of the vesicles produced by the vesiculation process is needed to determine if AChR is present on their surface in their native orientation and function, as described in the original study. Variables in the vesiculation process, such as cytochalasin concentration, incubation time, and centrifugation speeds may also need to be optimized for the particular cell line being used. In addition, if the issue is that there is not a high enough density of AChR on the vesicle surface, a cell line expressing only AChR at high density could be tested, for example the HEK293 cell line described by Leite *et al.*[93] which expresses AChR clustered with rapsyn.

4.3 General Conclusion

Myasthenia gravis is an autoimmune disease of the neuromuscular junction where patients are a very heterogenic population in terms of clinical presentation, antibody profile, severity, disease progression, treatment regimen and response to treatment. There is a need for clinical biomarkers

that could be used alongside clinical evaluations in predicting treatment response and clinical outcome, in order to help with a patient-specific approach to disease management.

While the measurement of anti-AChR and anti-MuSK autoantibodies serves as an excellent diagnostic biomarker for MG, there is limited use in measuring these antibodies after diagnosis. Additionally, it is known that over the course of an immune response, antibody parameters like titer, isotype/subclass, and affinity change, and that these parameters influence the pathogenicity of autoantibodies. In this thesis we hypothesized that tracking changes in titer, dissociation rate, and IgG subclass of autoantibodies in MG may help in predicting disease exacerbations, treatment response, and therefore prognosis. The objectives of this thesis were the development of biosensor assays that could be used to easily measure and characterize autoantibodies in MG.

The Biacore assay presented for measuring MuSK-Abs is highly specific, sensitive, and reproducible, and can be performed more rapidly and using very low volumes of serum compared to more conventional immunoassays. We demonstrated the use of this assay not only to measure MuSK antibodies for diagnostic purposes, but also be used to provide a more comprehensive long-term profiling and characterization of MuSK antibodies that has the potential to be useful in a clinical setting for monitoring disease progression and response to treatment. Towards the same goal for AChR antibodies, we also demonstrated preliminary experiments to immobilize AChR in its native membrane-bound form, and discussed the difficulties associated with developing assays for transmembrane proteins.

This thesis was focused on autoantibodies in myasthenia gravis patients, however the principles described here can be applied to other autoimmune and immune-mediated diseases.

References

1. Pascuzzi, R.M. The history of myasthenia gravis. *Neurol Clin* 12, 231-42 (1994).
2. Conti-Fine, B.M., Milani, M. & Kaminski, H.J. Myasthenia gravis: past, present, and future. *J Clin Invest* 116, 2843-54 (2006).
3. Walker, M.B. Case showing the Effect of Prostigmin on Myasthenia Gravis. *Proc R Soc Med* 28, 759-61 (1935).
4. Nastuk, W.L., Strauss, A.J. & Osserman, K.E. Search for a neuromuscular blocking agent in the blood of patients with myasthenia gravis. *Am J Med* 26, 394-409 (1959).
5. Simpson, J. Myasthenia gravis, a new hypothesis. *Scott Med J* 5, 419-436 (1960).
6. Patrick, J. & Lindstrom, J. Autoimmune response to acetylcholine receptor. *Science* 180, 871-2 (1973).
7. Meriggioli, M.N. & Sanders, D.B. Autoimmune myasthenia gravis: emerging clinical and biological heterogeneity. *Lancet Neurol* 8, 475-90 (2009).
8. Grob, D., Brunner, N., Namba, T. & Pagala, M. Lifetime course of myasthenia gravis. *Muscle Nerve* 37, 141-9 (2008).
9. Hopkins, L.C. Clinical features of myasthenia gravis. *Neurol Clin* 12, 243-61 (1994).
10. Drachman, D.B. Myasthenia gravis. *N Engl J Med* 330, 1797-810 (1994).
11. Thomas, C.E. et al. Myasthenic crisis: clinical features, mortality, complications, and risk factors for prolonged intubation. *Neurology* 48, 1253-60 (1997).
12. Leite, M.I. et al. Myasthenia gravis thymus: complement vulnerability of epithelial and myoid cells, complement attack on them, and correlations with autoantibody status. *Am J Pathol* 171, 893-905 (2007).
13. Evoli, A. et al. Clinical correlates with anti-MuSK antibodies in generalized seronegative myasthenia gravis. *Brain* 126, 2304-11 (2003).
14. McConville, J. et al. Detection and characterization of MuSK antibodies in seronegative myasthenia gravis. *Ann Neurol* 55, 580-4 (2004).
15. Lavrnic, D. et al. The features of myasthenia gravis with autoantibodies to MuSK. *J Neurol Neurosurg Psychiatry* 76, 1099-102 (2005).
16. Guptill, J.T., Sanders, D.B. & Evoli, A. Anti-MuSK antibody myasthenia gravis: clinical findings and response to treatment in two large cohorts. *Muscle Nerve* 44, 36-40 (2011).
17. Sanders, D.B., El-Salem, K., Massey, J.M., McConville, J. & Vincent, A. Clinical aspects of MuSK antibody positive seronegative MG. *Neurology* 60, 1978-80 (2003).
18. Lauriola, L. et al. Thymus changes in anti-MuSK-positive and -negative myasthenia gravis. *Neurology* 64, 536-8 (2005).
19. Leite, M.I. et al. Fewer thymic changes in MuSK antibody-positive than in MuSK antibody-negative MG. *Ann Neurol* 57, 444-8 (2005).
20. Carr, A.S., Cardwell, C.R., McCarron, P.O. & McConville, J. A systematic review of population based epidemiological studies in Myasthenia Gravis. *BMC Neurol* 10, 46 (2010).
21. Heldal, A.T., Eide, G.E., Gilhus, N.E. & Romi, F. Geographical distribution of a seropositive myasthenia gravis population. *Muscle Nerve* 45, 815-9 (2012).
22. Heldal, A.T., Owe, J.F., Gilhus, N.E. & Romi, F. Seropositive myasthenia gravis: a nationwide epidemiologic study. *Neurology* 73, 150-1 (2009).
23. Kurtzke, J.F. Epidemiology of myasthenia gravis. *Adv Neurol* 19, 545-66 (1978).

24. Christensen, P.B. et al. Incidence and prevalence of myasthenia gravis in western Denmark: 1975 to 1989. *Neurology* 43, 1779-83 (1993).
25. Phillips, L.H., 2nd, Torner, J.C., Anderson, M.S. & Cox, G.M. The epidemiology of myasthenia gravis in central and western Virginia. *Neurology* 42, 1888-93 (1992).
26. Phillips, L.H., 2nd & Torner, J.C. Epidemiologic evidence for a changing natural history of myasthenia gravis. *Neurology* 47, 1233-8 (1996).
27. Schon, F., Drayson, M. & Thompson, R.A. Myasthenia gravis and elderly people. *Age Ageing* 25, 56-8 (1996).
28. Aarli, J.A. Late-onset myasthenia gravis: a changing scene. *Arch Neurol* 56, 25-7 (1999).
29. Matsuda, M. et al. Increase in incidence of elderly-onset patients with myasthenia gravis in Nagano Prefecture, Japan. *Intern Med* 44, 572-7 (2005).
30. Vincent, A. et al. Evidence of underdiagnosis of myasthenia gravis in older people. *J Neurol Neurosurg Psychiatry* 74, 1105-8 (2003).
31. Somnier, F.E. Increasing incidence of late-onset anti-AChR antibody-seropositive myasthenia gravis. *Neurology* 65, 928-30 (2005).
32. Pakzad, Z., Aziz, T. & Oger, J. Increasing incidence of myasthenia gravis among elderly in British Columbia, Canada. *Neurology* 76, 1526-8 (2011).
33. Koneczny, I., Cossins, J. & Vincent, A. The role of muscle-specific tyrosine kinase (MuSK) and mystery of MuSK myasthenia gravis. *J Anat* (2013).
34. Sine, S.M. End-plate acetylcholine receptor: structure, mechanism, pharmacology, and disease. *Physiol Rev* 92, 1189-234 (2012).
35. Buckley, C. & Vincent, A. Autoimmune channelopathies. *Nat Clin Pract Neurol* 1, 22-33 (2005).
36. Horton, R.M., Manfredi, A.A. & Conti-Tronconi, B.M. The 'embryonic' gamma subunit of the nicotinic acetylcholine receptor is expressed in adult extraocular muscle. *Neurology* 43, 983-6 (1993).
37. Kim, N. et al. Lrp4 is a receptor for Agrin and forms a complex with MuSK. *Cell* 135, 334-42 (2008).
38. Zhang, B. et al. LRP4 serves as a coreceptor of agrin. *Neuron* 60, 285-97 (2008).
39. Zhang, W., Coldefy, A.S., Hubbard, S.R. & Burden, S.J. Agrin binds to the N-terminal region of Lrp4 protein and stimulates association between Lrp4 and the first immunoglobulin-like domain in muscle-specific kinase (MuSK). *J Biol Chem* 286, 40624-30 (2011).
40. Okada, K. et al. The muscle protein Dok-7 is essential for neuromuscular synaptogenesis. *Science* 312, 1802-5 (2006).
41. Sanes, J.R. & Lichtman, J.W. Induction, assembly, maturation and maintenance of a postsynaptic apparatus. *Nat Rev Neurosci* 2, 791-805 (2001).
42. Hughes, B.W., Kusner, L.L. & Kaminski, H.J. Molecular architecture of the neuromuscular junction. *Muscle Nerve* 33, 445-61 (2006).
43. Lin, W. et al. Distinct roles of nerve and muscle in postsynaptic differentiation of the neuromuscular synapse. *Nature* 410, 1057-64 (2001).
44. Weatherbee, S.D., Anderson, K.V. & Niswander, L.A. LDL-receptor-related protein 4 is crucial for formation of the neuromuscular junction. *Development* 133, 4993-5000 (2006).
45. Gomez, A.M. et al. Antibody effector mechanisms in myasthenia gravis-pathogenesis at the neuromuscular junction. *Autoimmunity* 43, 353-70 (2010).

46. Wood, S.J. & Slater, C.R. Safety factor at the neuromuscular junction. *Prog Neurobiol* 64, 393-429 (2001).
47. Lindstrom, J.M., Seybold, M.E., Lennon, V.A., Whittingham, S. & Duane, D.D. Antibody to acetylcholine receptor in myasthenia gravis. Prevalence, clinical correlates, and diagnostic value. *Neurology* 26, 1054-9 (1976).
48. De Baets, M. & Stassen, M.H. The role of antibodies in myasthenia gravis. *J Neurol Sci* 202, 5-11 (2002).
49. Vincent, A. AChR from cell line TE671 cannot replace human muscle AChR in the conventional diagnostic immunoprecipitation RIA. *J Neuroimmunol* 53, 115 (1994).
50. Somnier, F.E. Anti-acetylcholine receptor (AChR) antibodies measurement in myasthenia gravis: the use of cell line TE671 as a source of AChR antigen. *J Neuroimmunol* 51, 63-8 (1994).
51. Voltz, R. et al. Myasthenia gravis: measurement of anti-AChR autoantibodies using cell line TE671. *Neurology* 41, 1836-8 (1991).
52. Beeson, D., Jacobson, L., Newsom-Davis, J. & Vincent, A. A transfected human muscle cell line expressing the adult subtype of the human muscle acetylcholine receptor for diagnostic assays in myasthenia gravis. *Neurology* 47, 1552-5 (1996).
53. Beeson, D., Amar, M., Bermudez, I., Vincent, A. & Newsom-Davis, J. Stable functional expression of the adult subtype of human muscle acetylcholine receptor following transfection of the human rhabdomyosarcoma cell line TE671 with cDNA encoding the epsilon subunit. *Neurosci Lett* 207, 57-60 (1996).
54. Hoedemaekers, A.C., van Breda Vriesman, P.J. & De Baets, M.H. Myasthenia gravis as a prototype autoimmune receptor disease. *Immunol Res* 16, 341-54 (1997).
55. Toyka, K.V., Brachman, D.B., Pestronk, A. & Kao, I. Myasthenia gravis: passive transfer from man to mouse. *Science* 190, 397-9 (1975).
56. Newsom-Davis, J., Pinching, A.J., Vincent, A. & Wilson, S.G. Function of circulating antibody to acetylcholine receptor in myasthenia gravis: investigation by plasma exchange. *Neurology* 28, 266-72 (1978).
57. Tzartos, S.J. et al. Anatomy of the antigenic structure of a large membrane autoantigen, the muscle-type nicotinic acetylcholine receptor. *Immunol Rev* 163, 89-120 (1998).
58. Lindstrom, J.M. Acetylcholine receptors and myasthenia. *Muscle Nerve* 23, 453-77 (2000).
59. Vincent, A. et al. Determinant spreading and immune responses to acetylcholine receptors in myasthenia gravis. *Immunol Rev* 164, 157-68 (1998).
60. Drachman, D.B., Adams, R.N., Stanley, E.F. & Pestronk, A. Mechanisms of acetylcholine receptor loss in myasthenia gravis. *J Neurol Neurosurg Psychiatry* 43, 601-10 (1980).
61. Drachman, D.B., Adams, R.N., Josifek, L.F., Pestronk, A. & Stanley, E.F. Antibody-mediated mechanisms of ACh receptor loss in myasthenia gravis: clinical relevance. *Ann N Y Acad Sci* 377, 175-88 (1981).
62. Sahashi, K., Engel, A.G., Linstrom, J.M., Lambert, E.H. & Lennon, V.A. Ultrastructural localization of immune complexes (IgG and C3) at the end-plate in experimental autoimmune myasthenia gravis. *J Neuropathol Exp Neurol* 37, 212-23 (1978).
63. Rodgaard, A., Nielsen, F.C., Djurup, R., Somnier, F. & Gammeltoft, S. Acetylcholine receptor antibody in myasthenia gravis: predominance of IgG subclasses 1 and 3. *Clin Exp Immunol* 67, 82-8 (1987).

64. Lefvert, A.K., Cuenoud, S. & Fulpius, B.W. Binding properties and subclass distribution of anti-acetylcholine receptor antibodies in myasthenia gravis. *J Neuroimmunol* 1, 125-35 (1981).
65. Engel, A.G. & Arahata, K. The membrane attack complex of complement at the endplate in myasthenia gravis. *Ann N Y Acad Sci* 505, 326-32 (1987).
66. Ruff, R.L. & Lennon, V.A. How myasthenia gravis alters the safety factor for neuromuscular transmission. *J Neuroimmunol* 201-202, 13-20 (2008).
67. Drachman, D.B., Angus, C.W., Adams, R.N., Michelson, J.D. & Hoffman, G.J. Myasthenic antibodies cross-link acetylcholine receptors to accelerate degradation. *N Engl J Med* 298, 1116-22 (1978).
68. Kao, I. & Drachman, D.B. Myasthenic immunoglobulin accelerates acetylcholine receptor degradation. *Science* 196, 527-9 (1977).
69. Drachman, D.B., Adams, R.N., Josifek, L.F. & Self, S.G. Functional activities of autoantibodies to acetylcholine receptors and the clinical severity of myasthenia gravis. *N Engl J Med* 307, 769-75 (1982).
70. Lennon, V.A., Seybold, M.E., Lindstrom, J.M., Cochrane, C. & Ulevitch, R. Role of complement in the pathogenesis of experimental autoimmune myasthenia gravis. *J Exp Med* 147, 973-83 (1978).
71. Heinemann, S., Bevan, S., Kullberg, R., Lindstrom, J. & Rice, J. Modulation of acetylcholine receptor by antibody against the receptor. *Proc Natl Acad Sci U S A* 74, 3090-4 (1977).
72. Burges, J., Wray, D.W., Pizzighella, S., Hall, Z. & Vincent, A. A myasthenia gravis plasma immunoglobulin reduces miniature endplate potentials at human endplates in vitro. *Muscle Nerve* 13, 407-13 (1990).
73. Whiting, P.J., Vincent, A. & Newsom-Davis, J. Acetylcholine receptor antibody characteristics in myasthenia gravis. Fractionation of alpha-bungarotoxin binding site antibodies and their relationship to IgG subclass. *J Neuroimmunol* 5, 1-9 (1983).
74. Vincent, A. & Newsom-Davis, J. Acetylcholine receptor antibody characteristics in myasthenia gravis. I. Patients with generalized myasthenia or disease restricted to ocular muscles. *Clin Exp Immunol* 49, 257-65 (1982).
75. Limburg, P.C., The, T.H., Hummel-Tappel, E. & Oosterhuis, H.J. Anti-acetylcholine receptor antibodies in myasthenia gravis. Part 1. Relation to clinical parameters in 250 patients. *J Neurol Sci* 58, 357-70 (1983).
76. Besinger, U.A. et al. Myasthenia gravis: long-term correlation of binding and bungarotoxin blocking antibodies against acetylcholine receptors with changes in disease severity. *Neurology* 33, 1316-21 (1983).
77. Leite, M.I., Waters, P. & Vincent, A. Diagnostic use of autoantibodies in myasthenia gravis. *Autoimmunity* 43, 371-9 (2010).
78. Vincent, A. Unravelling the pathogenesis of myasthenia gravis. *Nat Rev Immunol* 2, 797-804 (2002).
79. Oosterhuis, H.J., Limburg, P.C., Hummel-Tappel, E. & The, T.H. Anti-acetylcholine receptor antibodies in myasthenia gravis. Part 2. Clinical and serological follow-up of individual patients. *J Neurol Sci* 58, 371-85 (1983).
80. Newsom-Davis, J., Wilson, S.G., Vincent, A. & Ward, C.D. Long-term effects of repeated plasma exchange in myasthenia gravis. *Lancet* 1, 464-8 (1979).

81. Seybold, M.E. Plasmapheresis in myasthenia gravis. *Ann N Y Acad Sci* 505, 584-7 (1987).
82. Somnier, F.E. Clinical implementation of anti-acetylcholine receptor antibodies. *J Neurol Neurosurg Psychiatry* 56, 496-504 (1993).
83. Carter, B., Harrison, R., Lunt, G.G., Behan, P.O. & Simpson, J.A. Anti-acetylcholine receptor antibody titres in the sera of myasthenia patients treated with plasma exchange combined with immunosuppressive therapy. *J Neurol Neurosurg Psychiatry* 43, 397-402 (1980).
84. Seybold, M.E. & Lindstrom, J.M. Patterns of acetylcholine receptor antibody fluctuation in myasthenia gravis. *Ann N Y Acad Sci* 377, 292-306 (1981).
85. Hoch, W. et al. Auto-antibodies to the receptor tyrosine kinase MuSK in patients with myasthenia gravis without acetylcholine receptor antibodies. *Nat Med* 7, 365-8 (2001).
86. Vincent, A. & Leite, M.I. Neuromuscular junction autoimmune disease: muscle specific kinase antibodies and treatments for myasthenia gravis. *Curr Opin Neurol* 18, 519-25 (2005).
87. Shigemoto, K. et al. Induction of myasthenia by immunization against muscle-specific kinase. *J Clin Invest* 116, 1016-24 (2006).
88. Cole, R.N., Reddel, S.W., Gervasio, O.L. & Phillips, W.D. Anti-MuSK patient antibodies disrupt the mouse neuromuscular junction. *Ann Neurol* 63, 782-9 (2008).
89. Plomp, J.J., Huijbers, M.G., van der Maarel, S.M. & Verschuuren, J.J. Pathogenic IgG4 subclass autoantibodies in MuSK myasthenia gravis. *Ann N Y Acad Sci* 1275, 114-22 (2012).
90. van der Zee, J.S., van Swieten, P. & Aalberse, R.C. Inhibition of complement activation by IgG4 antibodies. *Clin Exp Immunol* 64, 415-22 (1986).
91. Shiraishi, H. et al. Acetylcholine receptors loss and postsynaptic damage in MuSK antibody-positive myasthenia gravis. *Ann Neurol* 57, 289-93 (2005).
92. Mori, S. et al. Antibodies against muscle-specific kinase impair both presynaptic and postsynaptic functions in a murine model of myasthenia gravis. *Am J Pathol* 180, 798-810 (2012).
93. Leite, M.I. et al. IgG1 antibodies to acetylcholine receptors in 'seronegative' myasthenia gravis. *Brain* 131, 1940-52 (2008).
94. Boneva, N., Frenkian-Cuvelier, M., Bidault, J., Brenner, T. & Berrih-Aknin, S. Major pathogenic effects of anti-MuSK antibodies in myasthenia gravis. *J Neuroimmunol* 177, 119-31 (2006).
95. Bartoccioni, E. et al. Anti-MuSK antibodies: correlation with myasthenia gravis severity. *Neurology* 67, 505-7 (2006).
96. Niks, E.H. et al. Clinical fluctuations in MuSK myasthenia gravis are related to antigen-specific IgG4 instead of IgG1. *J Neuroimmunol* 195, 151-6 (2008).
97. Sanders, D.B. & Evoli, A. Immunosuppressive therapies in myasthenia gravis. *Autoimmunity* 43, 428-35 (2010).
98. Zhou, L. et al. Clinical comparison of muscle-specific tyrosine kinase (MuSK) antibody-positive and -negative myasthenic patients. *Muscle Nerve* 30, 55-60 (2004).
99. Romi, F., Aarli, J.A. & Gilhus, N.E. Seronegative myasthenia gravis: disease severity and prognosis. *Eur J Neurol* 12, 413-8 (2005).
100. Vrolix, K. et al. The auto-antigen repertoire in myasthenia gravis. *Autoimmunity* 43, 380-400 (2010).

101. Higuchi, O., Hamuro, J., Motomura, M. & Yamanashi, Y. Autoantibodies to low-density lipoprotein receptor-related protein 4 in myasthenia gravis. *Ann Neurol* 69, 418-22 (2011).
102. Cossins, J. et al. The search for new antigenic targets in myasthenia gravis. *Ann N Y Acad Sci* 1275, 123-8 (2012).
103. Motomura, M. & Higuchi, O. [Progress of myasthenia gravis: discovery of Lrp4 antibodies]. *Rinsho Shinkeigaku* 52, 1303-5 (2012).
104. Pevzner, A. et al. Anti-LRP4 autoantibodies in AChR- and MuSK-antibody-negative myasthenia gravis. *J Neurol* 259, 427-35 (2012).
105. Richman, D.P. Antibodies to low density lipoprotein receptor-related protein 4 in seronegative myasthenia gravis. *Arch Neurol* 69, 434-5 (2012).
106. Zhang, B. et al. Autoantibodies to lipoprotein-related protein 4 in patients with double-seronegative myasthenia gravis. *Arch Neurol* 69, 445-51 (2012).
107. Romi, F., Skeie, G.O., Aarli, J.A. & Gilhus, N.E. Muscle autoantibodies in subgroups of myasthenia gravis patients. *J Neurol* 247, 369-75 (2000).
108. Vincent, A., Palace, J. & Hilton-Jones, D. Myasthenia gravis. *Lancet* 357, 2122-8 (2001).
109. Melms, A. et al. Thymus in myasthenia gravis. Isolation of T-lymphocyte lines specific for the nicotinic acetylcholine receptor from thymuses of myasthenic patients. *J Clin Invest* 81, 902-8 (1988).
110. Sims, G.P., Shiono, H., Willcox, N. & Stott, D.I. Somatic hypermutation and selection of B cells in thymic germinal centers responding to acetylcholine receptor in myasthenia gravis. *J Immunol* 167, 1935-44 (2001).
111. Schluep, M., Willcox, N., Vincent, A., Dhoot, G.K. & Newsom-Davis, J. Acetylcholine receptors in human thymic myoid cells in situ: an immunohistological study. *Ann Neurol* 22, 212-22 (1987).
112. Hohlfeld, R. & Wekerle, H. Reflections on the "intrathymic pathogenesis" of myasthenia gravis. *J Neuroimmunol* 201-202, 21-7 (2008).
113. Scadding, G.K., Vincent, A., Newsom-Davis, J. & Henry, K. Acetylcholine receptor antibody synthesis by thymic lymphocytes: correlation with thymic histology. *Neurology* 31, 935-43 (1981).
114. Newsom-Davis, J., Willcox, N., Scadding, G., Calder, L. & Vincent, A. Anti-acetylcholine receptor antibody synthesis by cultured lymphocytes in myasthenia gravis: thymic and peripheral blood cell interactions. *Ann N Y Acad Sci* 377, 393-402 (1981).
115. Schonbeck, S., Padberg, F., Hohlfeld, R. & Wekerle, H. Transplantation of thymic autoimmune microenvironment to severe combined immunodeficiency mice. A new model of myasthenia gravis. *J Clin Invest* 90, 245-50 (1992).
116. Morgenthaler, T.I., Brown, L.R., Colby, T.V., Harper, C.M., Jr. & Coles, D.T. Thymoma. *Mayo Clin Proc* 68, 1110-23 (1993).
117. Aarli, J.A., Stefansson, K., Marton, L.S. & Wollmann, R.L. Patients with myasthenia gravis and thymoma have in their sera IgG autoantibodies against titin. *Clin Exp Immunol* 82, 284-8 (1990).
118. Mygland, A. et al. Ryanodine receptor autoantibodies in myasthenia gravis patients with a thymoma. *Ann Neurol* 32, 589-91 (1992).
119. Kadota, Y. et al. Altered T cell development in human thymoma is related to impairment of MHC class II transactivator expression induced by interferon-gamma (IFN-gamma). *Clin Exp Immunol* 121, 59-68 (2000).

120. Fujii, Y. The thymus, thymoma and myasthenia gravis. *Surg Today* (2012).
121. Scarpino, S. et al. Expression of autoimmune regulator gene (AIRE) and T regulatory cells in human thymomas. *Clin Exp Immunol* 149, 504-12 (2007).
122. Strobel, P. et al. Selective loss of regulatory T cells in thymomas. *Ann Neurol* 56, 901-4 (2004).
123. Compston, D.A., Vincent, A., Newsom-Davis, J. & Batchelor, J.R. Clinical, pathological, HLA antigen and immunological evidence for disease heterogeneity in myasthenia gravis. *Brain* 103, 579-601 (1980).
124. Giraud, M., Vandiedonck, C. & Garchon, H.J. Genetic factors in autoimmune myasthenia gravis. *Ann N Y Acad Sci* 1132, 180-92 (2008).
125. Chen, W.H., Chiu, H.C. & Hseih, R.P. Association of HLA-Bw46DR9 combination with juvenile myasthenia gravis in Chinese. *J Neurol Neurosurg Psychiatry* 56, 382-5 (1993).
126. Matsuki, K. et al. HLA antigens in Japanese patients with myasthenia gravis. *J Clin Invest* 86, 392-9 (1990).
127. Niks, E.H. et al. Strong association of MuSK antibody-positive myasthenia gravis and HLA-DR14-DQ5. *Neurology* 66, 1772-4 (2006).
128. Garchon, H.J., Djabiri, F., Viard, J.P., Gajdos, P. & Bach, J.F. Involvement of human muscle acetylcholine receptor alpha-subunit gene (CHRNA) in susceptibility to myasthenia gravis. *Proc Natl Acad Sci U S A* 91, 4668-72 (1994).
129. Feng, H.Y. et al. A retrospective review of 15 patients with familial myasthenia gravis over a period of 25 years. *Neurol Sci* 33, 771-7 (2012).
130. Askmark, H., Haggard, L., Nygren, I. & Punga, A.R. Vitamin D deficiency in patients with myasthenia gravis and improvement of fatigue after supplementation of vitamin D3: a pilot study. *Eur J Neurol* 19, 1554-60 (2012).
131. Cavalcante, P. et al. Inflammation and epstein-barr virus infection are common features of myasthenia gravis thymus: possible roles in pathogenesis. *Autoimmune Dis* 2011, 213092 (2011).
132. Serafini, B., Cavalcante, P., Bernasconi, P., Aloisi, F. & Mantegazza, R. Epstein-Barr virus in myasthenia gravis thymus: a matter of debate. *Ann Neurol* 70, 519 (2011).
133. Pascuzzi, R.M. The edrophonium test. *Semin Neurol* 23, 83-8 (2003).
134. Golnik, K.C., Pena, R., Lee, A.G. & Eggenberger, E.R. An ice test for the diagnosis of myasthenia gravis. *Ophthalmology* 106, 1282-6 (1999).
135. Meriggioli, M.N. & Sanders, D.B. Advances in the diagnosis of neuromuscular junction disorders. *Am J Phys Med Rehabil* 84, 627-38 (2005).
136. Sanders, D.B., Howard, J.F., Jr. & Johns, T.R. Single-fiber electromyography in myasthenia gravis. *Neurology* 29, 68-76 (1979).
137. Oh, S.J., Kim, D.E., Kuruoglu, R., Bradley, R.J. & Dwyer, D. Diagnostic sensitivity of the laboratory tests in myasthenia gravis. *Muscle Nerve* 15, 720-4 (1992).
138. Jayam Trouth, A., Dabi, A., Solieman, N., Kurukumbi, M. & Kalyanam, J. Myasthenia gravis: a review. *Autoimmune Dis* 2012, 874680 (2012).
139. Vincent, A. & Newsom-Davis, J. Acetylcholine receptor antibody as a diagnostic test for myasthenia gravis: results in 153 validated cases and 2967 diagnostic assays. *J Neurol Neurosurg Psychiatry* 48, 1246-52 (1985).
140. Chan, K.H., Lachance, D.H., Harper, C.M. & Lennon, V.A. Frequency of seronegativity in adult-acquired generalized myasthenia gravis. *Muscle Nerve* 36, 651-8 (2007).

141. Romi, F., Skeie, G.O., Gilhus, N.E. & Aarli, J.A. Striational antibodies in myasthenia gravis: reactivity and possible clinical significance. *Arch Neurol* 62, 442-6 (2005).
142. Vincent, A. & Drachman, D.B. Myasthenia gravis. *Adv Neurol* 88, 159-88 (2002).
143. Skeie, G.O. et al. Guidelines for treatment of autoimmune neuromuscular transmission disorders. *Eur J Neurol* 17, 893-902 (2010).
144. El-Salem, K. et al. Treatment of MuSK-Associated Myasthenia Gravis. *Curr Treat Options Neurol* 16, 283 (2014).
145. Skeie, G.O. et al. Guidelines for the treatment of autoimmune neuromuscular transmission disorders. *Eur J Neurol* 13, 691-9 (2006).
146. Punga, A.R., Flink, R., Askmark, H. & Stalberg, E.V. Cholinergic neuromuscular hyperactivity in patients with myasthenia gravis seropositive for MuSK antibody. *Muscle Nerve* 34, 111-5 (2006).
147. Batocchi, A.P., Evoli, A., Di Schino, C. & Tonali, P. Therapeutic apheresis in myasthenia gravis. *Ther Apher* 4, 275-9 (2000).
148. Gilhus, N.E. et al. Myasthenia gravis: a review of available treatment approaches. *Autoimmune Dis* 2011, 847393 (2011).
149. Zisimopoulou, P. et al. Towards antigen-specific apheresis of pathogenic autoantibodies as a further step in the treatment of myasthenia gravis by plasmapheresis. *J Neuroimmunol* 201-202, 95-103 (2008).
150. Psaridi-Linardaki, L., Trakas, N., Mamalaki, A. & Tzartos, S.J. Specific immunoadsorption of the autoantibodies from myasthenic patients using the extracellular domain of the human muscle acetylcholine receptor alpha-subunit. Development of an antigen-specific therapeutic strategy. *J Neuroimmunol* 159, 183-91 (2005).
151. Gajdos, P. et al. Treatment of myasthenia gravis exacerbation with intravenous immunoglobulin: a randomized double-blind clinical trial. *Arch Neurol* 62, 1689-93 (2005).
152. Zinman, L., Ng, E. & Bril, V. IV immunoglobulin in patients with myasthenia gravis: a randomized controlled trial. *Neurology* 68, 837-41 (2007).
153. Gajdos, P., Chevret, S., Clair, B., Tranchant, C. & Chastang, C. Clinical trial of plasma exchange and high-dose intravenous immunoglobulin in myasthenia gravis. Myasthenia Gravis Clinical Study Group. *Ann Neurol* 41, 789-96 (1997).
154. Barth, D., Nabavi Nouri, M., Ng, E., Nwe, P. & Bril, V. Comparison of IVIg and PLEX in patients with myasthenia gravis. *Neurology* 76, 2017-23 (2011).
155. Samuelsson, A., Towers, T.L. & Ravetch, J.V. Anti-inflammatory activity of IVIG mediated through the inhibitory Fc receptor. *Science* 291, 484-6 (2001).
156. Brannagan, T.H., 3rd, Nagle, K.J., Lange, D.J. & Rowland, L.P. Complications of intravenous immune globulin treatment in neurologic disease. *Neurology* 47, 674-7 (1996).
157. Pascuzzi, R.M., Coslett, H.B. & Johns, T.R. Long-term corticosteroid treatment of myasthenia gravis: report of 116 patients. *Ann Neurol* 15, 291-8 (1984).
158. Sghirlanzoni, A., Peluchetti, D., Mantegazza, R., Fiacchino, F. & Cornelio, F. Myasthenia gravis: prolonged treatment with steroids. *Neurology* 34, 170-4 (1984).
159. Cosi, V. et al. Effectiveness of steroid treatment in myasthenia gravis: a retrospective study. *Acta Neurol Scand* 84, 33-9 (1991).

160. Evoli, A., Batocchi, A.P., Palmisani, M.T., Lo Monaco, M. & Tonali, P. Long-term results of corticosteroid therapy in patients with myasthenia gravis. *Eur Neurol* 32, 37-43 (1992).
161. Seybold, M.E. & Drachman, D.B. Gradually increasing doses of prednisone in myasthenia gravis. Reducing the hazards of treatment. *N Engl J Med* 290, 81-4 (1974).
162. Frauman, A.G. An overview of the adverse reactions to adrenal corticosteroids. *Adverse Drug React Toxicol Rev* 15, 203-6 (1996).
163. Jani-Acsadi, A. & Lisak, R.P. Myasthenia gravis. *Curr Treat Options Neurol* 12, 231-43 (2010).
164. Kumar, V. & Kaminski, H.J. Treatment of myasthenia gravis. *Curr Neurol Neurosci Rep* 11, 89-96 (2011).
165. Kuks, J.B., Djojoatmodjo, S. & Oosterhuis, H.J. Azathioprine in myasthenia gravis: observations in 41 patients and a review of literature. *Neuromuscul Disord* 1, 423-31 (1991).
166. Palace, J., Newsom-Davis, J. & Lecky, B. A randomized double-blind trial of prednisolone alone or with azathioprine in myasthenia gravis. Myasthenia Gravis Study Group. *Neurology* 50, 1778-83 (1998).
167. Evoli, A. et al. Response to therapy in myasthenia gravis with anti-MuSK antibodies. *Ann N Y Acad Sci* 1132, 76-83 (2008).
168. Kissel, J.T., Levy, R.J., Mendell, J.R. & Griggs, R.C. Azathioprine toxicity in neuromuscular disease. *Neurology* 36, 35-9 (1986).
169. Hohlfeld, R., Michels, M., Heininger, K., Besinger, U. & Toyka, K.V. Azathioprine toxicity during long-term immunosuppression of generalized myasthenia gravis. *Neurology* 38, 258-61 (1988).
170. Finelli, P.F. Primary CNS lymphoma in myasthenic on long-term azathioprine. *J Neurooncol* 74, 91-2 (2005).
171. Herrlinger, U., Weller, M., Dichgans, J. & Melms, A. Association of primary central nervous system lymphoma with long-term azathioprine therapy for myasthenia gravis? *Ann Neurol* 47, 682-3 (2000).
172. Allison, A.C. & Eugui, E.M. Mycophenolate mofetil and its mechanisms of action. *Immunopharmacology* 47, 85-118 (2000).
173. Chaudhry, V., Cornblath, D.R., Griffin, J.W., O'Brien, R. & Drachman, D.B. Mycophenolate mofetil: a safe and promising immunosuppressant in neuromuscular diseases. *Neurology* 56, 94-6 (2001).
174. Ciafaloni, E., Massey, J.M., Tucker-Lipscomb, B. & Sanders, D.B. Mycophenolate mofetil for myasthenia gravis: an open-label pilot study. *Neurology* 56, 97-9 (2001).
175. Meriggioli, M.N. et al. Mycophenolate mofetil for myasthenia gravis: an analysis of efficacy, safety, and tolerability. *Neurology* 61, 1438-40 (2003).
176. Meriggioli, M.N., Rowin, J., Richman, J.G. & Leurgans, S. Mycophenolate mofetil for myasthenia gravis: a double-blind, placebo-controlled pilot study. *Ann N Y Acad Sci* 998, 494-9 (2003).
177. Muscle Study Group. A trial of mycophenolate mofetil with prednisone as initial immunotherapy in myasthenia gravis. *Neurology* 71, 394-9 (2008).
178. Sanders, D.B. et al. An international, phase III, randomized trial of mycophenolate mofetil in myasthenia gravis. *Neurology* 71, 400-6 (2008).

179. Sanders, D.B. & Siddiqi, Z.A. Lessons from two trials of mycophenolate mofetil in myasthenia gravis. *Ann N Y Acad Sci* 1132, 249-53 (2008).
180. Tindall, R.S., Phillips, J.T., Rollins, J.A., Wells, L. & Hall, K. A clinical therapeutic trial of cyclosporine in myasthenia gravis. *Ann N Y Acad Sci* 681, 539-51 (1993).
181. Ciafaloni, E., Nikhar, N.K., Massey, J.M. & Sanders, D.B. Retrospective analysis of the use of cyclosporine in myasthenia gravis. *Neurology* 55, 448-50 (2000).
182. Takamori, M. et al. Anti-ryanodine receptor antibodies and FK506 in myasthenia gravis. *Neurology* 62, 1894-6 (2004).
183. Konishi, T., Yoshiyama, Y., Takamori, M. & Saida, T. Long-term treatment of generalised myasthenia gravis with FK506 (tacrolimus). *J Neurol Neurosurg Psychiatry* 76, 448-50 (2005).
184. Nagane, Y., Utsugisawa, K., Obara, D., Kondoh, R. & Terayama, Y. Efficacy of low-dose FK506 in the treatment of Myasthenia gravis--a randomized pilot study. *Eur Neurol* 53, 146-50 (2005).
185. Ponseti, J.M. et al. Tacrolimus for myasthenia gravis: a clinical study of 212 patients. *Ann N Y Acad Sci* 1132, 254-63 (2008).
186. Pescovitz, M.D. Rituximab, an anti-cd20 monoclonal antibody: history and mechanism of action. *Am J Transplant* 6, 859-66 (2006).
187. Diaz-Manera, J. et al. Long-lasting treatment effect of rituximab in MuSK myasthenia. *Neurology* 78, 189-93 (2012).
188. Stein, B. & Bird, S.J. Rituximab in the treatment of MuSK antibody-positive myasthenia gravis. *J Clin Neuromuscul Dis* 12, 163-4 (2011).
189. Illa, I. et al. Sustained response to Rituximab in anti-AChR and anti-MuSK positive Myasthenia Gravis patients. *J Neuroimmunol* 201-202, 90-4 (2008).
190. Hain, B., Jordan, K., Deschauer, M. & Zierz, S. Successful treatment of MuSK antibody-positive myasthenia gravis with rituximab. *Muscle Nerve* 33, 575-80 (2006).
191. Keung, B. et al. Long-term benefit of rituximab in MuSK autoantibody myasthenia gravis patients. *J Neurol Neurosurg Psychiatry* 84, 1407-9 (2013).
192. Spring, P.J. & Spies, J.M. Myasthenia gravis: options and timing of immunomodulatory treatment. *BioDrugs* 15, 173-83 (2001).
193. Blalock, A., Harvey, A., Ford, F. & Lilienthal, J.J. The treatment of myasthenia gravis by removal of the thymus gland. *Br J Surg* 32, 201-214 (1946).
194. Gronseth, G.S. & Barohn, R.J. Practice parameter: thymectomy for autoimmune myasthenia gravis (an evidence-based review): report of the Quality Standards Subcommittee of the American Academy of Neurology. *Neurology* 55, 7-15 (2000).
195. Gronseth, G.S. & Barohn, R.J. Thymectomy for Myasthenia Gravis. *Curr Treat Options Neurol* 4, 203-209 (2002).
196. Jaretzki, A., Steinglass, K.M. & Sonett, J.R. Thymectomy in the management of myasthenia gravis. *Semin Neurol* 24, 49-62 (2004).
197. Wolfe, G.I., Kaminski, H.J., Jaretzki, A., 3rd, Swan, A. & Newsom-Davis, J. Development of a thymectomy trial in nonthymomatous myasthenia gravis patients receiving immunosuppressive therapy. *Ann N Y Acad Sci* 998, 473-80 (2003).
198. Kaminski, H.J. et al. Biomarker development for myasthenia gravis. *Ann N Y Acad Sci* 1275, 101-6 (2012).
199. Ghazanfari, N. et al. Muscle specific kinase: organiser of synaptic membrane domains. *Int J Biochem Cell Biol* 43, 295-8 (2011).

200. GE Healthcare. (Uppsala, Sweden, 2007).
201. Cooper, M.A. Optical biosensors in drug discovery. *Nat Rev Drug Discov* 1, 515-28 (2002).
202. GE Healthcare. (Uppsala, Sweden, 2008).
203. GE Healthcare. (Uppsala, Sweden, 2012).
204. Mason, S., La, S., Mytych, D., Swanson, S.J. & Ferbas, J. Validation of the BIACORE 3000 platform for detection of antibodies against erythropoietic agents in human serum samples. *Curr Med Res Opin* 19, 651-9 (2003).
205. Pasnoor, M. et al. Clinical findings in MuSK-antibody positive myasthenia gravis: a U.S. experience. *Muscle Nerve* 41, 370-4 (2010).
206. Ohta, K. et al. Clinical and experimental features of MuSK antibody positive MG in Japan. *Eur J Neurol* 14, 1029-34 (2007).
207. Tsiamalos, P., Kordas, G., Kokla, A., Poulas, K. & Tzartos, S.J. Epidemiological and immunological profile of muscle-specific kinase myasthenia gravis in Greece. *Eur J Neurol* 16, 925-30 (2009).
208. Takacs, M.A., Jacobs, S.J., Bordens, R.M. & Swanson, S.J. Detection and characterization of antibodies to PEG-IFN-alpha2b using surface plasmon resonance. *J Interferon Cytokine Res* 19, 781-9 (1999).
209. Sem, D.S., McNeeley, P.A. & Linnik, M.D. Antibody affinities and relative titers in polyclonal populations: surface plasmon resonance analysis of anti-DNA antibodies. *Arch Biochem Biophys* 372, 62-8 (1999).
210. Wolfe, G.I. et al. Myasthenia gravis activities of daily living profile. *Neurology* 52, 1487-9 (1999).
211. Boye, J., Elter, T. & Engert, A. An overview of the current clinical use of the anti-CD20 monoclonal antibody rituximab. *Ann Oncol* 14, 520-35 (2003).
212. Yi, J.S., Decroos, E.C., Sanders, D.B., Weinhold, K.J. & Guptill, J.T. Prolonged B-cell depletion in MuSK myasthenia gravis following rituximab treatment. *Muscle Nerve* 48, 992-3 (2013).
213. Baek, W.S., Bashey, A. & Sheean, G.L. Complete remission induced by rituximab in refractory, seronegative, muscle-specific, kinase-positive myasthenia gravis. *J Neurol Neurosurg Psychiatry* 78, 771 (2007).
214. Burns, T.M., Conaway, M.R., Cutter, G.R., Sanders, D.B. & Muscle Study, G. Less is more, or almost as much: a 15-item quality-of-life instrument for myasthenia gravis. *Muscle Nerve* 38, 957-63 (2008).
215. Barohn, R.J. et al. Reliability testing of the quantitative myasthenia gravis score. *Ann N Y Acad Sci* 841, 769-72 (1998).
216. Thakre, M., Inshasi, J. & Marashi, M. Rituximab in refractory MuSK antibody myasthenia gravis. *J Neurol* 254, 968-9 (2007).
217. Fruh, V., AP, I.J. & Siegal, G. How to catch a membrane protein in action: a review of functional membrane protein immobilization strategies and their applications. *Chem Rev* 111, 640-56 (2011).
218. Sevin-Landais, A. et al. Functional immobilisation of the nicotinic acetylcholine receptor in tethered lipid membranes. *Biophys Chem* 85, 141-52 (2000).
219. Kroger, D., Hucho, F. & Vogel, H. Ligand binding to nicotinic acetylcholine receptor investigated by surface plasmon resonance. *Anal Chem* 71, 3157-65 (1999).

220. Pick, H. et al. Investigating cellular signaling reactions in single attoliter vesicles. *J Am Chem Soc* 127, 2908-12 (2005).
221. Luther, M.A. et al. A muscle acetylcholine receptor is expressed in the human cerebellar medulloblastoma cell line TE671. *J Neurosci* 9, 1082-96 (1989).
222. Ke, L., Eisenhour, C.M., Bencherif, M. & Lukas, R.J. Effects of chronic nicotine treatment on expression of diverse nicotinic acetylcholine receptor subtypes. I. Dose- and time-dependent effects of nicotine treatment. *J Pharmacol Exp Ther* 286, 825-40 (1998).
223. Siegel, H.N. & Lukas, R.J. Nicotinic agonists regulate alpha-bungarotoxin binding sites of TE671 human medulloblastoma cells. *J Neurochem* 50, 1272-8 (1988).
224. Blaes, F., Beeson, D., Plested, P., Lang, B. & Vincent, A. IgG from "seronegative" myasthenia gravis patients binds to a muscle cell line, TE671, but not to human acetylcholine receptor. *Ann Neurol* 47, 504-10 (2000).
225. French, M.A. & Harrison, G. Serum IgG subclass concentrations in healthy adults: a study using monoclonal antisera. *Clin Exp Immunol* 56, 473-5 (1984).
226. Bruggemann, M. et al. Comparison of the effector functions of human immunoglobulins using a matched set of chimeric antibodies. *J Exp Med* 166, 1351-61 (1987).
227. Ferrante, A., Beard, L.J. & Feldman, R.G. IgG subclass distribution of antibodies to bacterial and viral antigens. *Pediatr Infect Dis J* 9, S16-24 (1990).
228. Siber, G.R., Schur, P.H., Aisenberg, A.C., Weitzman, S.A. & Schiffman, G. Correlation between serum IgG-2 concentrations and the antibody response to bacterial polysaccharide antigens. *N Engl J Med* 303, 178-82 (1980).
229. Conti-Fine, B.M., Milani, M. & Wang, W. CD4+ T cells and cytokines in the pathogenesis of acquired myasthenia gravis. *Ann N Y Acad Sci* 1132, 193-209 (2008).
230. Schuurman, J. et al. Normal human immunoglobulin G4 is bispecific: it has two different antigen-combining sites. *Immunology* 97, 693-8 (1999).
231. Townsend, M.J., Monroe, J.G. & Chan, A.C. B-cell targeted therapies in human autoimmune diseases: an updated perspective. *Immunol Rev* 237, 264-83 (2010).
232. Khosroshahi, A., Bloch, D.B., Deshpande, V. & Stone, J.H. Rituximab therapy leads to rapid decline of serum IgG4 levels and prompt clinical improvement in IgG4-related systemic disease. *Arthritis Rheum* 62, 1755-62 (2010).
233. Stasi, R. et al. Analysis of regulatory T-cell changes in patients with idiopathic thrombocytopenic purpura receiving B cell-depleting therapy with rituximab. *Blood* 112, 1147-50 (2008).
234. Sfikakis, P.P. et al. Increased expression of the FoxP3 functional marker of regulatory T cells following B cell depletion with rituximab in patients with lupus nephritis. *Clin Immunol* 123, 66-73 (2007).
235. Lund, F.E. & Randall, T.D. Effector and regulatory B cells: modulators of CD4+ T cell immunity. *Nat Rev Immunol* 10, 236-47 (2010).
236. Fattorossi, A. et al. Circulating and thymic CD4 CD25 T regulatory cells in myasthenia gravis: effect of immunosuppressive treatment. *Immunology* 116, 134-41 (2005).
237. Thiruppathi, M. et al. Functional defect in regulatory T cells in myasthenia gravis. *Ann N Y Acad Sci* 1274, 68-76 (2012).
238. Balandina, A., Lecart, S., Dartevelle, P., Saoudi, A. & Berrih-Aknin, S. Functional defect of regulatory CD4(+)CD25+ T cells in the thymus of patients with autoimmune myasthenia gravis. *Blood* 105, 735-41 (2005).

239. Catzola, V. et al. Changes in regulatory T cells after rituximab in two patients with refractory myasthenia gravis. *J Neurol* 260, 2163-5 (2013).

Appendix

The Biacore-derived parameters of binding response and antibody dissociation rates for the 65 serial serum samples analyzed are shown in table A-1.

Table A-1 Biacore-derived parameters of 65 serial serum samples.

Patient No.	Sample Month (Year)	Binding Response (RU)	Antibody Dissociation Rate (s^{-1})
1	0	156.80	$2.05x10^{-4}$
1	6	136.35	$2.16x10^{-4}$
1	66 (5.5)	74.99	$7.70x10^{-5}$
2	0	228.48	$4.49x10^{-4}$
2	34 (2.8)	339.29	$3.25x10^{-4}$
2	133 (11.1)	78.89	$6.69x10^{-4}$
3	0	116.56	$2.02x10^{-4}$
3	7 (0.6)	132.44	$1.81x10^{-4}$
4	0	129.66	$2.18x10^{-4}$
4	1	142.37	$1.99x10^{-4}$
5	0	69.77	$3.99x10^{-4}$
5	2	48.95	$4.39x10^{-4}$
6	0	294.95	$1.71x10^{-4}$
6	2	346.44	$1.58x10^{-4}$
6	3	99.94	$1.23x10^{-4}$
6	60 (5.0)	122.43	$1.61x10^{-4}$
7	0	323.35	$2.82x10^{-4}$
7	13 (1.1)	240.93	$2.94x10^{-4}$
7	22 (1.8)	94.04	$1.80x10^{-4}$
8	0	121.56	$1.43x10^{-4}$
8	5	123.46	$1.51x10^{-4}$
8	161 (13.4)	21.28 (negative)	-
9	0	112.68	$2.67x10^{-5}$
9	2	96.62	$3.85x10^{-4}$
10	0	10.57 (negative)	-
10	1	13.36 (negative)	-
10	5	17.44 (negative)	-
10	25 (2.1)	18.24 (negative)	-
10	72 (6.0)	33.09 (negative)	-
10	189 (15.8)	44.93	ND
11	0	73.65	$4.74x10^{-4}$
11	3	42.08	$2.64x10^{-4}$
11	17 (1.4)	119.69	$3.92x10^{-4}$
11	34 (2.8)	54.23	$2.72x10^{-4}$
11	37 (3.1)	69.62	$2.29x10^{-4}$

Patient No.	Sample Month (Year)	Binding Response (RU)	Antibody Dissociation Rate (s^{-1})
11	40 (3.3)	106.51	$2.55x10^{-4}$
11	44 (3.7)	72.81	ND
12	0	169.56	$1.21x10^{-4}$
12	1	223.54	$1.20x10^{-4}$
12	9	33.55 (negative)	-
12	17 (1.4)	79.97	$5.94x10^{-5}$
12	145 (12.1)	188.36	$1.35x10^{-4}$
12	154 (12.8)	113.90	$1.02x10^{-4}$
12	157 (13.1)	139.40	$1.01x10^{-4}$
13	0	238.46	$2.32x10^{-4}$
13	0.3	165.10	$2.11x10^{-4}$
13	14 (1.2)	293.84	$1.31x10^{-4}$
14	0	122.63	$5.27x10^{-4}$
14	33 (2.8)	73.83	$3.16x10^{-4}$
14	128 (10.7)	207.56	$1.99x10^{-4}$
15	0	103.64	$2.32x10^{-4}$
15	3	47.95	$2.31x10^{-4}$
16	0	80.42	$4.90x10^{-4}$
16	7	129.10	$3.91x10^{-4}$
16	14 (1.2)	154.47	$3.29x10^{-4}$
16	15 (1.3)	38.06	$5.24x10^{-4}$
17	0	312.60	$1.70x10^{-4}$
17	1	75.54	$2.28x10^{-4}$
18	0	113.30	$2.66x10^{-4}$
18	11	145.04	$3.23x10^{-4}$
18	16 (1.3)	-8.52 (negative)	-
18	17 (1.4)	-8.90 (negative)	-
18	20 (1.7)	-11.06 (negative)	-
19	0	99.99	$5.74x10^{-4}$
19	1	196.74	$5.05x10^{-4}$